03

7.9 - 10.10 2.

OR - 158058

(E79-10102)   APPLICATION OF LANDSAT DATA AND   N79-17291
DIGITAL IMAGE PROCESSING Technical Report,
1975 - 1978 (Zentralstelle fuer
Geo-Photogrammetrie) 169 p HC A08/MF A01   Unclas
                              CSCL 05B G3/43 00102

28380

RECEIVED

JAN 2 6 1979

SIS/902.6

ZGF - ZENTRALSTELLE FUR GEO-PHOTOGRAMMETRIE UND FERNERKUNDUNG (DFG)

am Institut für allgemeine und angewandte Geologie der Universität, Luisenstr 37, D-8 München 2

ORIGINAL CONTAINS
COLOR ILLUSTRATIONS

1. SR No. 28380	2. Type of Report III	3. Recipient's Catalog No.

4. Title: Application of LANDSAT-data and digital image processing.	5. Report Data May 1978

7. Principal Investigator Prof. Dr. J. Bodechtel	6. Period Covered 1975 – 1978

9. Name and Address of Principal Investigators Organization Zentralstelle für Geo-Photogrammetrie und Fernerkundung	8. Number of Pages: 164
	1o. Principal Investig. Rept.No.

12. Sponsoring Agency and Address Deutsche Forschungsgemeinschaft Kennedyallee 4o 53oo Bonn – Bad Godesberg 1	11. GSFC Technical Monitor James Broderick
	13. Key words (selected by PI) Geology, Landuse, Landsat-application, data and image processing

Supplementary notes

This report consists of the results of research work carried out at the Zentralstelle für Geo-Photogrammetrie und Fernerkundung der Deutschen Forschungsgemeinschaft (Central Laboratory of geophotogrammetry and remote sensing of the German Research Council)

Summary:
On the basis of Landsat-1 and -2 data, part I of the following report demonstrates applications in the fields of coal mining, lignite exploration, and thematic mapping in geology. Section II describes the hybrid image processing system of the ZGF, its software and its utilization for educational purposes.
In Part III a proposal for a pre-operational European satellite which has been prepared in cooperation with Messerschmitt-Bölkow-Blohm is being discussed.

Content   page

page

Introduction

With respect to several discussions with the Mission Utilization
Office, the following Landsat-2 final report covers a wider
field of activities based on the availability of Landsat data
through the PI-contract with NASA and through the receiving
capabilities of Fuccino.
The generous data contribution by NASA has initiated a tremendous
increase in carrying out more application oriented investigations
also by user groups which have not been involved at all by
Landsat-1 investigations.
Besides a constantly increasing user community and improved
capabilities of handling remote sensing data, the potential
of space borne remote sensing has become evident, even though
it can be stated , that Landsat-2 does not provide an optimum
data base for all relevant European key applications.
Encouraged by the increased interest in Landsat data, we have
put effort in providing the user community with sophisticated
data processing techniques and in discussing the specific user
requirements towards operatinal remote sensing systems.
With respect to Landsat investigations carried out and to above
mentioned activities the submitted final Landsat-2 report consists
of 3 parts:

Part 1 describes various applications of Landsat data and in
       accordance with the Mission Utilization Office also
       the use of aircraft data, within several projects.
       These studies involved the application of conventional
       photo interpretation techniques and digital data processing.

Part 2 describes in detail technical aspects of the hybrid image
       processing system and discusses how we are using our
       technical capabilities in order to approach the potential
       user community.

Part 3 summarizes our experience gained by discussing the needs
for remote sensing with several user groups. These results
in combination with the technical design considerations by
MBB on the basis of an experimental CCD scanner has led
to a proposal for an european earth resources satellite.

PART   I

EVALUATION OF LANDSAT DATA BY CONVENTIONAL

INTERPRETATION TECHNIQUES AND BY DIGITAL

IMAGE PROCESSING

With respect to the sophisticated image
data processing techniques available today,
the visual interpretation of Landsat images
with an eye to linear features seems not
anymore to be of specific interest.
Furthermore, methodological aspects of
extracting photolineations from space borne
images have been described by many authors
and have also been discussed in our Landsat-1
final report.

Nevertheless, we continued to apply above
methods of lineament interpretation and
have decided to adapt these activities in
the final report, because we strongly feel,
that the interpretation and evaluation of
linear features is still of basic interest
and often provides significant information
not only under scientific aspects but also
for direct application.
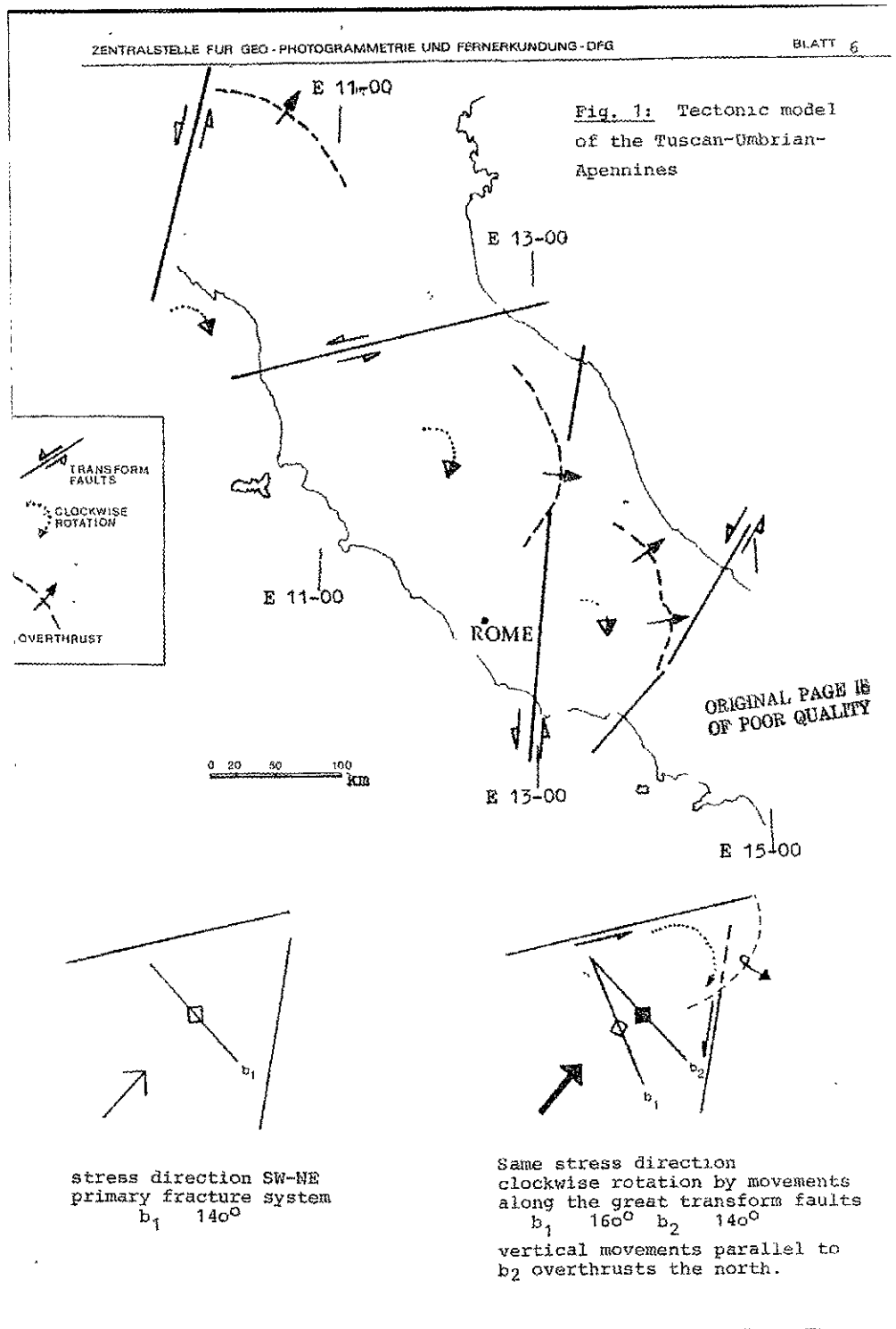
A   Satellite Lineations in Comparison with
         Structural Field Measurements

         - A Tectonical Model of the Northern Apennines

Since 1970 the Photogeologic Department of the University
of Munich has participated in a research project "Geo-
dynamics" of the German Research Council. The research
work within this program has been based on the combination
of satellite and aircraft data interpretation and structural
field measurements. The first interpretation phase (since
1973) showed already reasonable results, which have been
published in GEOFORUM (1974), and will be briefly reviewed
here (fig. 1).

1. The evaluation of Landsat-1 images suggests two large
   horizontal fault zones within the Northern Apennines:
   - the first zone (80° striking) follows the Arno
     Valley resp. its eastern prolongation
   - the second zone ($0 - 10^O$ striking) is well known
     as the "Ancona-Anzio-Line".

   The sense of movement derived by photointerpretation
   techniques is sinistral for both the Arno fault and
   the Ancona-Anzio Line. The result of these opposite
   movements is a clockwise rotation of the block bounded
   by the two faults.

2. This rotation is confirmed by joint-plane-measurements
   in an area SE Siena (Tuscany), which indicates the
   existence of two different fabric systems. The b-axis
   of the older system strikes about 160° (NNW), the b-
   axis of the younger system strikes about 140° (NW),
   and corresponds to the main fold axes of the region.

Fig. 1: Tectonic model
of the Tuscan-Umbrian-
Apennines

TRANSFORM
FAULTS

CLOCKWISE
ROTATION

OVERTHRUST

E 11-00

E 13-00

E 11-00

ROME

E 13-00

E 15-00

0   20   50   100
km

stress direction SW-NE
primary fracture system
b_1 140°

Same stress direction
clockwise rotation by movements
along the great transform faults
    b_1 160° b_2 140°

vertical movements parallel to
b_2 overthrusts the north.

3. The statistical analysis of lineament directions
   visible on satellite images and aerial photographs
   (BODECHTEL 1969) confirm the two "axis systems" for
   wide parts of the Southern Tuscany.

Based on these results and the work done by the research
team of the FU Berlin (especially in the region of the
Prato-Sillaro-Line) and, before all, the almost totally
lacking information on joint configurations in the entire
Northern Apennines, a final working program was started.
It includes the following objects:

1. Tectonic field measurements along two traverses
   through the Northern Apennines.[*] The position of
   the two sections was chosen with respect to the
   previous described results based on the evaluation
   of satellite imagery. The position of profiles is
   indicated by fig. 2.
   The southern profile (measurement points 1 through
   1o - fig. 2) was selected in order to classify the
   problem of the clockwise rotation of the Tuscan-
   Umbrian Apennines.
   Furthermore, the influence of a fault zone in the
   eastern part of the section should be tested. The
   northern section (measurement points 11 through 16)
   should serve for clearing the structural implications
   of the Prato-Sillaro-Line.

2. Detailed evaluation, especially lineament analysis,
   of satellite images covering the Northern Apennines.
   The additional use of SKYLAB data has also been incorporated.
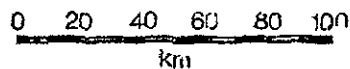
---

[*] A description of the relationship between in situ
    point measurements and their statistical evaluation
    is given in the Landsat-1 final report.

ORIGINAL PAGE IS
OF POOR QUALITY

FOLDOUT FRAME 2

A D R I A T I S C H E S   M E E R

ORIGINAL PAGE IS
OF POOR QUALITY

T Y R R H E N I S C H E S   M E E R

FOLDOUT FRAME

1 Mti.dell'
   Uccellina
2 Scansano
3 Poggio il Sasso
4 Castell'Azzara
5 Mte.Cetona
6 Trasumeno Sud
7 Mte.Malbe
8 Gualdo Tadino-
   Fabriano
9 Mte. S.Vicino
1o Mte.Conero
11 Mte. Albano South
12 Mte.Albano North
13 La Querce-Filettole
14 Montepiano-Vernio
15 Valle Santerno

A Line Sestri-
     Voltaggio
B Line Prato-
     Sillaro
C Cervarola-Over-
     thrust
D Line Ancona-Anzio

.... Grenzen der Fazieszüge
——————— Haupt-Querstörungen
††††††††† Haupt-Aufschiebungen
——————— Faltenzüge

④ Großmeßbereich

Fig.2: Position of
in situ measurements
(map after ABBATE et
al. 197o)

1. Field Measurements

About 15.ooo joint planes were measured along the two
profiles, the largest part by use of terrestrial-photo-
grammetric techniques. These techniques give an optimum
base for digital processing of the data. In the southern
part the measurements were concentrated on the several
"horst"-zones in which the Tuscan-Umbrian-Apennines are
arranged from West to East. The analysis of the joint-
pole configurations on an equal-area-net led to the
following results.

1. The existence of two (or more) fabric systems has
   been confirmed for all sites but two: Nearly at all
   the localities the striking of the b-axes of the two
   systems is significantly different (see fig. 3).

2. The differences of the axis-trends vary uniformly
   between +1o´ and +25´ in the southern section. The
   amount does not depend on the age of the measured
   rock formation. Only on the limbs of overturned or
   upright folds (Mte. Cetona, Umbrian Apennines)
   higher differences up to 4o - 6o^{o} can be observed.
   This phenomenon has to be explained by the fact that
   on the outer arc of a fold formed by buckling the
   original angle between rotated linears (b_1-axis) and
   fold axis (b_2-axis) is increased. An exact re-
   orientation of the upfolded linears is not possible
   without knowledge of the state of strain (RAMSAY 1966).
   Data for defining this state of strain cannot be
   obtained in this region.
   In the northern section the pattern exhibited by
   the axis differences is not uniform. This is caused
   by the influence of the Prato-Sillaro-Line. The
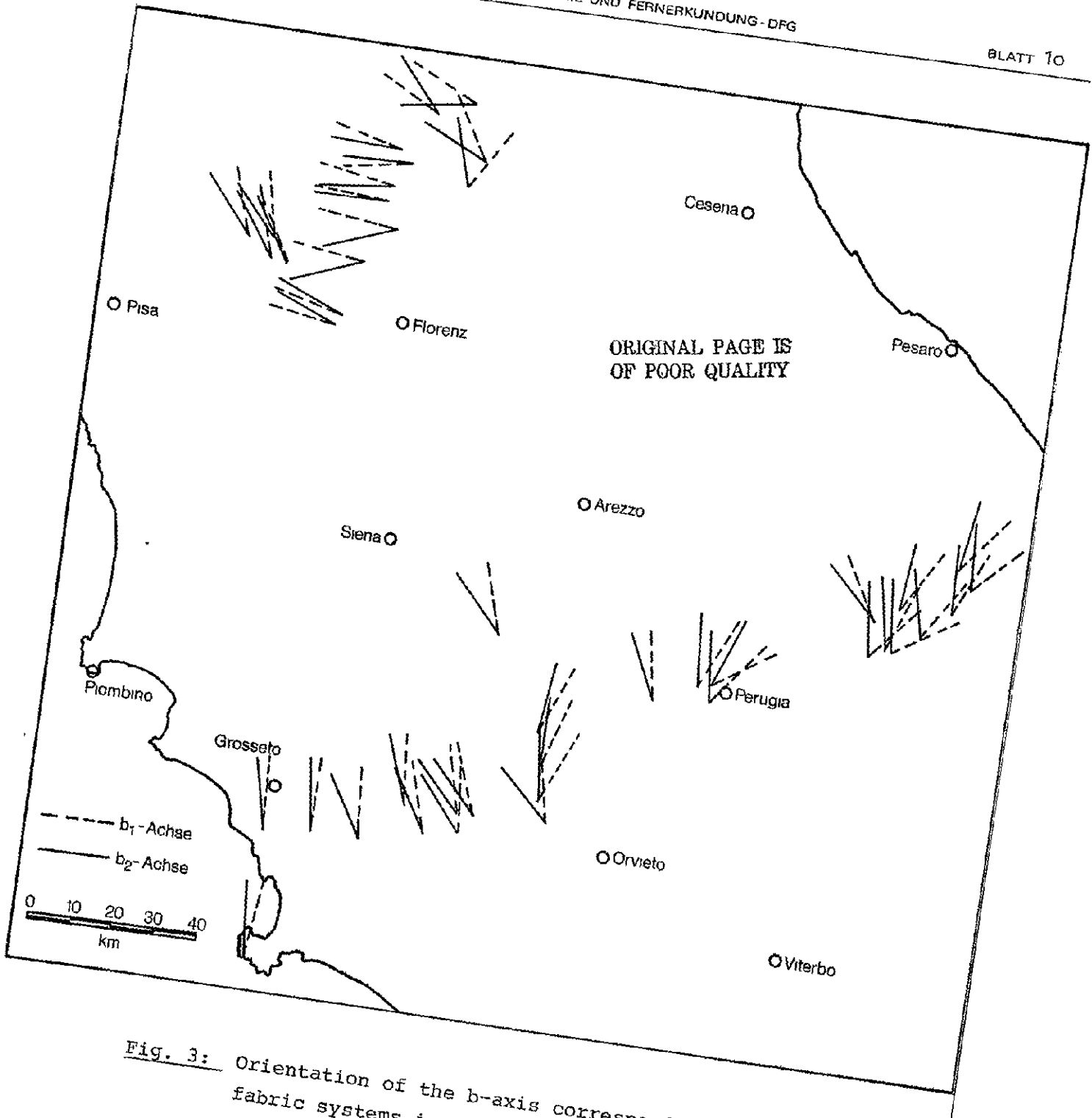   following angle differences could be derived:

Fig. 3: Orientation of the b-axis corresponding to fabric systems in the northern Apennin.
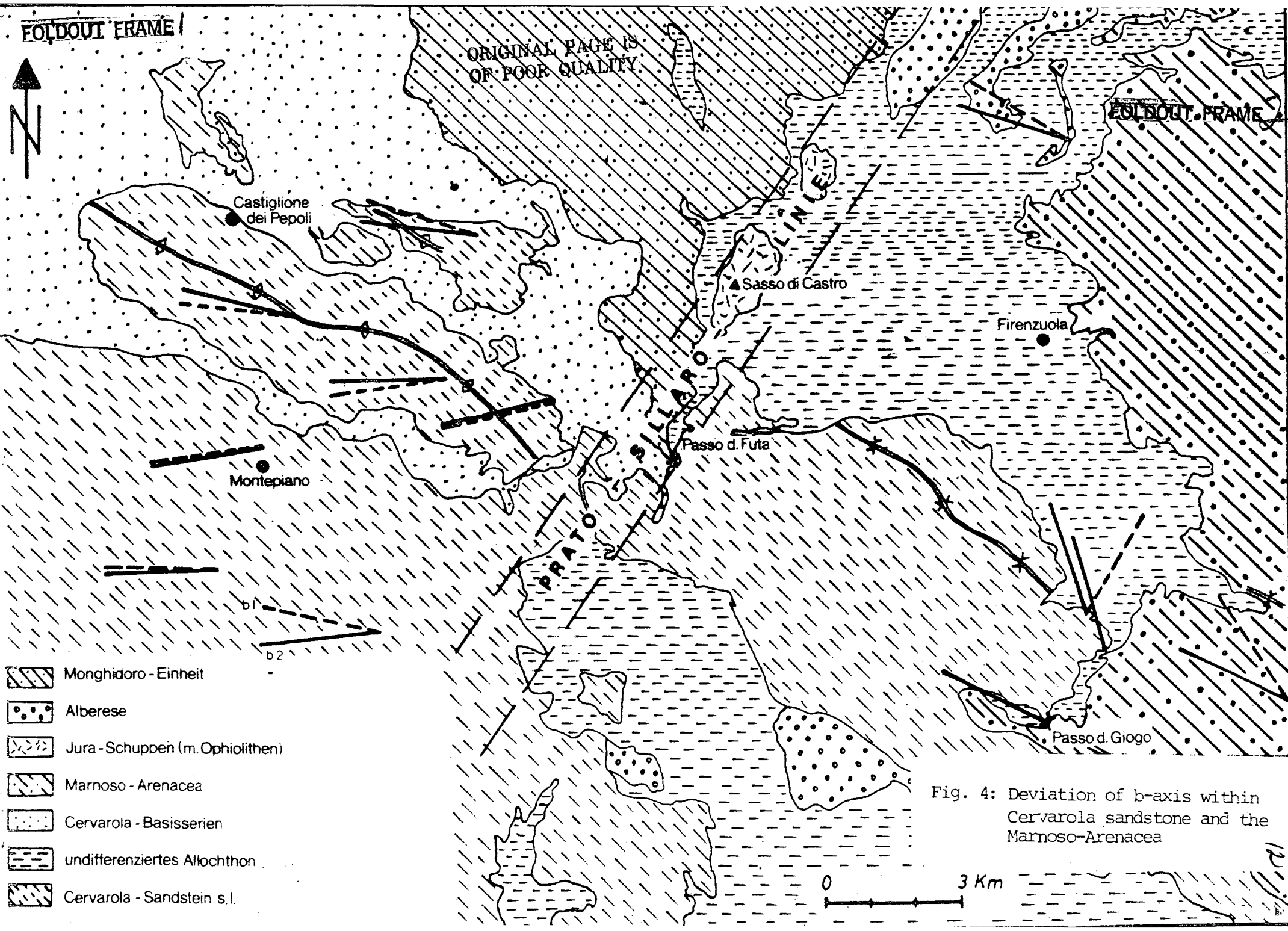
For the Marnoso-Arenacea-formation (South of Prato-Sillaro-Line) $+25°$; $(-15)- (-45°)$ for the Cervarola-Sandstone (North of Prato-Sillaro-Line); $(+35) - (+50°)$ for the Morello-Alberese (immediately in the Prato-Sillaro-Line-Zone), and $\pm$ O for the Macigno of the Mte. Albano (southern prolongation of the Prato-Sillaro-Line?) (see fig. 1). Only at the Passo Giogo the situation is veiled by the main overthrust of the Cervarola-Sandstone.

3. At the localities situated near large faults or fault zones the b_2-axis do not follow the general striking of the main fold structures (fig.4). These deviations can be considered as drag effects indicating the sense of movement occurred on the fault. For example, near the fault marked by the Esino Valley (Gola della Rossa) and its prolongation to the W the axis deflection suggests a dextral movement. In the same way the axis deviations in the Cervarola-Sandstone and the Morello-Alberese near the Prato-Sillaro-Line indicate a sinistral sense of movement. The same movement was postulated by BORTOLOTTI (1968) based on rather intuitive arguments. It has to be mentioned that also at the southern end of the Mte. Albano a similar axis deviation can be observed.

4. Concerning the fact, that the Marnoso-Arenacea-formation cannot be observed in the North of the Prato-Sillaro-Line, bedding plane measurements indicate its plunging with $15°$ to NW.

Castiglione dei Pepoli

Sasso di Castro

Firenzuola

Passo d. Futa

PRATO PULLARO LINIE

Montepiano

b1

b2

Passo d. Giogo

Fig. 4: Deviation of b-axis within Cervarola sandstone and the Marnoso-Arenacea

Monghidoro - Einheit

Alberese

Jura - Schuppen (m. Ophiolithen)

Marnoso - Arenacea

Cervarola - Basisserien

undifferenziertes Allochthon

Cervarola - Sandstein s.l.

0   3 Km

2. Evaluation of Satellite Imagery

On the basis of various data sources a lineation map
was prepared in a scale of 1 : 5oo.ooo. The result is
 iven in fig. 5. This map ony exhibits lineations longer
than 5 km. If detectable the sense of movement was marked
and the major fold axes were traced.

For the Prato-Sillaro-Line and the southern adjacent
profile zones a special map indicating satellite
lineation and in situ mapped faults were prepared in
a scale of 1:1oo.ooo (fig. 6 a and b).

In addition to above interpretation, the lineament
orientation has been systematically plotted over the
entire region of interest (fig. 7).
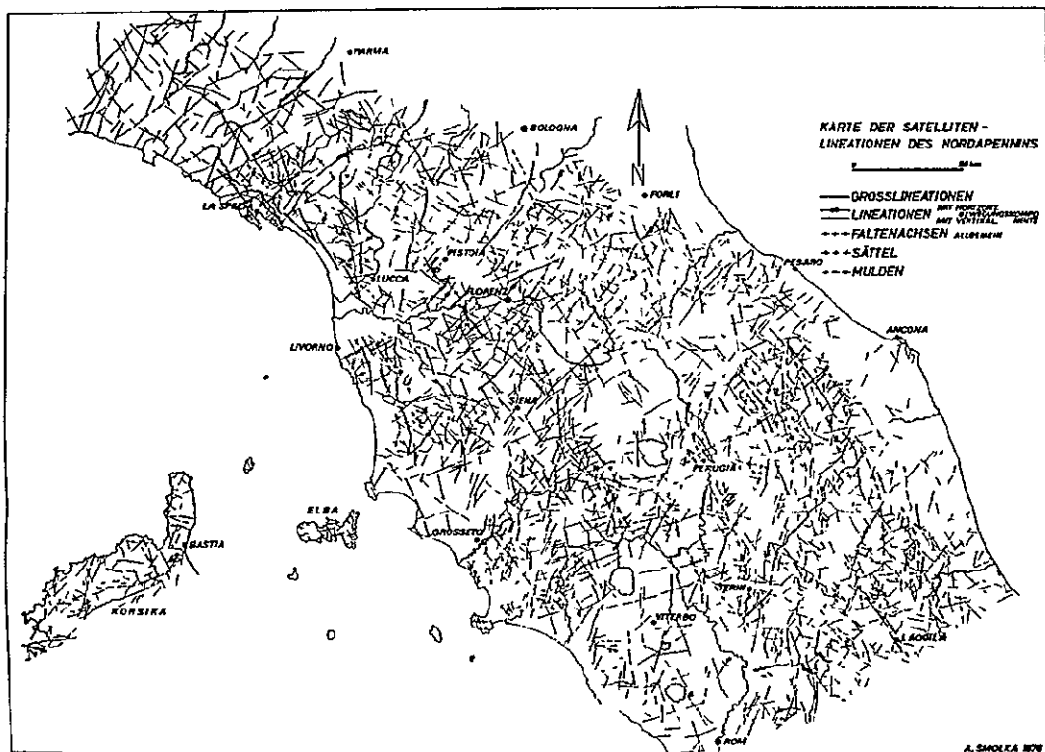
Fig. 5: Map of satellite lineations of the northern Apennine.
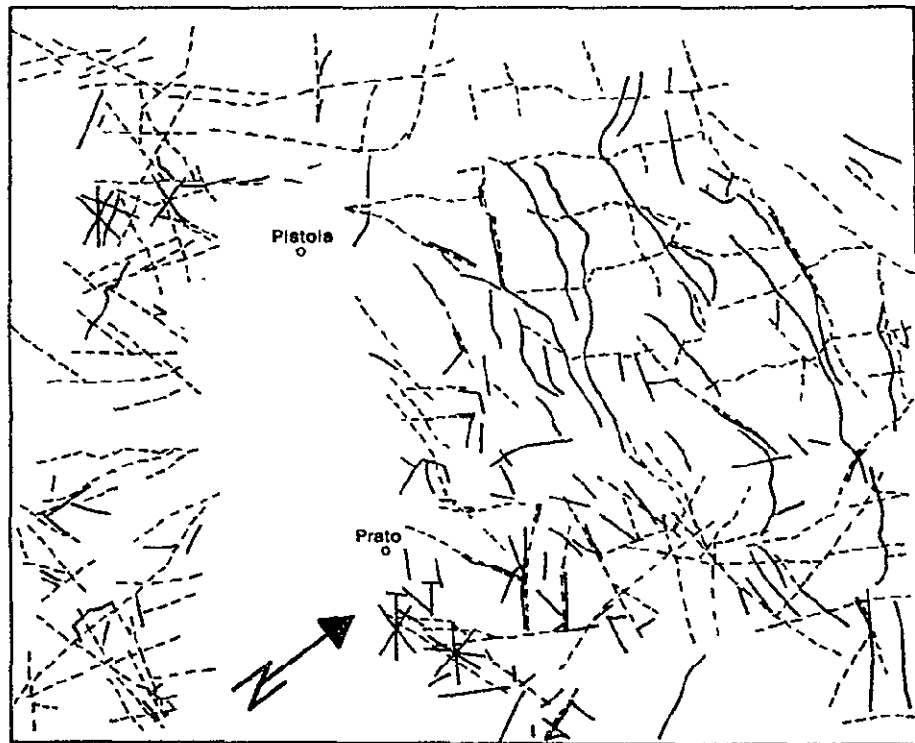
——— Faults mapped in the field (after Carta Geologica
                                    d'Italia, 1:100.000)
——— Satellite lineations

Fig. 6 a: Comparison of mapped faults with satellite
            lineations. Northern profile.
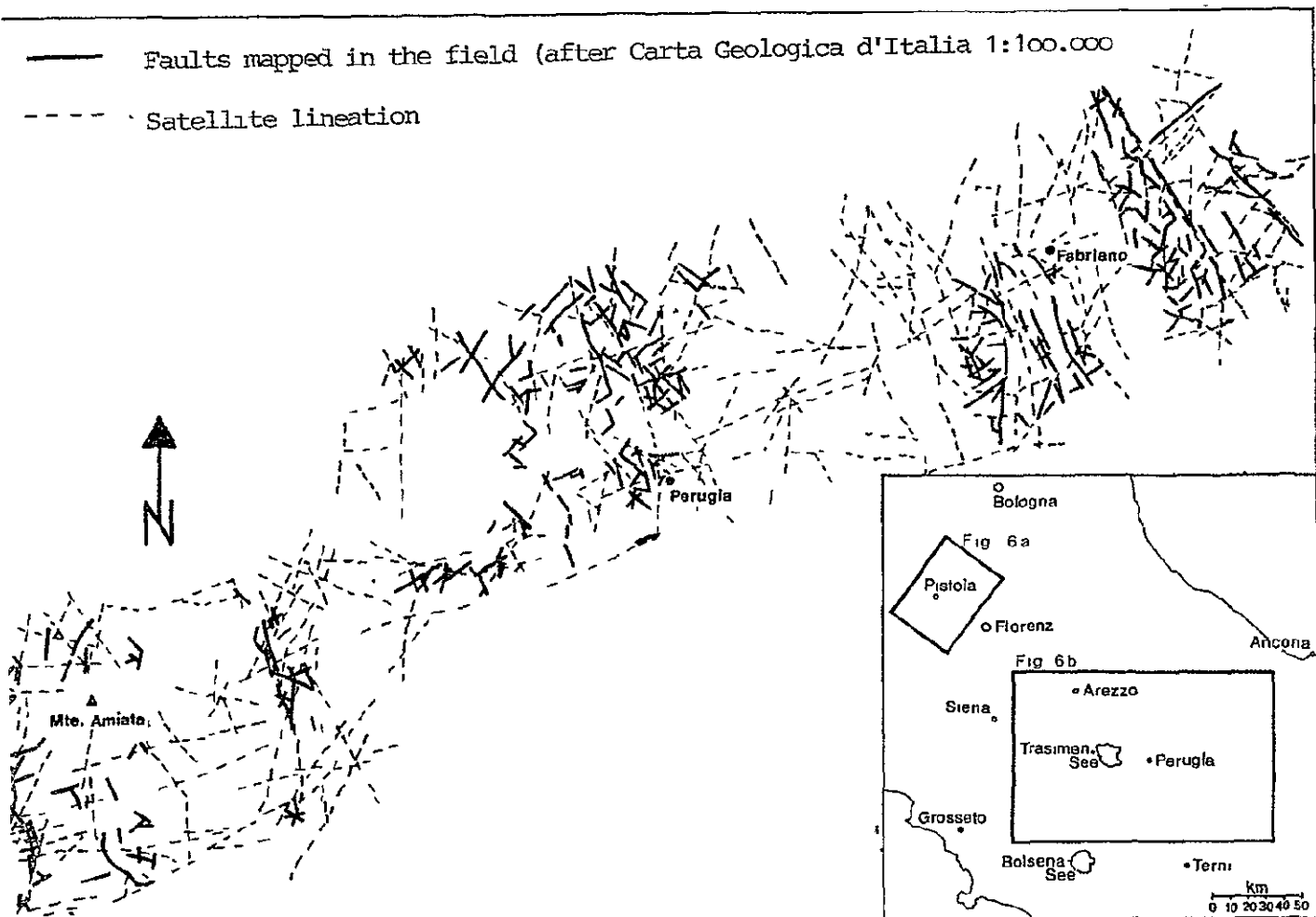
Fig. 6 b: Comparison of faults with satellite
            lineations. Southern profile.
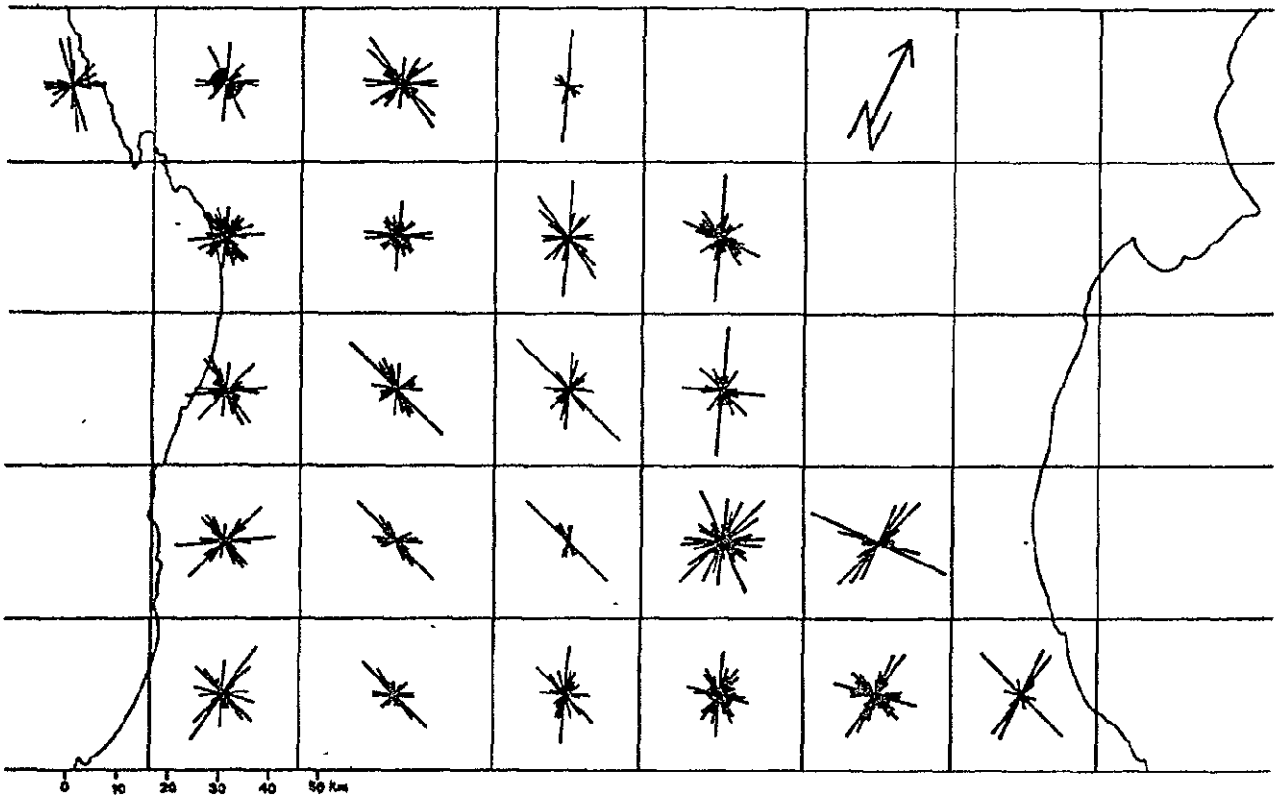
NORTHERN REGION
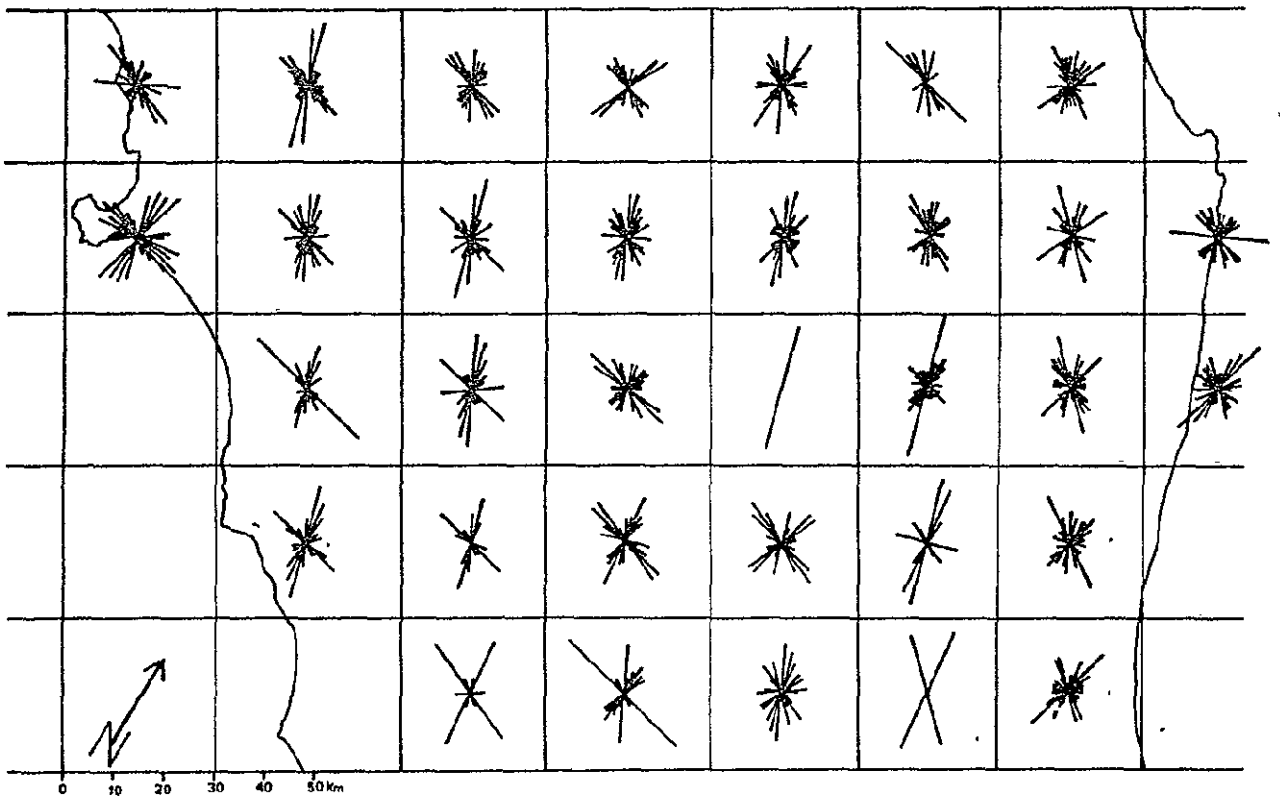
SOUTHERN REGION

Fig. 7: Statistical representation of lineament orientation.

From this work the following results could be obtained hitherto:

1. There are only few lineaments crossing several tectonic units, e.g. the Prato-Sillaro-Line, which touches Macigno, Morello-Alberese, Cervarola-Sandstone, Cantiere-Monghidoro-Unit, Bismantova-Sandstone and the Pliocene. Another lineament begins N of La Spezia and extends to the ENE along the Magra valley, over the Passo di Lagastrello to the Enza valley. This fault crosses the Tuscan formations, the Ligurian Ophiolith-Unit, the Orocco-Caio-Unit. Nearly all the other lineaments, even very long ones as the normal fault accompanying the Cetona-Orsaro-Structure are running within the same tectonic unit or separating diverse tectonic domains (e.g. Ancona-Anzio-Line). These lineations must be interpreted basement structures penetrating the young sedimentary cover.

2. There is neither morphological nor geological evidence for a large fault zone in the Arno valley and its prolongation to the E. On the contrary, the assumption of such a fault zone is in a strong contradiction to the strange turning of the Arno River around the Prato-magno.

3. The following main lineament trends can be derived from fig. 5 and 7.

   - a perpendicular set of lineaments ($65^{\circ}/155^{\circ}$) occupying the whole area mapped. This set corresponds to the antiapenninic and apenninic directions S of the Arno River

   - another perpendicular set of lineaments with a preferred $35^{\circ} - 45^{\circ}$ trend and a subordinated $125^{\circ} - 135^{\circ}$ trend. This set is well developed N of the

Arno River and corresponds to the antiapenninic
and apenninic directions in this region. The 35°
- 45° trend is still prominent in the southern
Tuscany and the Nera valley (Umbria), whereas the
$13o^O$ direction disappears almost totally S of the
Arno River.

- some curved lineaments striking $35o^O$ - 25° (Prato-
  Sillaro-Line, Ancona-Anzio-Line; the long lineation
  beginning in the Mti. di Campiglia and running to
  the eastern border of the mesozoic nucleus of the
  Lima valley; the two large lineaments in the young
  volcanites). These lineations are not strongly
  referred to the orogenic structures. Therefore
  they should have existed already in the pre-apenninic
  crystalline basement. In the Umbrian arc the linea-
  ment pattern is generally more complicated because
  of the bending of the fold axis from NW/SE direction
  to NS direction.

4. Regarding the satellite image the main element of the
   Prato-Sillaro-Line is made up by a well recognizable
   lineament, which follows the Idice valley and limits
   the Cantiere-Monghidoro-Unit to E. The lineament
   prolonges southwards cutting the Morello-Alberese in
   direction of Calenzano.

   The detailed analysis of lineament directions for the
   Prato-Sillaro-Line and the adjacent areas shows some
   interesting aspects (fig. 8).

   - in the Mte. Albano the antiapenninic direction is
     still predominating in comparison to the Prato-
     Sillaro-Line direction ($2o^O$)

   - in the region S of the Cervarola-overthrust the
     Prato-Sillaro-Line direction becomes much more

prominent than the antiapenninic one

- N of the Cervarola-overthrust the Prato-Sillaro-
  Line direction changes to 5 - 1o^O striking.

In all the three zones subordinated maxima are developed
at 75°, 95° and 16o^O. The first two directions have to
be considered as shears to the 4o^O- and 65° directions
respectively. It is very characteristic that only these
shears are developed, which allow sinistral movements.
The 16o^O trend is common in the entire Northern Apennines.

Bologna O

La Spezia

I

II

III

O Florenz

Livorno

km
0 10 20 30 40 50

N
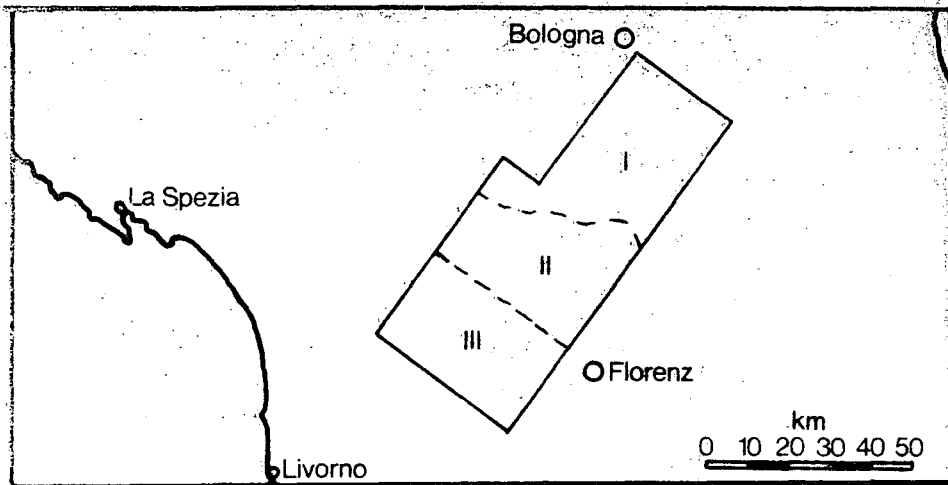
N CERVAROLA - AUFSCHIEBUNG (I)   S CERVAROLA - AUFSCHIEBUNG (II)   MTE.ALBANO (III)

Generalstreichen

Fig. 8

20
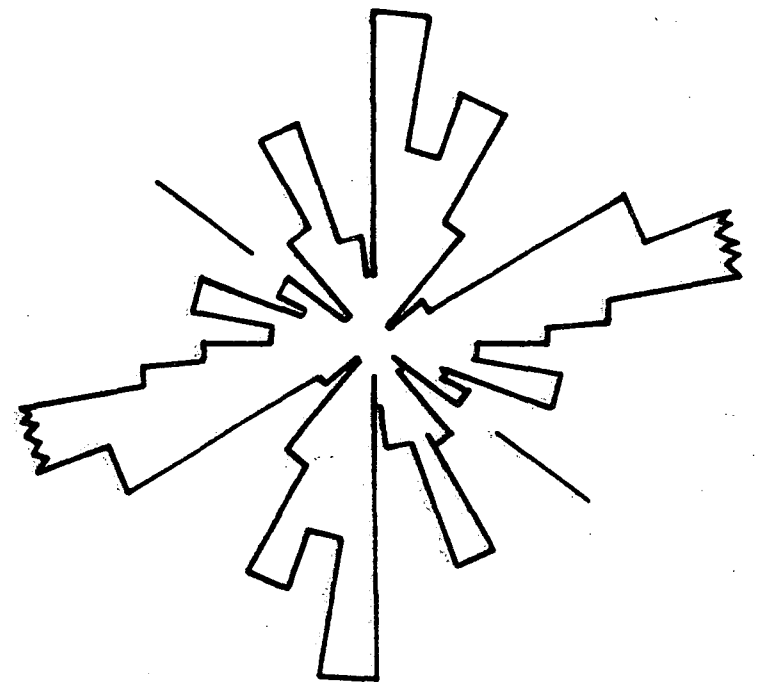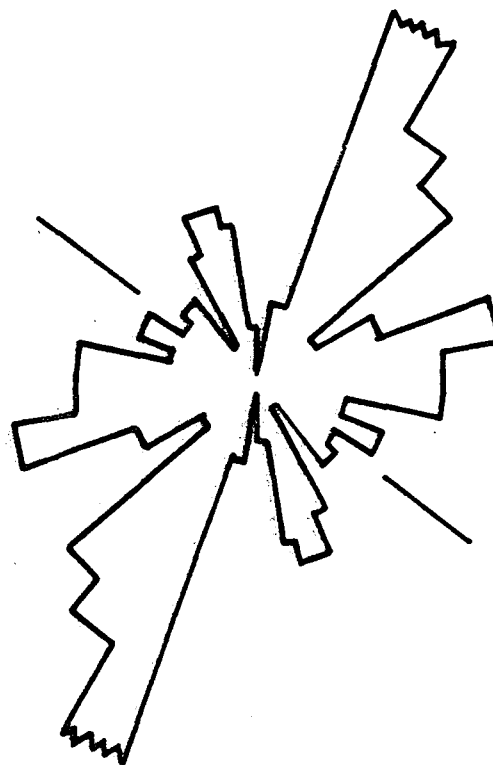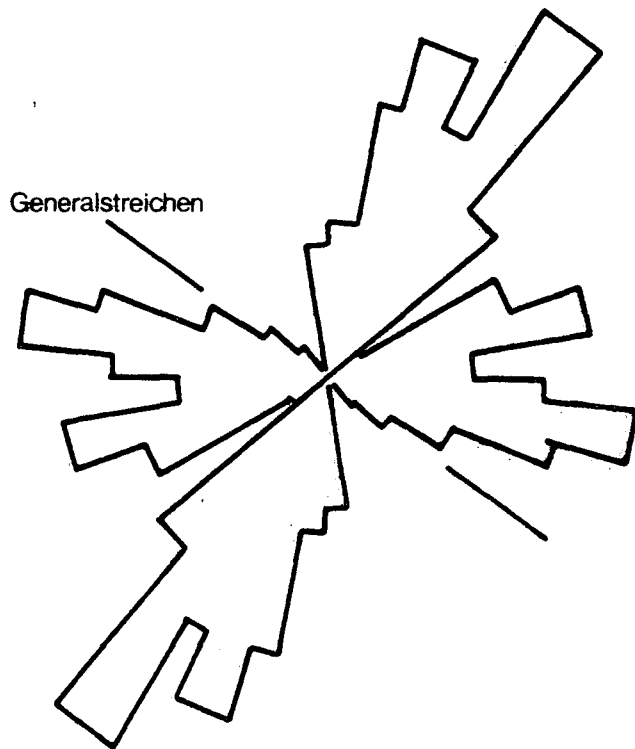
3. Conclusions

The clockwise rotation of the Tuscan-Umbrian region
stated in a previous publication (BODECHTEL & NITHACK
1975) can be regarded as well established by tectonic
field measurements and satellite image interpretation.
However, it has been proved by new results that the
northern boundary of the rotated block is not given by
the "Arno fault zone".
The part of the Arno fault in the proposed rotation
model is taken over by the Prato-Sillaro-Line. From
this is resulting a change in the shape of the rotated
block, which represents a parallelogram instead of a
triangle. Consequently, using the terms of the physics
of solids the movement causing the rotation of the b_1-
axes has to be described as torsion rather than as
rotation. The horizontal movement component on the
Ancona-Anzio-Line is considered rather small. Concerning
the continuation of the Prato-Sillaro-Line to the SW the
sinistral faults and the axis-deviations in the southern
Mte. Albano region suggest a prolongation of the fault
zone to the Tyrrhenian coast near Leghorn with slightly
curved trend. The existence of two lineation systems
visible on the satellite images ($4o/13o^{\circ}$ and $65/155^{\circ}$
resp.) agrees well with the conception of clockwise
rotation of the block S of the Prato-Sillaro-Line.
Considering the extension of these two systems to N
of the Prato-Sillaro-Line, BODECHTEL & NITHACK (1975)
inferred a similar rotation of this northern block.
However, such movement should be confirmed by additional
field work.

It has to be emphasized, that the conception proposed
here does not oppose to the idea of the anticlockwise
rotation of Italy (ALVAREZ 1974, 1976; SOFFEL 1974, 1975).
This rotation finished in the Eocene according to SOFFEL.

The above described clockwise torsion, however, took
place between the two main orogenic phases in the
Northern Apennines, that is between Aquitanian and
Tortonian after BALDACCI et al. (1966).

B. Comparison of Photo Lineations Derived from Satellite
   Images and Aerial Photographs –
   A photogeological evaluation of Calabria and Sicily.

The entire southern part of Italy with an area of approximately
4900 km^2 (fig. 9) was mapped on the basis of MSS bands 5 and 7.
The lineaments interpreted were displayed at a scale of
1:500.000 and statistically evaluated. By this a total of
12.500 elements with an overall length of 6500 km could be
digitally registered. Some major lineations could be optimally
derived from prints in a scale of 1:1.000.000 (fig. 10).
Besides the interpretation of Landsat images aerial photographs
(27 stereo-pairs, scale 1:10.000 and 1:20.000 were evaluated
under same objectives.

Results.

The interpretation of the satellite images has clearly shown
that above major lineations are accompanied by parallel
striking minor elements. They occur either in the direct
vicinity or as parallel elements at greater distances. The
interelationship between major and minor lineations is strongly
indicating the existance of large fracture zones described by
CASSINIS et al.

The statistical representation of all counted lineations
clearly reveals 3 directional maxima to N, NE, and SE (fig. 10).
The evaluation on the basis of areal photographs shows a
strong similarity between the directional distribution of
lineation detectable on the island of Vulcano (fig. 10 and
11) with those from the Italian peninsula and Sicily. A
further correlation can be observed between the major linea-
ment directions and the areal distribution of the eolian
islands.
The islands Salina Paraneo and Stromboli are arranged along
the NE-SW striking lineament maximum whereas Salina, Lipari
and Vulcano indicate above NW-SE direction. This phenomenon

Fig. 9: Landsat photo mosaic of Calabria and Sicily.
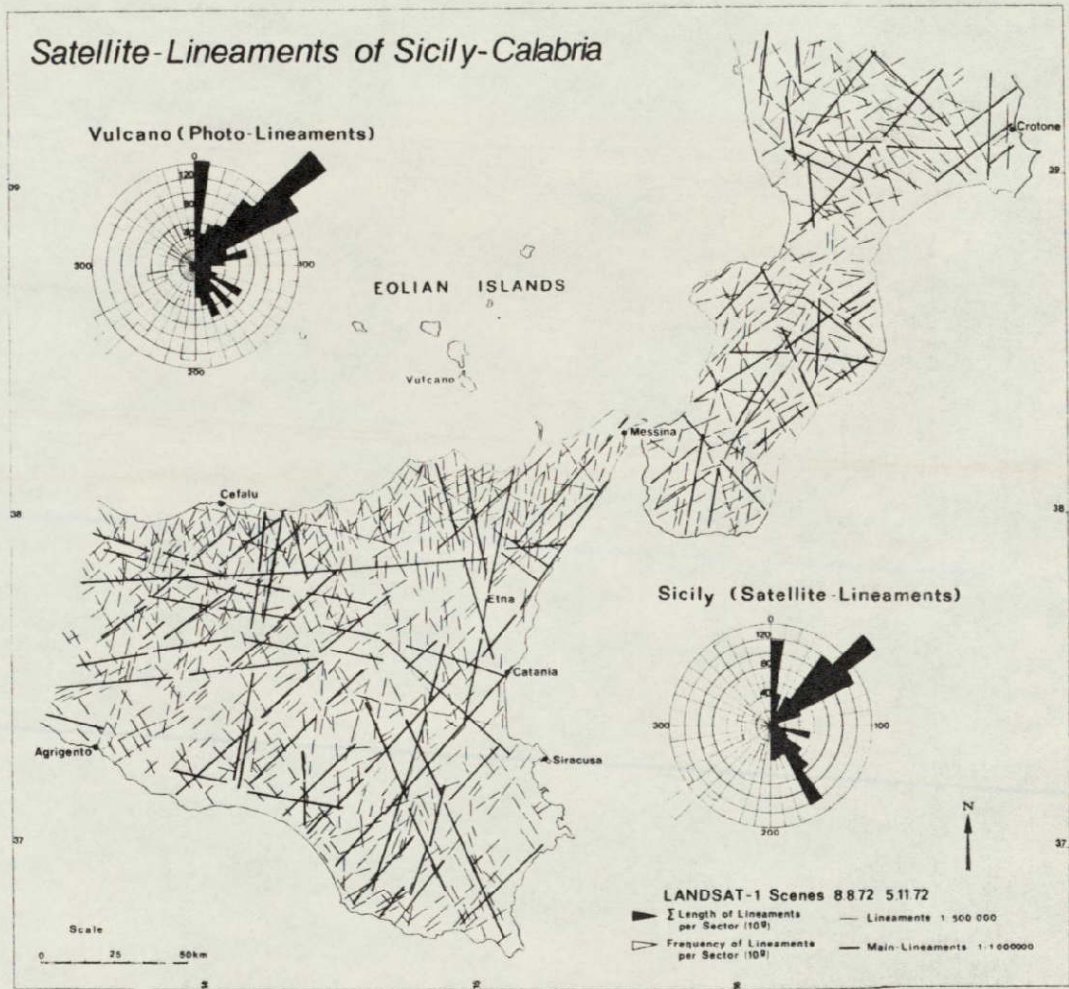
Fig. 1o: Photolineaments map derived from Landsat images of various scales.
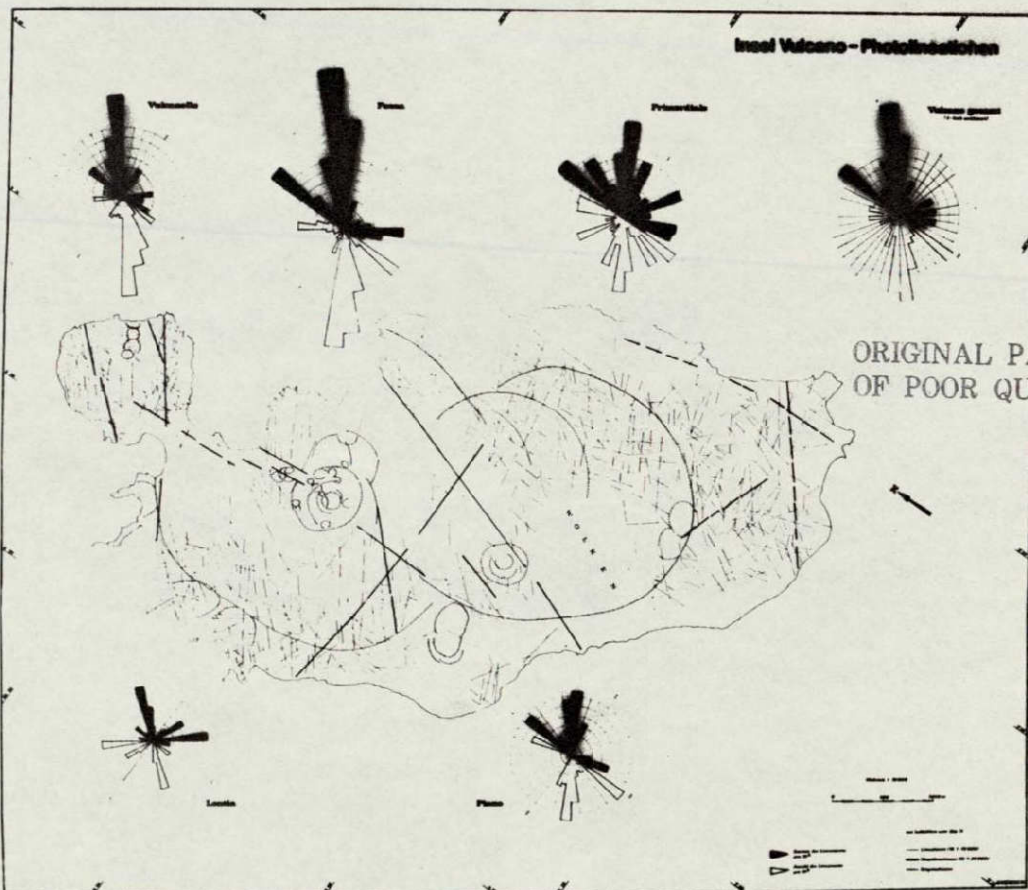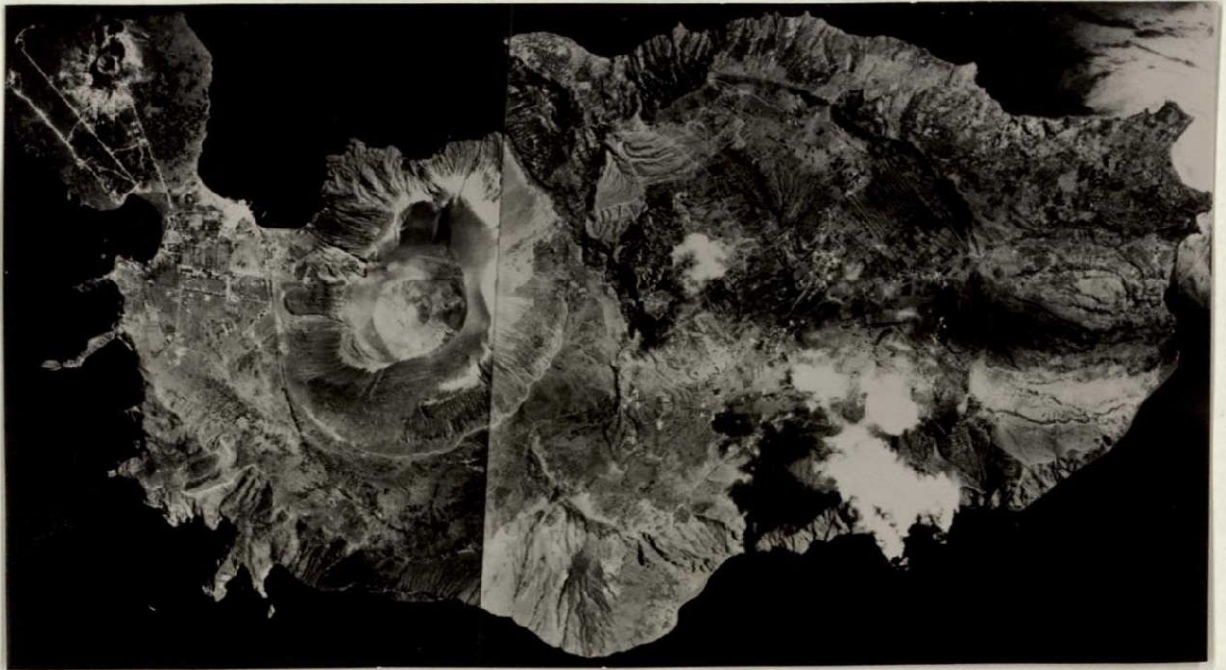
Fig. 11: Photomosaic of Vulcano and photolineament evaluation.

characterizes the relationship of the volcanism with major
fracture systems of the Tyrrhenian block.
The study demonstrated that the lineations derived from
satellite images indicate a simplified structural pattern
which is of special significance in defining the young
fault tectonics of the southern Tyrrhenian block. The
major directions of photo- and satellite lineaments coin-
cide with seismotectonic results in the central mediterranean
area and confirm also earlier results.

C. The Significance of Lineament Techniques for Practical
   Application in the North German Coal District.

1. Introduction

The coal reservoires in the southern and central part of the
"Rheinisch-Westfälische" Coal Mining Region are far reaching
exhausted. In order to keep up with the coal output, mining
activities have to be extended to the northern part of the
Ruhr Varlley. In this area the coal bearing layers are
covered by mighty overlaying formations. Today prospection
in this area is being carried out by drillings and seismo-
logical measurements above ground. Seismometer profiles
deliver primarely information on the position of the coal
bearing layers. In addition to this, large tectonical fracture
systems can be detected, unter certain circumstances along the
profiles.

Due to the basis of drillings only pointwise information on
the petrography, the stratigraphy and the position of coal
bearing layers is obtainable.
Clues on the fracture tectonical situation however can only
be obtained if faults are sunk through.

Because of the lacking synoptic information obtainable by
above prospection techniques the application of further
methods such as photo-lineament evaluations is regarded to
be of specific interest. Therefore, the following investigation
has been directed towards an evaluation of the feasibility of
"satellite lineaments " in order to describe the tectonical
situation of the northern not yet explored mining region.

The area of interest (fig. 12) has been subdivided into 6
sub areas (fig. 13) which were individually investigated on
the basis of Landsat frames representing various seasons and
including Landsat-1 bulk   products and Landsat-2 enhanced
displays.

Rhein
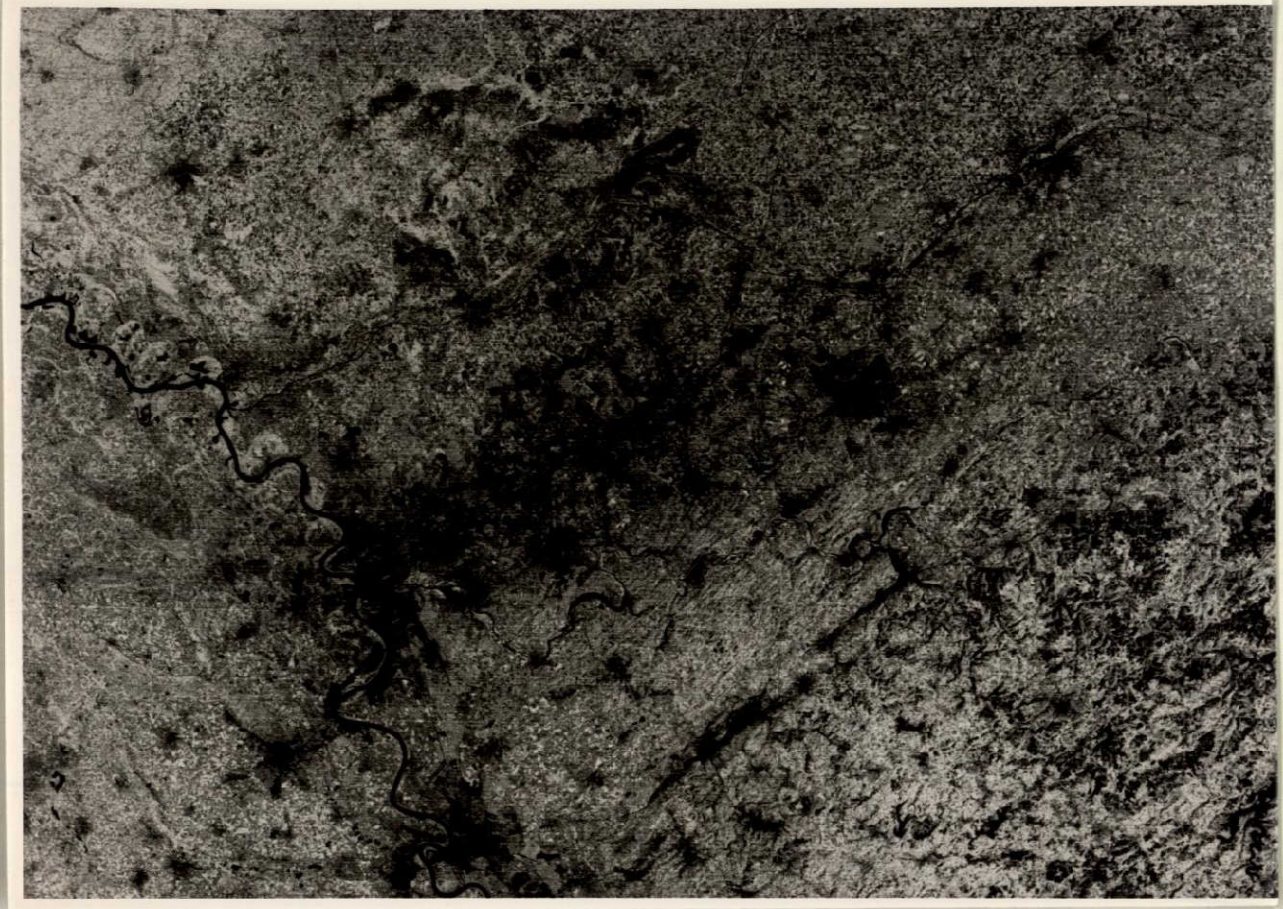
Düsseldorf

Scale   1 : 67o ooo

Fig. 12:   Computer enhanced display of Landsat MSS
           exhibiting the north German coal mining area
           (Ruhr Valley).
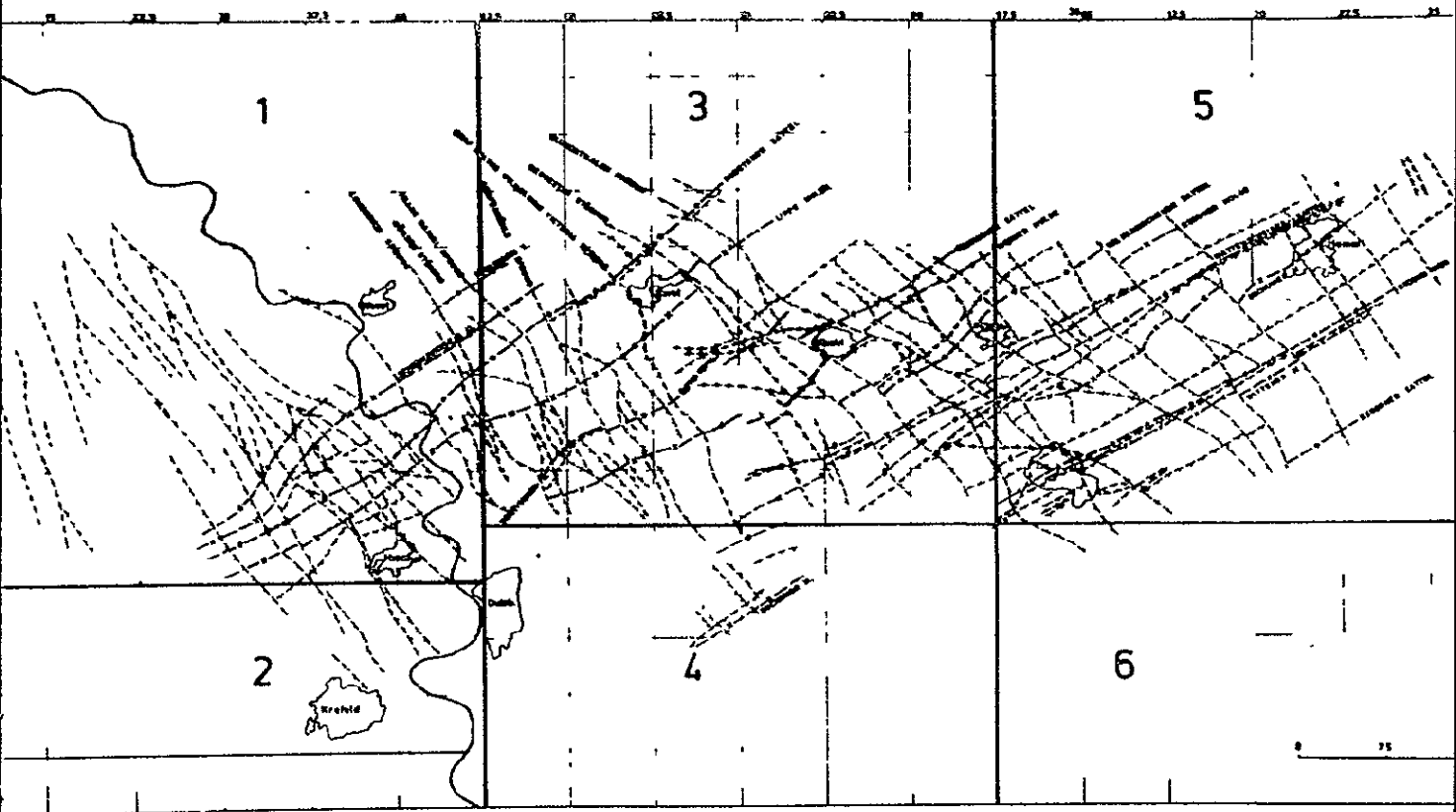
Fig. 13: Map of the major tectonical situation of the
Ruhr-Valley with sub areas investigated individually.

In order to investigate the significance of the mapped
photolineations with respect to the tectonical inventory
obtained by intensive in situ measurements below ground
(photogrammetric joint analysis), all photolineations which
could be correlated to the known tectonical systems were
indicated by special signatures (fig. 14 a,b).

An explanation of the signatures is given by fig. 15.
The graphs indicate that the lineations could be inter-
preted with respect to two tectonical fracture systems -
the B 1 -shear system (——) and the B 2 system (—·—)
which is belonging to the asturian folding phase.
Further indices represent lineations parallel to the
system's B-axis ····》· and B-parallel striking upthrusts
or dip slip faults. Perpenticular to B striking lineations
in direction of cross cutting dip slip faults and fractures
are indicated by····》 . The remaining elements ···· represent
transcurrent fault systems or diagonal shear ruptures typical
for the tectonical systems of the Ruhr Valley.

The rose diagram of fig. 16 is a synoptic representation of
all mapped photolineations (are 1 - 6) in combination with
the striking directions of the main elements of the tectonical
systems B_1 and B_2.
The fare reaching correspondence of photolineations with the
major tectonical fracture systems of the Ruhr Valley indicates
the high potential of linear features for the description of
subsurfacial tectonics.

In the following a detailed lineament tectonical description
of the various subareas demonstrated by fig. 13 is given.
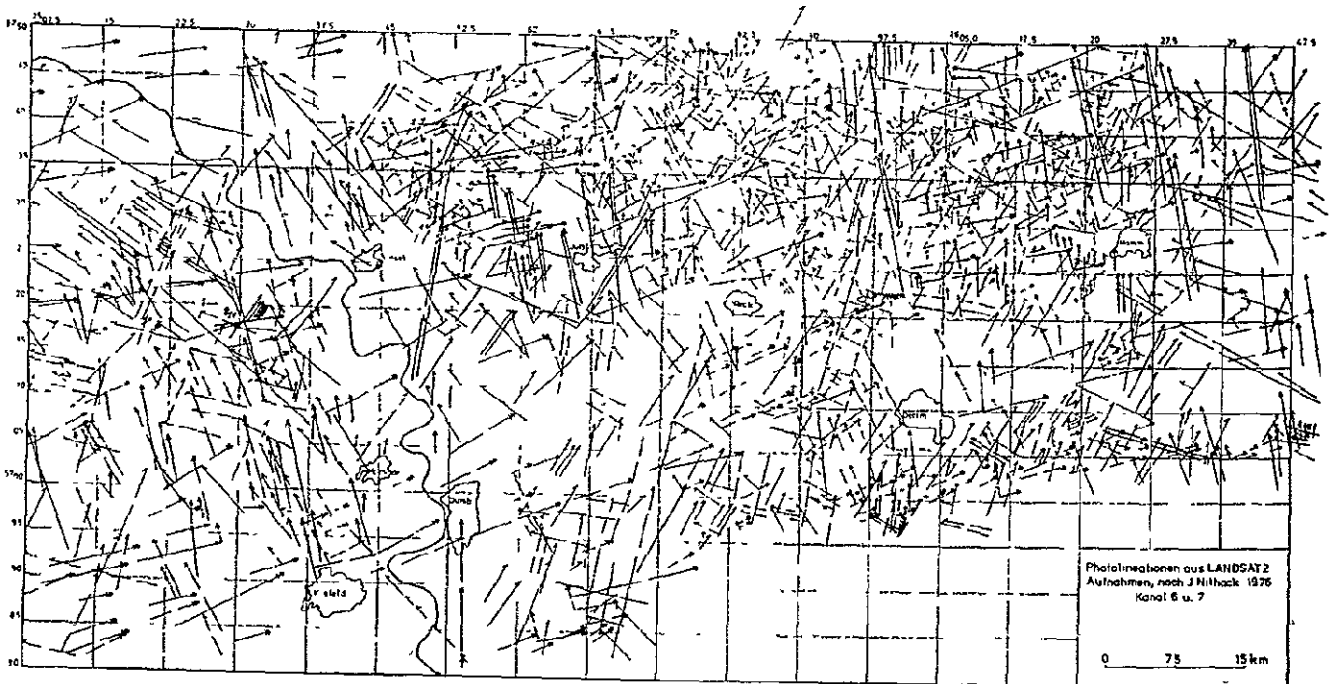
ORIGINAL PAGE IS
OF POOR QUALITY
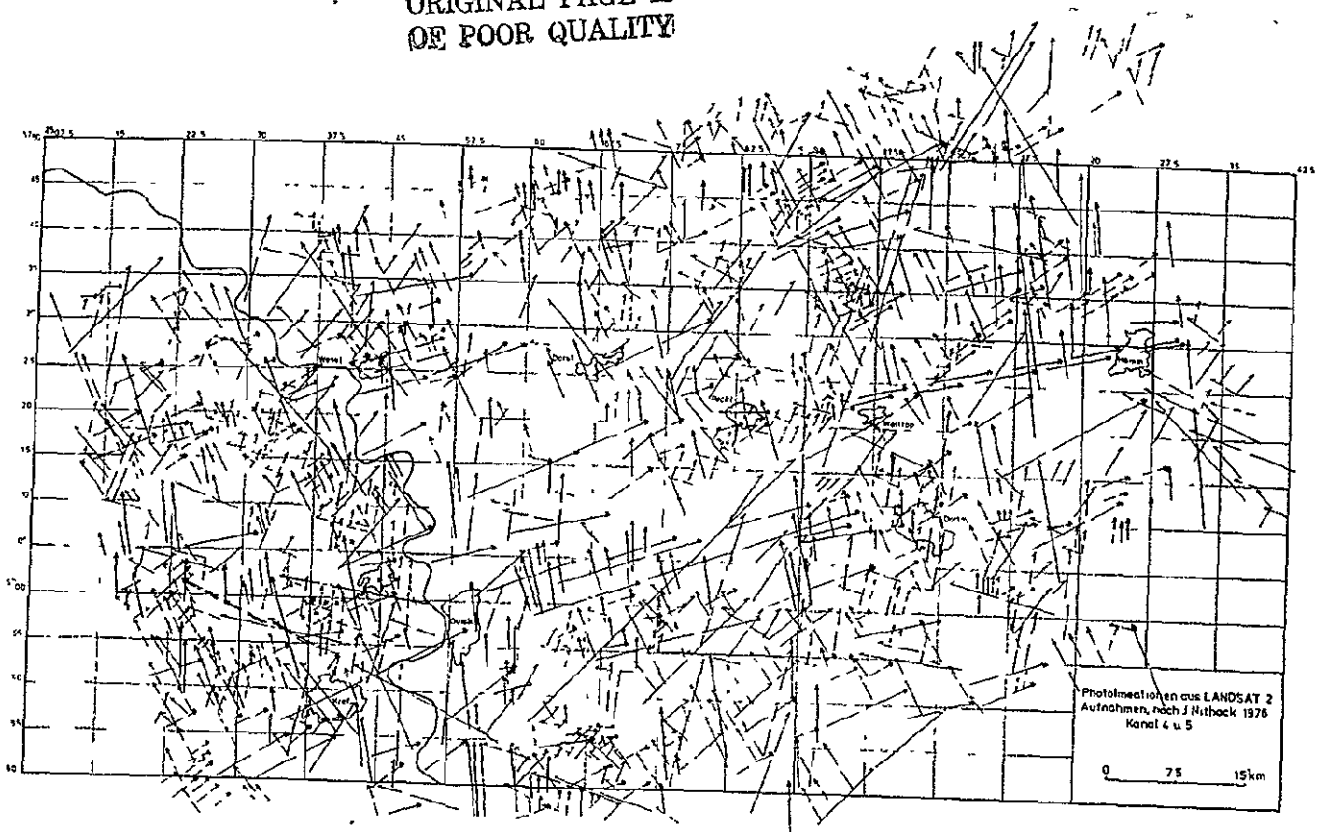
Fig. 14 a/b: Photo lineament maps of the Ruhr Valley derived
from MSS bands 6/7 and 4/5 resp.
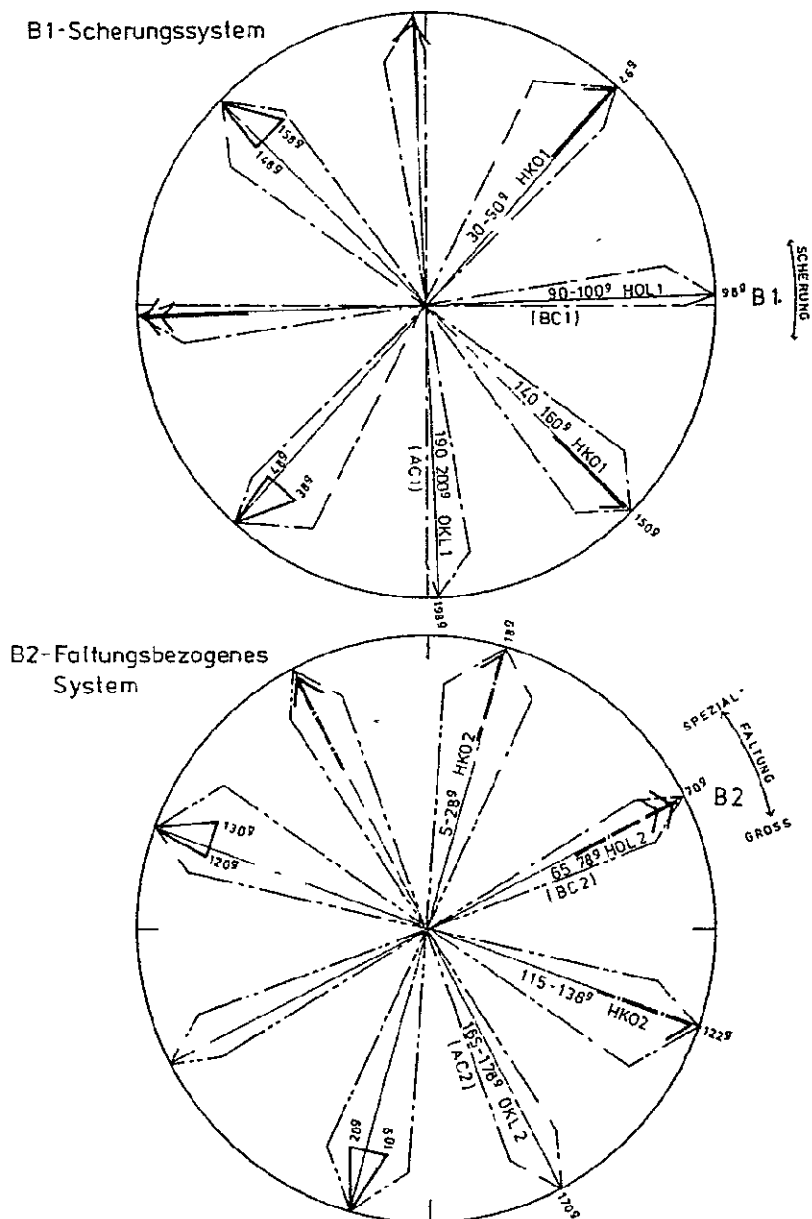
Fig. 15: Tectonical inventory of the Ruhr Valley. B1-shear
         system and B2 folding system with symbols indicating
         corresponding lineaments.

Fig. 16: Photo lineations of regions 1 - 6 in comparison with major tectonical systems B_1 B_2 (signatures around the circle).

2. Photolineations of the norther part of the Niederrhein
(Area 1)

As it can be derived from the maps of figure 14 a,b and the
rose diagram of fig. 17 area 1 is mainly characterized by
lineations striking with 190g (oKL1). Additional diagonal
striking shear structures HKo1 can be derived with two
crossings. These lineations indicate fracture systems of
the carbon layers, which have been active beyond the Meso-
zoicum.
In this area B_1-parallel striking elements are under-
represented.
The rose diagrams (fig. 18 a,b) obtained by analysing
computer enhanced Landsat-2 images deliver additional infor-
mation especially on elements indicating the fracture system
of the asturian folding phase (B_2).
A comparison of the rose diagrams exhibited by fig. 18 a,b
demonstrates a special phenomenon. MSS bands 6 and 7 deliver
primarily good possibilities to extract lineations belonging
to the B_1 system with NS striking elements accompanied by
HKO-1 shear crossings (Fig. 18 a). MSS bands 4 and 5 mainly
reveal those lineaments which characterize the B-2 system
with a strong maximum of OK12 elements perpenticular to the
direction of the B_2-axis (fig. 18 b) The same phenomenon could
also be observed in other subregions where the coal bearing
layers are covered with mighty overlaying formations.

MSS bands 6 and 7 exhibit more information on the drainage
system which seems to be primarilly controlled by structures
belonging to the earlier tectonical system (B 1).
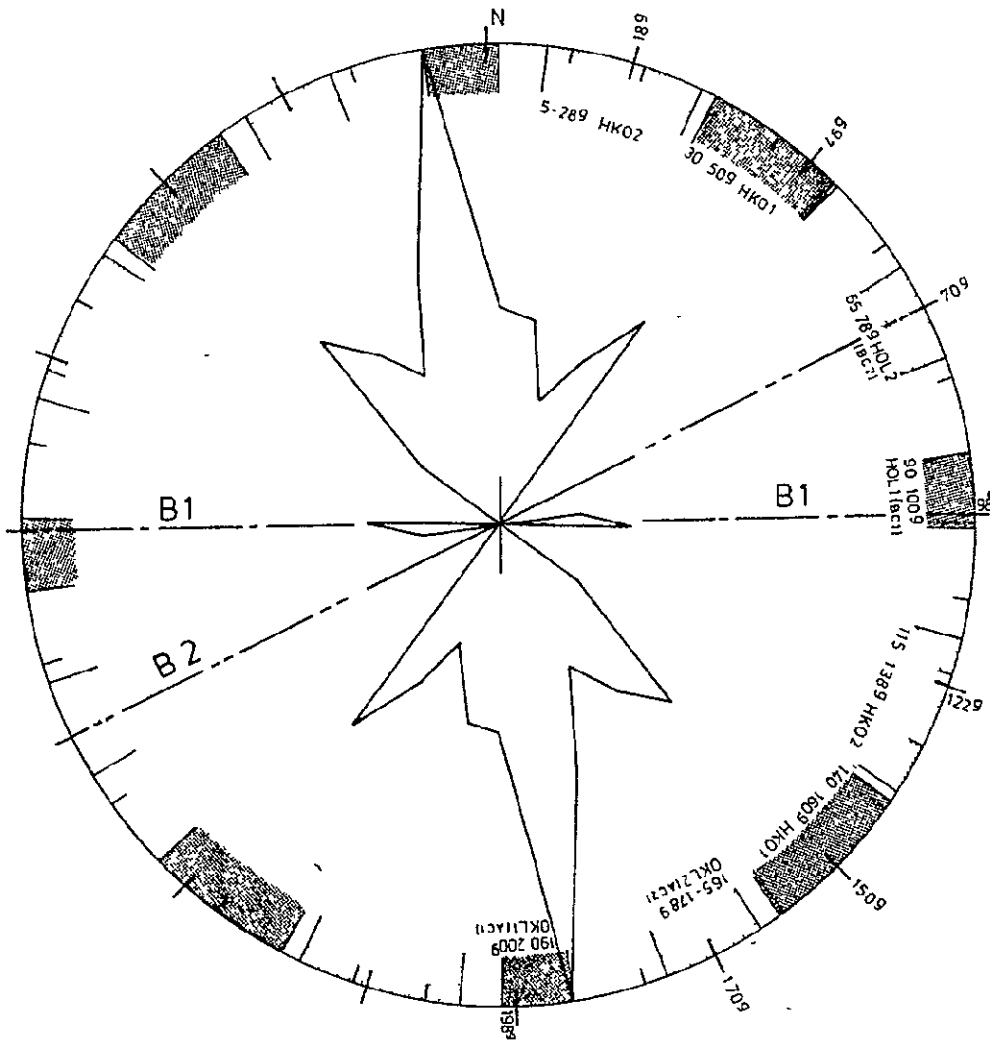
Fig. 17: Lineament distribution Area 1.
The major lineament orientation is NS
indication OKl 1.
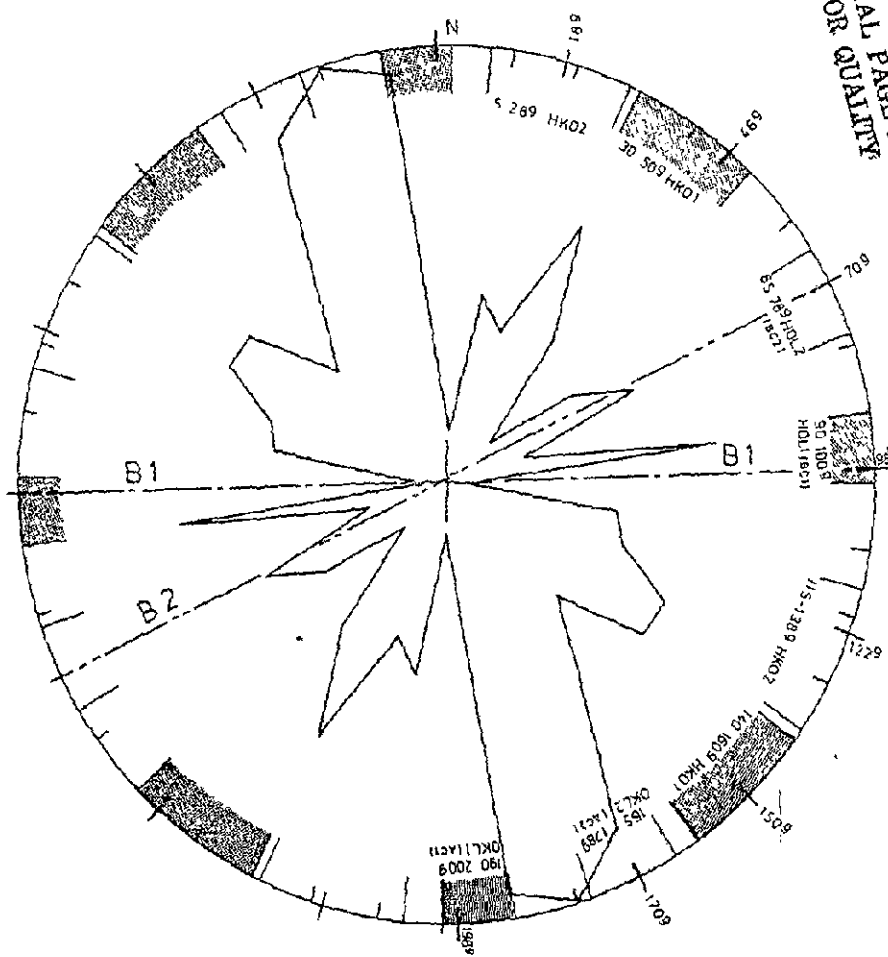
Fig. 18 a: Lineations derived from MSS
bands 6 and 7.
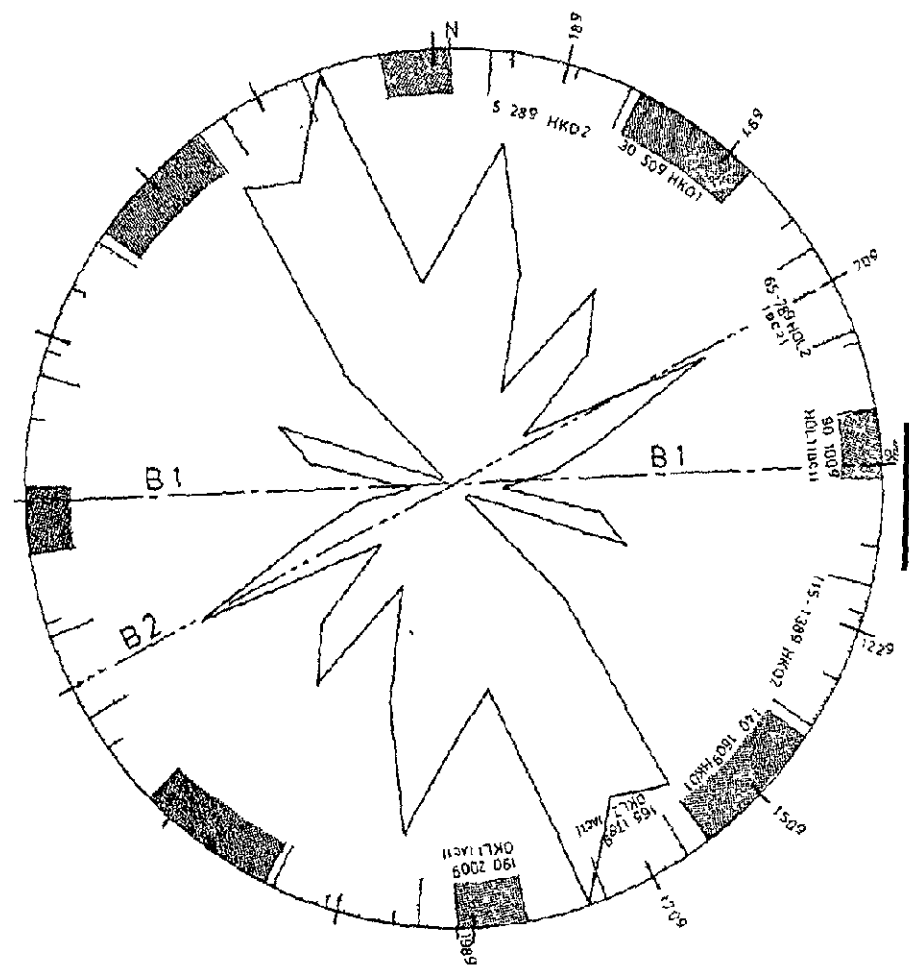
Fig. 18 b: Lineations derived from MSS
bands 4 and 5.

3. Photolineations of the northern Ruhr Valley
   (Area 3)

This area covers the region of mining activities and its
zone in front of the face.
The rose diagrams derived from Landsat-1 (fig. 19 a) (bulk
product) indicates nearly the same situation as for area 1 with
dominant NS striking (OK1-1) linear features. The interpretation
on the basis of the enhanced Landsat-2 image again demon-
strates a much higher degree of directional distributions
indicating the presence of the B_2 system (fig. 19 b). Of
special interest is the large number of lineations which
follow the general direction of the B_2-axis (= fold axis)
in connection with those lineaments striking perpenticular
(OK12).
Photogrammetric measurements below ground have shown that
above situation is typical for this area.
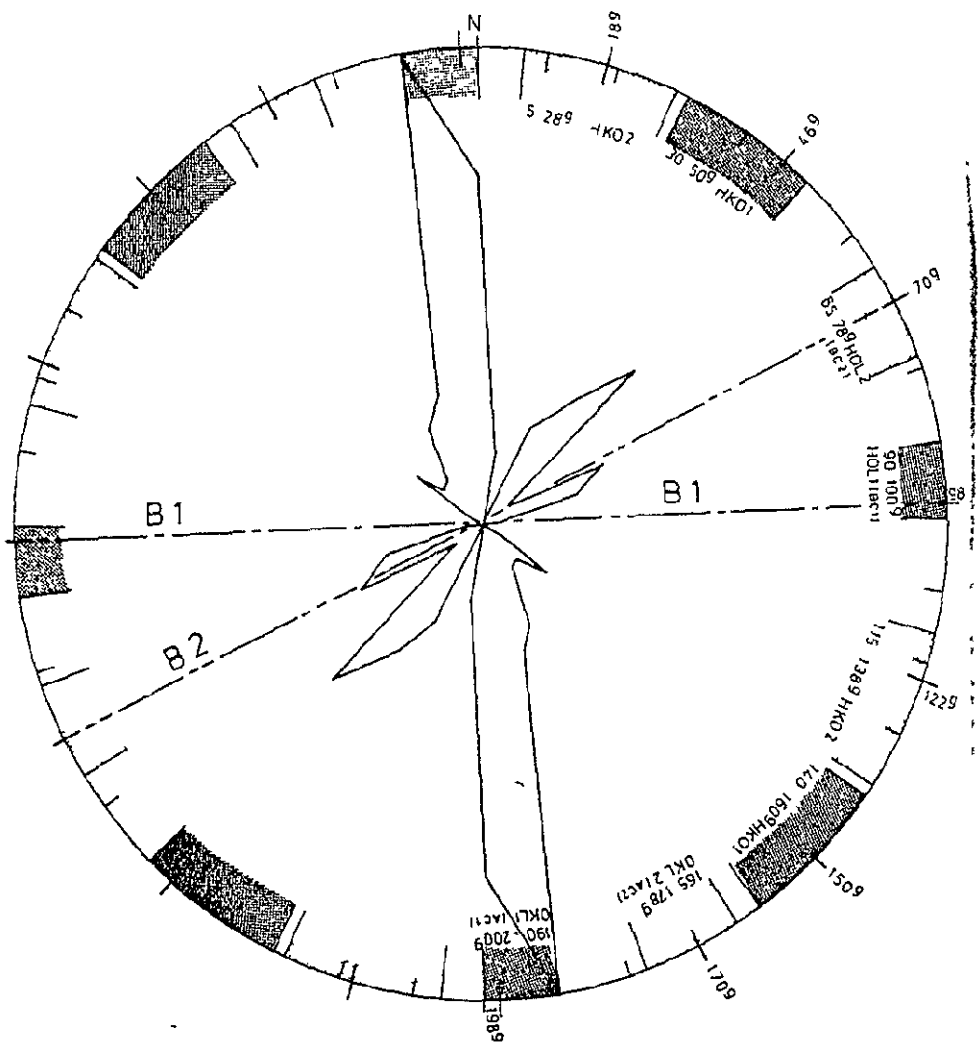
Fig. 19 a: Photolineation (Area 3) derived from Landsat-1 bulk products
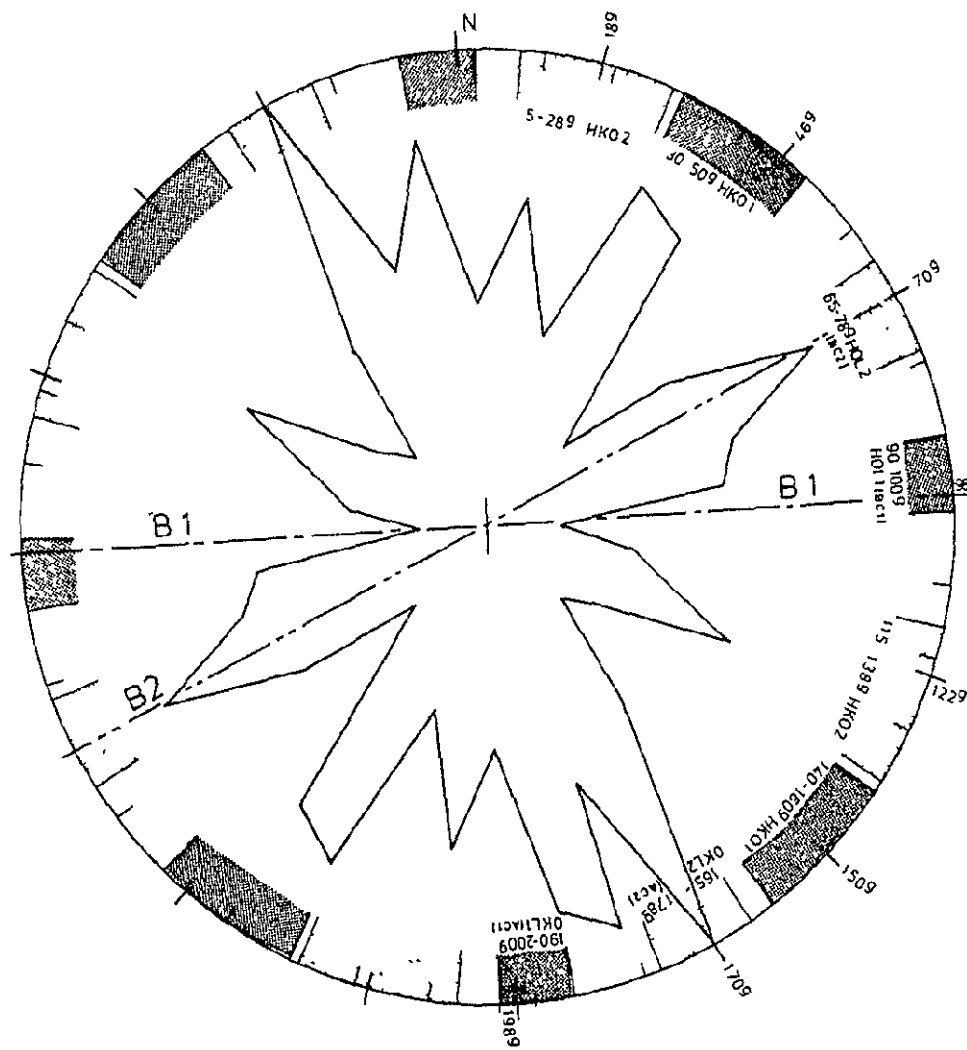
Fig. 19 b: Photolineations derived from Landsat-2. Computer enhanced images

4. Photolineations of the eastern Ruhr-Valley
    (Area 5)

The rose diagram of this area (fig. 2o) reveals besides the
N/S striking elements HoL-parallel lineations which strike
with 9o^g. In addition NE-, SW striking lineations represent
diagonal shear structures (HKo1).

The weak maxima between 12o and 13o^g can be related to shear
systems (HKo2) and 17o^g cross fractures which belong to the
tectonic fabric of the folding phase which is not very
expressed in this area.

5. Photolineations of the southern Ruhr-Valley
    (Area 4)

Area 4 ist characterized by an intensive folding of the coal
layers. In correspondence to this tectonical situation,
photolineations which occur parallel to the B2 system (folding
system), are more expressed as those lineaments which indicate
the B 1 system. This fact can be clearly demonstrated by the
diagrams of fig 21.
Thus, these diagrams do not only represent north-south
striking elements but also diagonal shear fractures indicating
Ho2 and oKL2 tectonical elements.
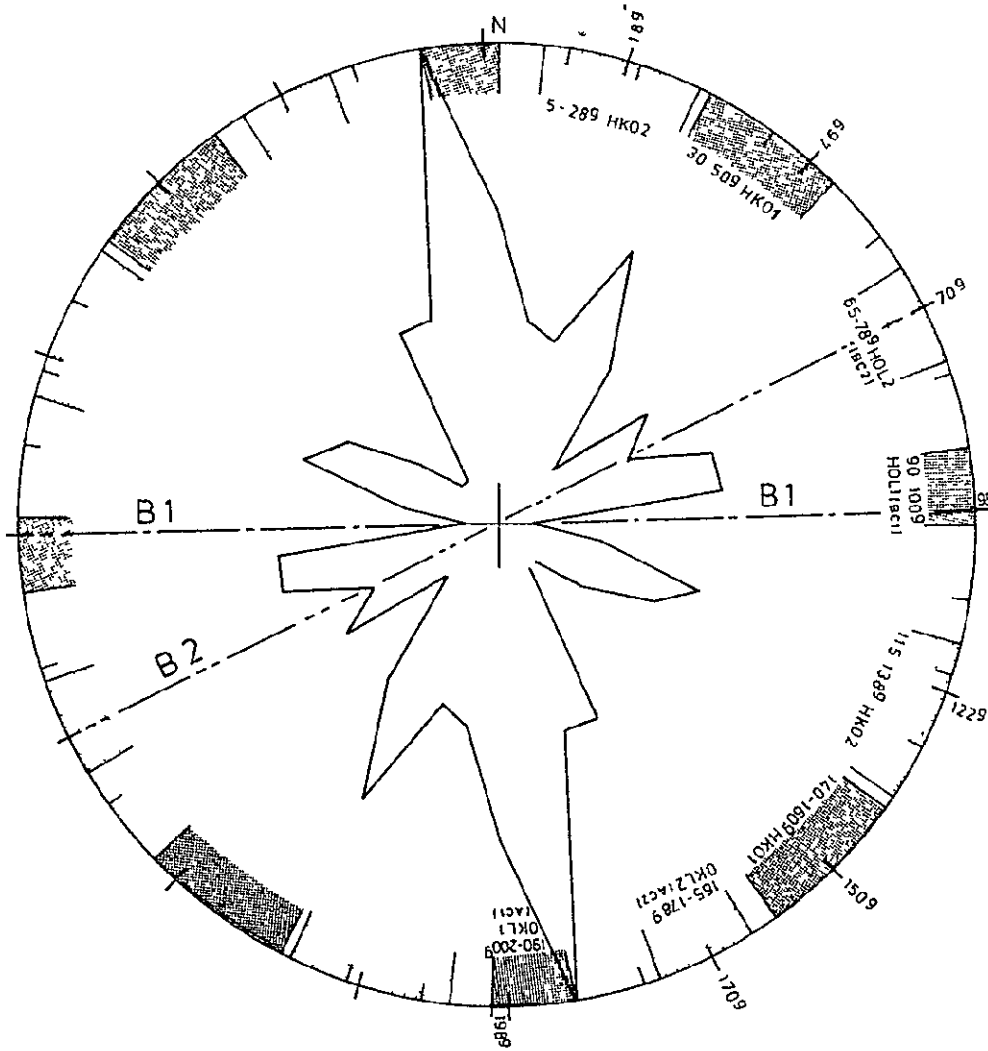
Fig. 2o: Photolineation (area 5)

Fig. 21: Photolineation (area 4)

6. Density maps

Besides the statistical representation of photolineation
on the basis of rose diagrams, special maps, indicating
the density of lineation and the directions of "density
axis" were produced.
The map of fig. 22 represents the density distribution of
lineations on the basis of 5 x 5 km. The distribution of
the maxima can be related to the major tectonic divisions
in EW direction as it has been described by KIENOW (1955).
In addition to that, the axis of zones with maximum density
indicate NS occuring lineament zones which are characterized
by intensive expressed fracture systems. The axis relating
to density minima can be correlated with diagonal shearing
zones (fig. 23).
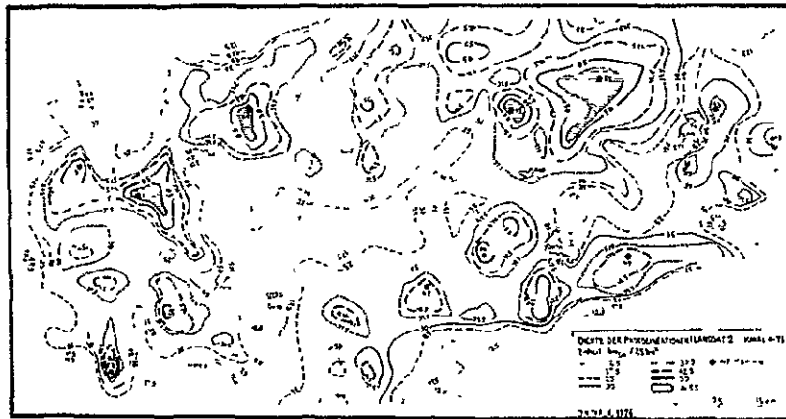
Fig. 22: Density map of photolineations (see also Fig. 12, 13 and 14)
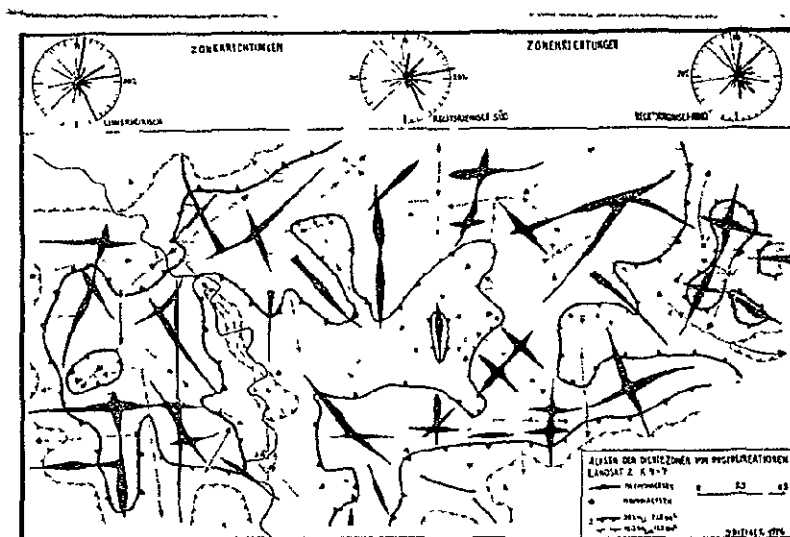
Fig. 23: Axis of zones with maximum(⟋) and minimum(⋯ ➤)lineament
densities

7. Conclusion

Above demonstrated examples are derived from ongoing
intensive investigations which are being carried out in
the mining district of the Ruhr-Valley. A detailed comparison
of photolineations with existing fracture systems has been
possible because of the excellent tectonical inventory which
is a result of a long term measurement program based on
in situ measurements below ground. The additional appli-
cation of Landsat imagery has definitely shown that there
exists a close relationship between photolineations and the
tectonical deformation plan of the Ruhr Valley. This corres-
ponds not only to the distribution of directions but also to
the detectability of structural elements of the deeper under-
ground which have influenced the folding phase of the carbon.

The interpretability of photolineations with respect to the
existing tectonical fracture systems leads to significant
practical applications.
Today, coal breaking below ground is being carried out on
the basis of far reaching automated machines. Experience has
shown, that displacements of the coal bearing layers typical
for regions with intensive tectonical influence may require
to rebuild all technical coal breaking installations which is
extremely costly.
A comparison with experienced difficulties in mining activities
due to typical fracture configurations also identifiable by
photolineations enable us to state, that in the northern not
yet explored part of the Ruhr Valley, which bears a high
potential for mining difficulties can be identified. These
areas are characterized by cross cutting and to a certain
degree diagonal striking elements.

REFERENCE

Photolineationen aus Landsat-2 Aufnahmen und ihre Beziehungen
zur Tektonik im Ruhrkarbon.
Forsch.Ber. Ld. Nordrhein-Westfalen, Fachgr. Bergbau und
Energie. 2556. Bd. 2. S. 137-143. 1977.

D. Application of Remote Sensing Data to Support Lignite Exploration in Northern Bavaria.

1. Introduction

The following section describes a research project which
has been carried out under the objective to investigate
remote sensing data in general for practical applications
in the field of lignite exploration in Germany.
It has to be seen under the aspect of combining modern
data and image data processing techniques with conventional
interpretation methods. An approach which emphasizes the
manifold possibilities to handle remote sensing information.

Within the frame of the project besides multispectral scanner
data obtained by an airborne M^2S-system also Landsat data
have been taken in consideration.

In the valley system of the "Urnaab" extensive lignite
deposits have been built up during the Tertiary. Since the
beginning of this century the known deposits in a depth
of about 1o m are being exploited by the Bavarian Browncoal
Industry.
With respect to problems in exploring new mining fields
various conventional exploration techniques such as geo-
electrcity, drillings and other geophysical methods have
not been too successful.

The described study deals for the first time with the possi-
bilities given by remote sensing techniques to support
exploration activities in the area of the bavarian Brown-
coal Industry. The basic idea that multispectral remote
sensing techniques may be a valuable tool has been derived
from the fact that brown coal is constantly releasing H_2S,
NH_3, CO_2, Co. These products of the coalification process, are
being absorbed by the surface vegetation directly, or via
the water cycle. By this it is expected that the reflection
characteristics of various vegetation types might be in-
fluenced in a detectable manner. Therefore the objective

of the study was directed towards an empirical investigation of a larger area (fig. 24) within the brown coal bearing valley systems due to spectral anomalies.

In order to meet above objectives the following data were acquired.
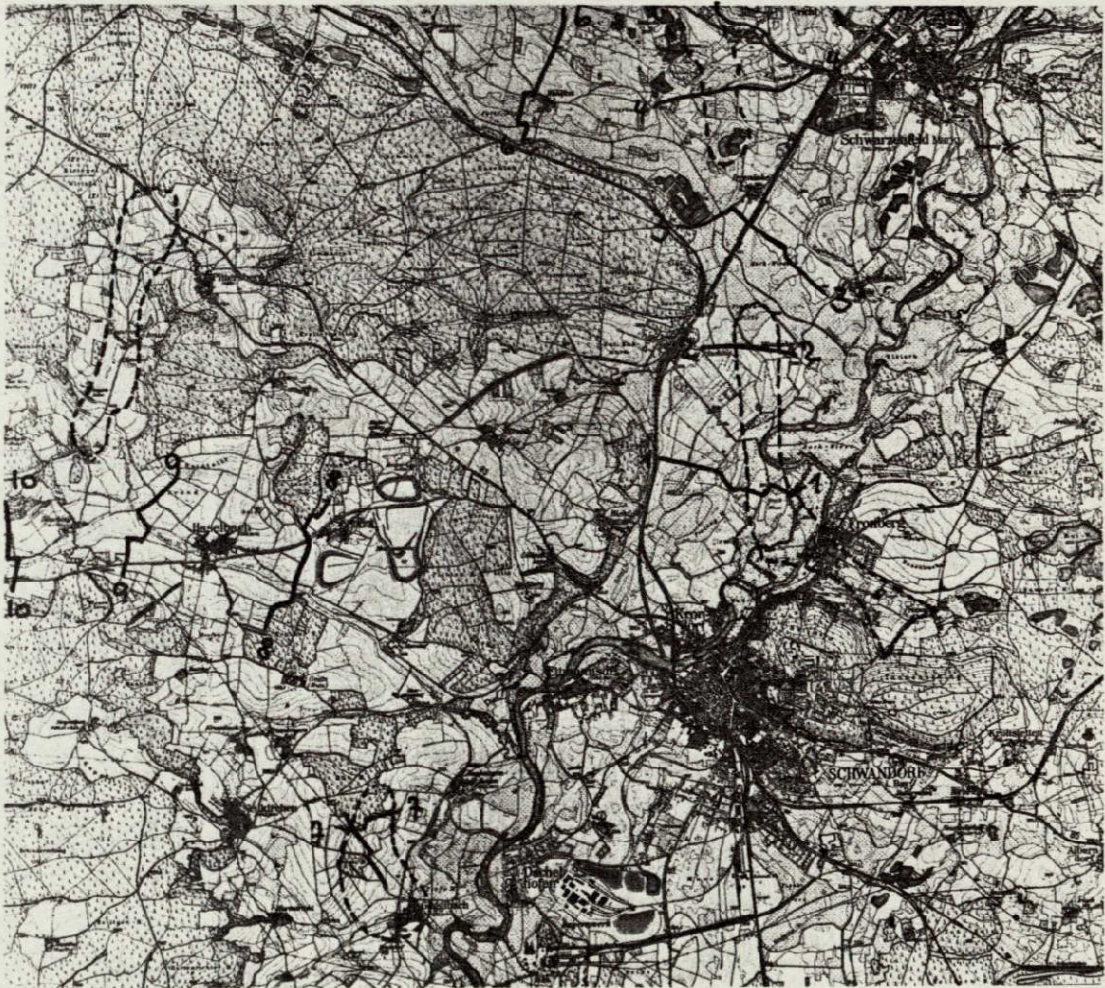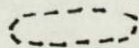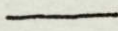
Fig. 24: Investigated area near Schwandorf

‹- - - - -› = known lignite deposits

——————— = vegetation profiles.

2. Data Acquisiton

During August 1976 the area of interest (fig.24) near
Schwandorf in northern Bavaria was covered by an aircraft
multispectral scanner flight from an altitude of ～ 4ooo m
above ground. From the same area Landsat data were processed
from CCT's and compared with the results of the scanner
flight. Unfortunately the Landsat data did not represent the
same time frame, (year, season) of the aircraft mission.

On the basis of above aircraft, Landsat and additional
collected ground truth data the following data evaluation
approaches were selected:

1) Statistical investigation of aircraft scanner data
   with respect to vegetation signatures.

2) Application of image processing techniques applied on
   M^2S and Landsat CCT's for enhancement and detection of
   possible spectral anomalies.

3. Statistical Investigation of Spectral Signatures

In order to statistically evaluate spectral characteristics
of selected vegetation types and to correlate these measure-
ments with the geological information an intensive and
detailed vegetation map along selected profiles was carried
out. As it can be derived from fig. 24 the selection of
profiles was related to areas with known lignite horizons
below ground to areas without lignite bearing layers and
to those areas which have not yet been explored. With respect
to ground truth activities,information about the plant species
(crop types), vegetation associations and soil moisture was
provided. A typical vegetation map along a profile is given in
fig. 25 . It shows that the major vegetation types have been
wheat, winter wheat, barley, maize and grass land.

For the correlation of spectral signatures with ground truth
information the image processing system of the Central Lab
was used and special software programs to establish a data
bank were implemented.
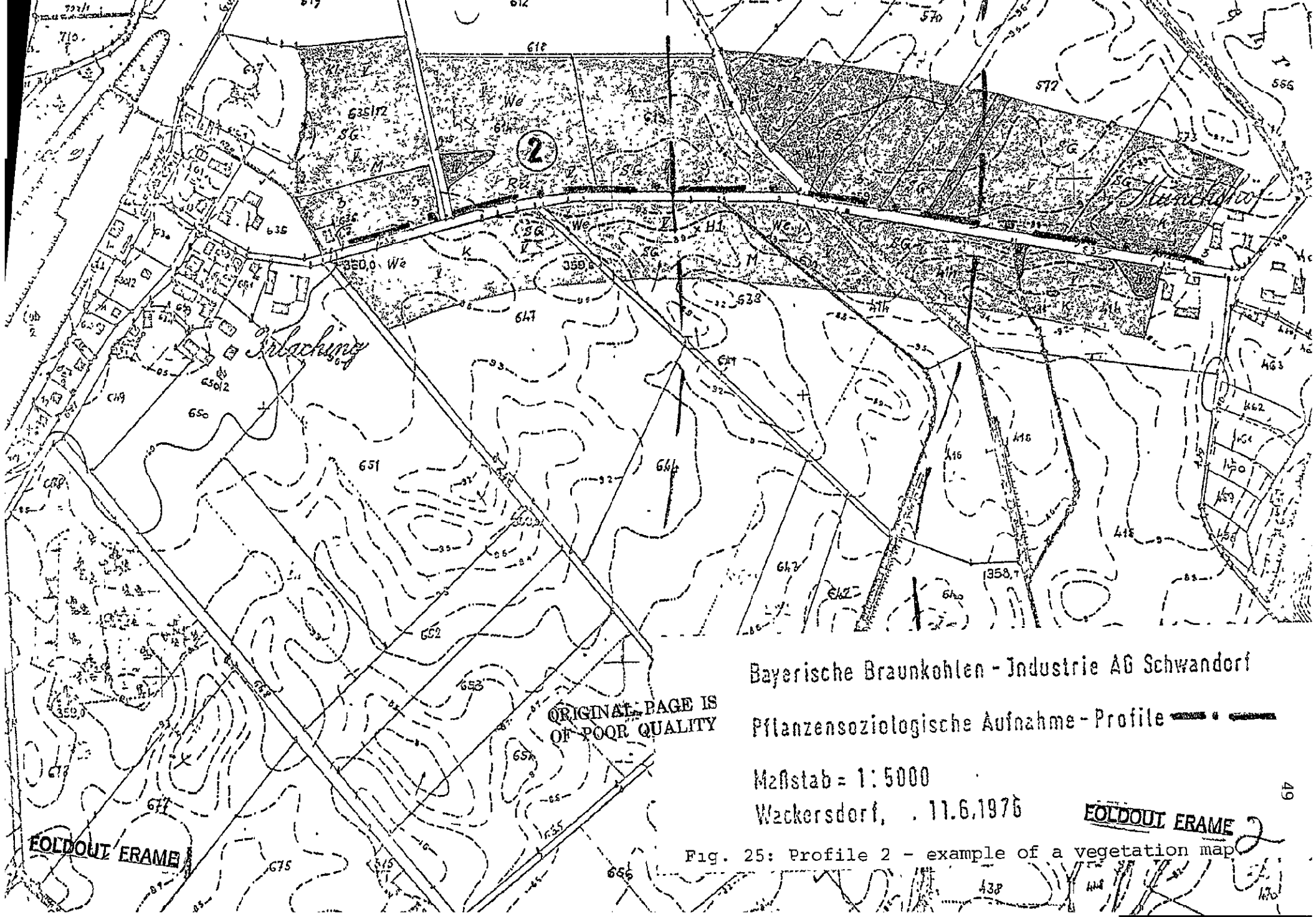
Bayerische Braunkohlen - Industrie AG Schwandorf

Pflanzensoziologische Aufnahme - Profile

Maßstab = 1:5000

Wackersdorf, . 11.6.1976

Fig. 25: Profile 2 - example of a vegetation map

The Data Bank

As it can be derived from fig. 26 larger areas containing
profiles with ground truth information can be displayed on
a color TV screen. The displayed image consists either of
three selected spectral bands within the visible and infra-
red region or of preprocessed bands such as PC-transformations

Fig. 26: Enlargement of M^2S exhibiting an area covering
         profile No. 1 and 2.

in order to obtain maximum grey-tone or color separation
for the visual identification of mapped fields.
In a next step (see fig. 27) the spectral signatures of
unumbiguously identifyable fields can be selected inter-
actively via the TV screen and stored into the data bank
by adding information on crop type, soil moisture, profile
number, position within scan stripe and information about
the occurrence of lignite in the underground.
The corresponding information is coded with symbols (f.e.
wheat = w, soil moisture levels F_1 ... $_3$ etc.).
For each measurement point the spectral information contains
the meanvalue, standard deviation and minimum/maximum intensities.

Fig. 28 demonstrates the use of the data bank for the
statistical investigation. By special filter programs
(F 1) the stored signatures can be retrieved due to
ground truth information described above. The execution
is carried out by keying in the corresponding symbols
Fig. 29 demonstrates a listing showing the ID-symbols
in the first line.
By this a fast evaluation of signatures is possible. By
using another set of filter programs (F 2) a further
selection of prefiltered data due to individual spectral
bands can be achieved in combination with the calculation
of several ratio transforms etc.

Results.

With respect to the manifold crop and vegetation types
covered by the mapped profiles only summer barley, wheat-
and corn-fields were selected for the comparative signature
study. The restriction of above vegetation types was necessary
because the other crop types were statistically underrepresented
within the profiles.
Out of a total of ∿ 4oo signature measurements the following
results could be derived:

DATA BANK — DATA STORAGE

```
┌─────────────────────┐     ┌─────────────────────┐
│ Scanner data        │     │   Ground Truth      │
│            (CCT)    │     │                     │
└─────────────────────┘     └─────────────────────┘
           │                           │
           ▼                           ▼
┌─────────────────────┐     ┌─────────────────────┐
│  TV-Display of      │     │  Vegetation Map     │
│  Test Areas         │     │                     │
└─────────────────────┘     └─────────────────────┘
           │                           │
           └──────┐        ┌───────────┘
                  ▼        ▼
         ┌─────────────────────┐
         │ Comparison/Identi-  │
         │ fication of test    │
         │      fields         │
         └─────────────────────┘
           │
           ▼
┌─────────────────────┐        ┌─────────────────────────────┐
│ Masking of identi-  │        │  Additional ID-Into         │
│ fied test fields    │        ├─────────────────────────────┤
└─────────────────────┘        │  crop type                  │
           │                   │  soil moisture level        │
           ▼                   │  profile ND.                │
┌─────────────────────┐        │  scan-stripe position       │
│ Coding of test      │◄───────│  lignite                    │
│ fields with ID-     │        │  no lignite                 │
│ symbols             │        │    ?                        │
└─────────────────────┘        └─────────────────────────────┘
           │
           ▼
┌─────────────────────┐
│ Storage of test fields│
│ into Data Bank      │
│ -spectral signatures│
│ -ID-symbols         │
└─────────────────────┘
```
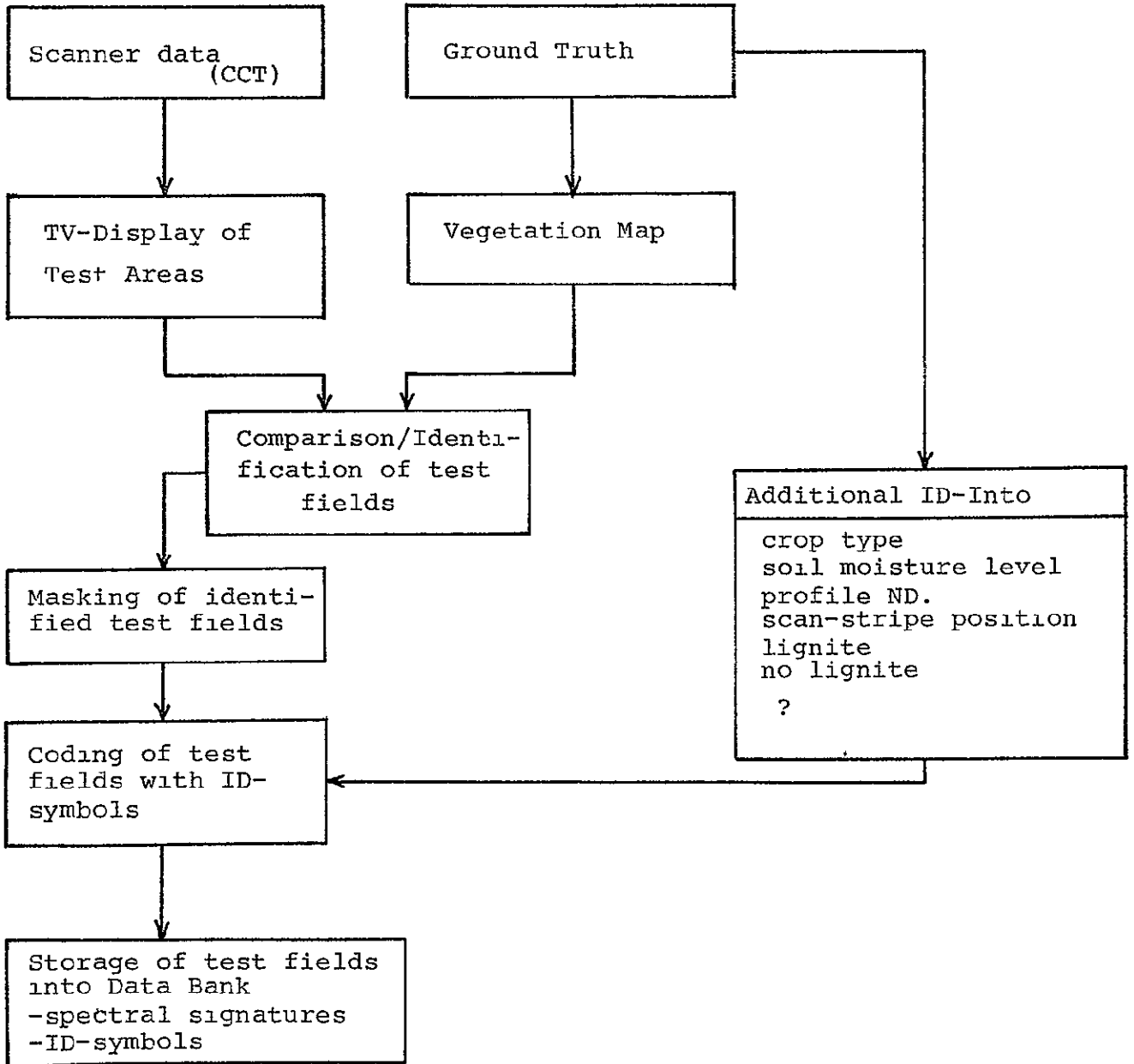
Fig. 27

DATA-BANK - DATA RETRIEVAL
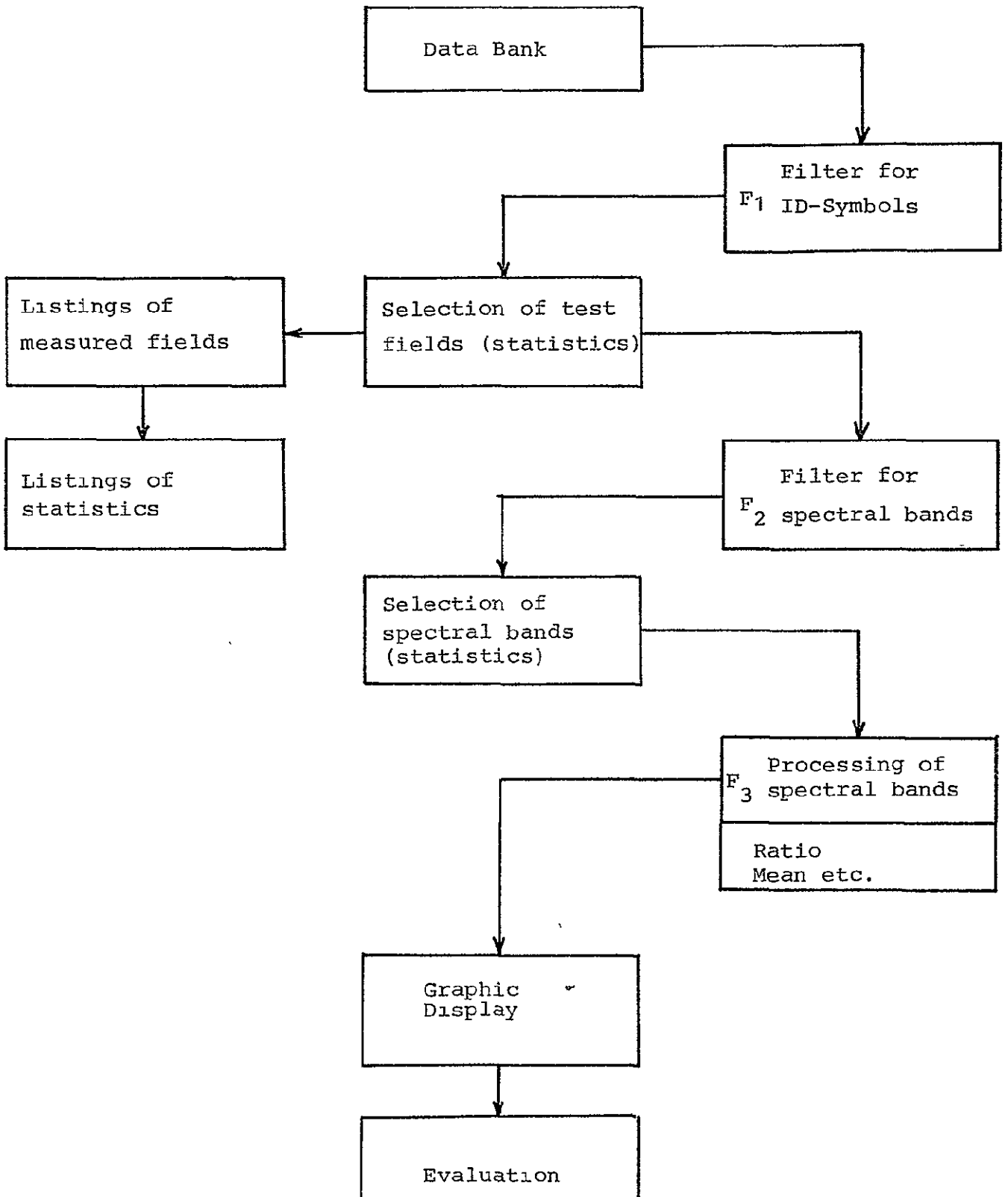
Fig. 28

```
I------I------I------I------I------I------I------I------I------I------I------I------I
I FIELD IDENTIFICATION = SGF2S300P2                                              I
I NUMBER OF PIXELS =        11                                                   I
I ANBAU =            SOMMERGERSTE      ORIGINAL PAGE IS                          I
I FEUCHTIGKEIT =     IV                                                          I
I STREIFEN =         3TER              OF POOR QUALITY                           I
I KOHLE? =           KEINE KOHLE                                                 I
I PROFIL =           2. PROFIL                                                   I
I------I------I------I------I------I------I------I------I------I------I------I------I
I CH   I   0 I   1 I   2 I   3 I   4 I   5 I   6 I   7 I   8 I   9 I  10 I
I------I------I------I------I------I------I------I------I------I------I------I------I
I MIN  I 161 I  84 I  53 I  49 I  29 I  37 I  27 I  53 I 124 I 101 I   0 I
I------I------I------I------I------I------I------I------I------I------I------I------I
I MAX  I 170 I  91 I  56 I  51 I  32 I  40 I  30 I  54 I 126 I 109 I   0 I
I------I------I------I------I------I------I------I------I------I------I------I------I
I MEAN I 164 I  86 I  54 I  49 I  30 I  37 I  27 I  53 I 125 I 104 I   0 I
I------I------I------I------I------I------I------I------I------I------I------I------I
I STDD I   3 I   2 I   1 I   0 I   1 I   1 I   1 I   0 I   1 I   3 I   0 I
I------I------I------I------I------I------I------I------I------I------I------I------I
```

```
I------I------I------I------I------I------I------I------I------I------I------I------I
I FIELD IDENTIFICATION = KOF2S300P2                                              I
I NUMBER OF PIXELS =       170                                                   I
I ANBAU =            KOHL                                                        I
I FEUCHTIGKEIT =     IV                                                          I
I STREIFEN =         3TER                                                        I
I KOHLE? =           KEINE KOHLE                                                 I
I PROFIL =           2. PROFIL                                                   I
I------I------I------I------I------I------I------I------I------I------I------I------I
I CH   I   0 I   1 I   2 I   3 I   4 I   5 I   6 I   7 I   8 I   9 I  10 I
I------I------I------I------I------I------I------I------I------I------I------I------I
I MIN  I 158 I  82 I  48 I  42 I  25 I   1 I  24 I  49 I 117 I   0 I   0 I
I------I------I------I------I------I------I------I------I------I------I------I------I
I MAX  I 170 I  89 I  53 I  46 I  30 I  36 I  28 I  50 I 129 I 128 I   0 I
I------I------I------I------I------I------I------I------I------I------I------I------I
I MEAN I 164 I  85 I  49 I  43 I  27 I  33 I  25 I  49 I 122 I 113 I   0 I
I------I------I------I------I------I------I------I------I------I------I------I------I
I STDD I   3 I   2 I   1 I   1 I   1 I   3 I   1 I   0 I   3 I  31 I   0 I
I------I------I------I------I------I------I------I------I------I------I------I------I
```

Fig. 29: Print out of selected vegetation types.

The spectral measurements taken from fields with summer barley
have clearly shown that those spectral signatures which were
derived from areas above lignite layers are characterized by
slightly decreased intensity values if compared with those
measurements over areas where drillings did not indicate
lignite.
Of special interest has been the fact that changes in reflection
intensities are not restricted only to the infrared band .

Comparisons of wheat measurements demonstrated a reverse
behaviour of spectral signatures. By this the intensity
values above lignite layers are higher than the others.

Corresponding measurements taken from maizefields and grass-
land also indicate increased intensities derived above
lignite horizons.

Similar investigations have been carried out over various
other crop types. These measurements, however, didn't show
the same correlations as they could be observed with above
vegetation types.

In order to select the optimum spectral regions for the
discrimination of above described phenomena, two-dimensional
representations of selected bands were visually interpreted.
Fig. 3o demonstrates an intensity plot of band 4 versus band 7.
The circle indicate the standard deviations.

The good separation between those measurements derived from
lignite bearing and lignite free areas can be clearly seen.

In order to compare spectral vegetation measurements from
profiles over yet unexplored areas an "intensity signature"
was established with respect to the positions of summer-
barley-, wheat- and maize values within above (fig. 3o)
two-dimensional space given by bands 4 and 7 (fig. 31).
The corresponding measurements were separated due to
information about lignite in the underground.

△ lignite
○ no lignite

maize

summer-
barley

grassland
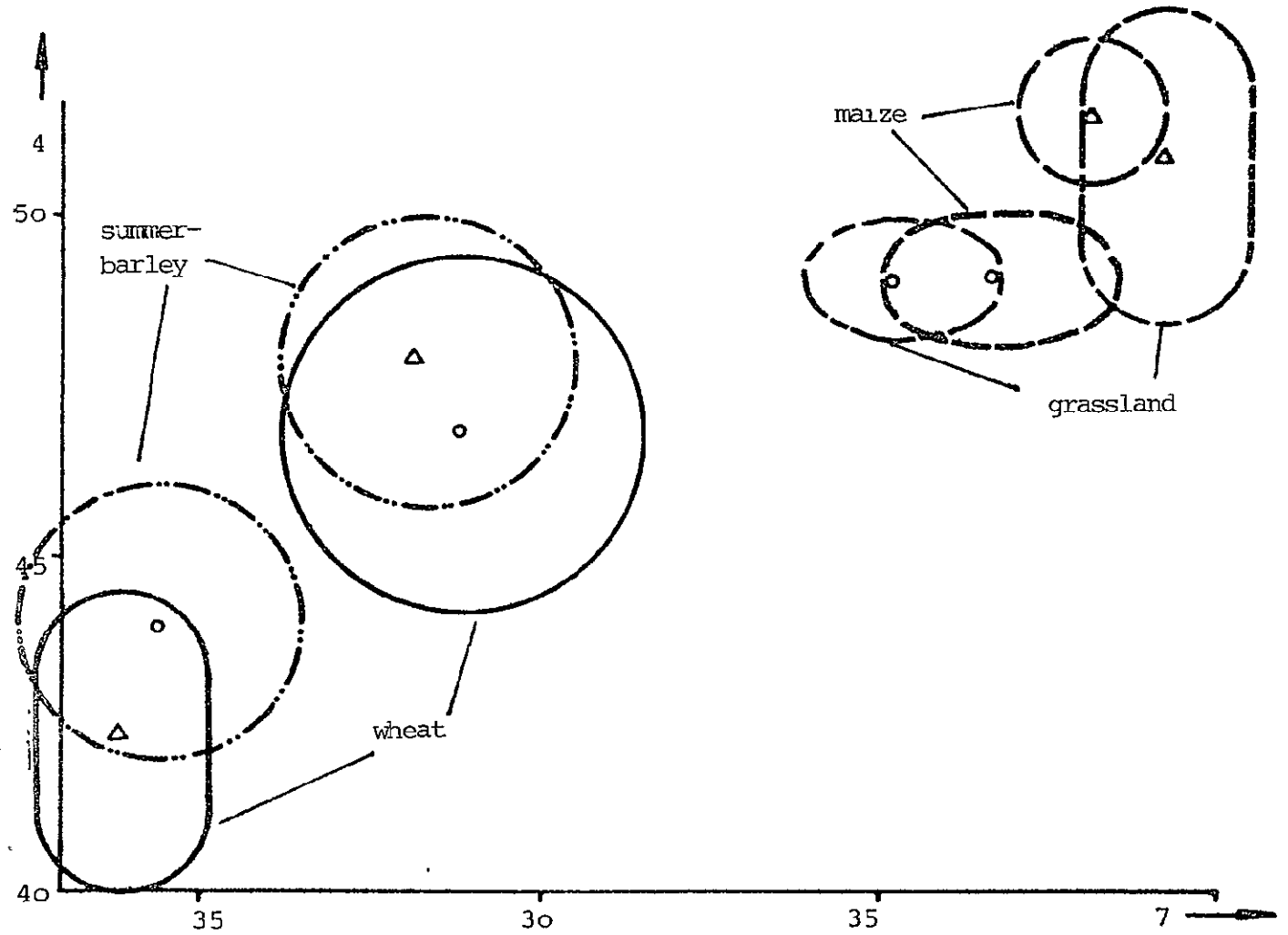
wheat

Fig. 3o: Two-dimensional display of intensity measurements
band 4 and 7.

Intensity signature derived from explored areas

Profile No. 9

Profile No. 8

1 = summer barley

2 = wheat

3 = maize
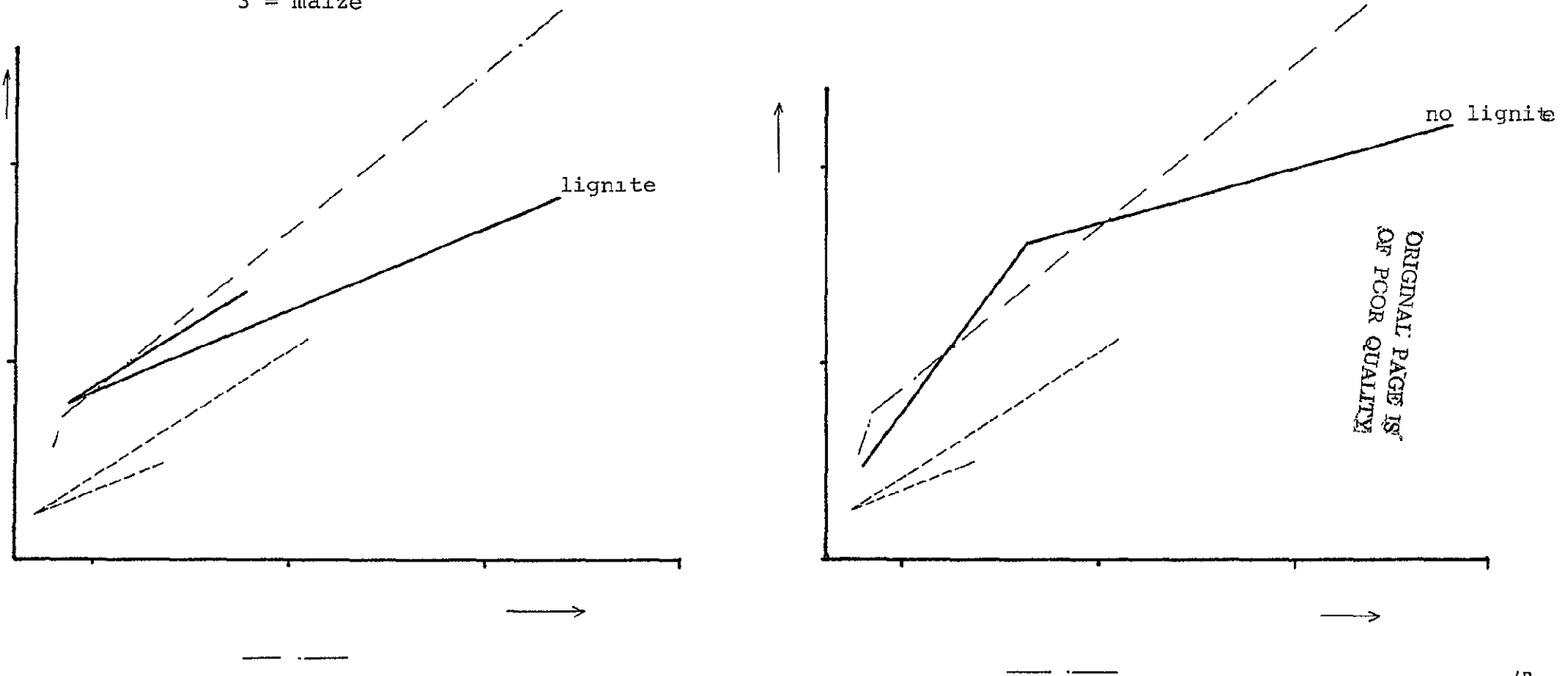
Fig. 31: Note the similarity of Profile No. 9 with measurements above lignite.

In a next step the measurements derived from profiles over
unexplored areas were transformed into the same "signature"
space". The comparative representation of fig. 3o shows that
the summer-barley-, wheat- and maize-measurements taken over
profile No. 9 indicate a trend similar to those measurements
above lignite horizons.
The corresponding data representing profile No. 8, however,
expresses a trend which indicates the absence of lignite.

The results obtained by above empirical approach only describe
spectral phenomena. The matter of fact that the near IR
measurements did not show any correlations with lignite
occurrence leads to the conclusion that a possible impact
of trace gases on vegetation is very unlikely.

4. Enhancement of spectral anomalies by image processing

In order to obtain more indications with respect to the obtained
results, various image enhancement techniques were tested
on the basis of M^2S and Landsat data.
Besides ratio transformations of selected bands, analog
carried out linear combinations and PC transformations
of all bands were produced. Best results could be obtained
by support of the PC transformations, in terms of inter-
preting the first PC transform or evaluating enhanced low
order transformations. The results of two selected areas
are demonstrated below. Area I (fig. 26) is located north
of Schwandorf (fig. 24) and covers Profile No. 1 and 2.

For a further interpretation a PC transformation was carried
out on the basis of all bands available. The corresponding
covariance matrix was obtained from samples representing
various vegetation types.
In order to enhance the low order transformations, a 3 x 3
convolusion and subsequent histogram stretch was carried out.
Out of the available transforms No. 6 and 8 were selected.
No. 8 (fig. 32) exhibits a grey tone distribution which
ca be related to somewhat increased soil moisture along
the river NAAB. The circular light area detectable on the
PC transformation No. 6 is very distinct - nevertheless it
could not be related to an a priori recorded earth scientific
phenomenon (fig. 33).

Fig. 32: 8th principal component
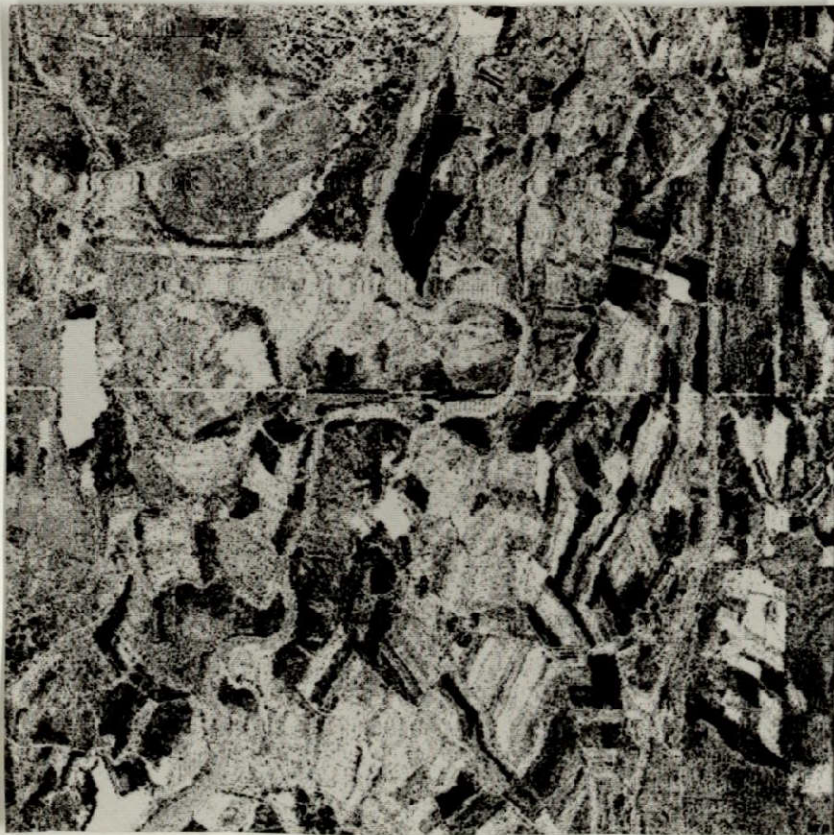
Fig. 33: 6th principal component
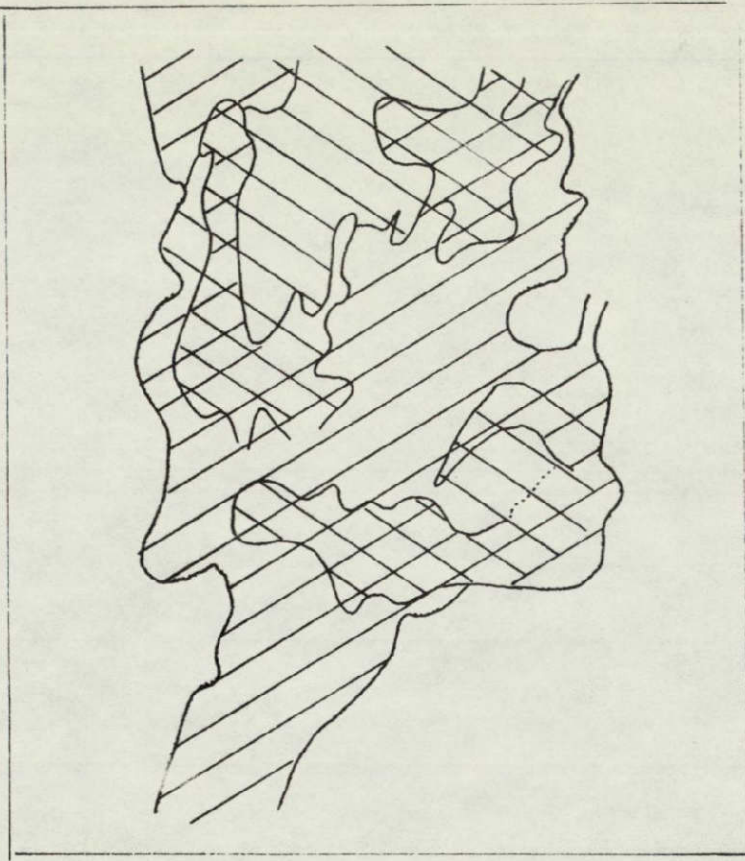
Fig. 34: Schematic overlay of grey tone distribution derived
from PC-axis No. 6 and 8.

Fig. 35: Overlay of extracted areas.

Fig. 34 represents a schematic overlay of both features.
Areas which indicate the overlapping of the two grey tone
phenomena represent a surprising correlation with explored
and mapped lignite horizons (compare fig. 35 and fig. 24).

The second area which has been digitally processed includes
profile No. 8 and 9 (fig. 24).
This time it is the 1st PC-transform which reveals an un-
ambignously detectable grey-tone anomaly (fig. 36).
This anomaly can be related to the occurrence of lignite
due to the fact that it covers exactly the already discussed
profile No. 9.
In addition to that, the anomaly can be interpreted as a
prolongation of a mapped lignite horizon in the north (fig.
24).

ORIGINAL PAGE IS
OF POOR QUALITY

Fig. 36: 1st PC transform exhibiting a distinct grey tone
        anomaly.

Further processing of Landsat data (fig. 37) did not bring
comparable results. This however does not lead to any
conclusions because of the seasonal difference between the
aircraft scanner flight and the Landsat overpass. In
addition it has to be mentioned that the scanner flight
was carried out after an unusual dry period in 1976.

Fig. 37:   Landsat, 1st principal component

E. Application of Landsat to Support Thematic Mapping in Geology

1. Introduction

During the last two years the experience was made, that the utilization of Landsat data for activities in the field of geology and thus exploration purposes is one of the applications which have proved to be of great practical potential.

In the beginning Landsat images acquired over arid and semi-arid areas have been primarily inspected and interpreted with an eye on linear features and textural information detectable on small scale synoptic data. The mapping of lineaments on the basis of aerial and satellite images can be regarded as an important approach to photogeological investigations, as it is demonstrated in the previous chapters. Lineaments and textural pattern often reveal tectonical phenomena on a small scale and thus contribute to a better understanding of the geological frame.

The application of conventional photogeological interpretation techniques with the analysis of grey- and color-tone variations for the determination and discrimination of lithological phenomena has not been very successful.

Based on physiological limitation, the human interpreter is not able to distinguish subtle grey and color-tone variations or even to recognize tonal phenomena in a quantitative way. Also grey tone variations in images as an expression of the spectral surface characteristics are not very indicative if the available spectral bands are interpreted individually. Even the interpretation of color representations composed by the MSS bands 4, 5 and 7 does not lead to satisfactory results. With respect to Landsat images this is mainly due to the similar reflection characteristics of various rock types within the wavelength regions covered by this MSS scanner system.

2. Requirements Towards Data Processing for Geology.

In order to fully utilize the spectral information avail-
able in Landsat images, data processing techniques have to
be applied. For landuse purposes thematic maps have been
produced by fully automated image processing. For geological
purposes, however, the application of digital processing can
not be fully automated. Experience in using spaceborne images
for geological applications has shown that the capabilities
of the interpreter in deriving significant information is
indispensible. Therefore, from a geological point of view
certain requirements concerning the data base, and the kind
of preprocessing methods applied have to be established:

a) Processing of multispectral and multitemporal informa-
   tion in order to enhance the spectral separability in-
   herent in the reflection properties of the surface;

b) Preservation of textural information exhibited in the
   original data;

c) Utilization of the synoptic properties provided by
   spaceborne images. This requires technological capa-
   bilities permitting the evaluation of full Landsat frames;

d) Production of processing results in form of orthophotos
   like images at a scale of 1:5oo.ooo and 1:25o.ooo.
   This requires high precision display capabilities.

Due to the manifold requirements we have constantly increased
our image processing software and have tested and still are
testing various methodological approaches to provide the
user with data products exhibiting an optimum information
basis.

In the following chapter some examples of data processing
are given. With respect to above mentioned requirements the
examples do not take into consideration the analysis of
multitemporal data, because software development for geometric

corrections could not yet be finished. For demonstration
purposes examples, taken from scenes covering a part of
Saudi Arabia and Iran were selected. The corresponding
frames (EROS -bulk products) are exhibited by fig. 38 and
fig. 39.

The selected data were processed and displayed by applying
the various methods available through the ISI system 47o
and the extensive software package (see part II).
With respect to the user requirements and an optimized use
of our processing unit, the various processing methods are
applied in terms of problem oriented processing (POP) and
post processing (PTP).

Problem oriented processing involves all the procedures
which may enhance the interpretability of data by digitally
combining multispectral information in one or the other way.
By this it is understood to perform f.e. logical operations
taking into account intensity values of pixels derived from
the multispectral data set, and any multispectral feature
transformations such as ratio processing principal components
or other linear and non linear transformations.
POP requires the presence of the earth scientist during the
processing phase in order to obtain optimum enhancements
for his task. The procedure of optimizing this process is
explained in part II.

Post processing includes more or less routine operations to
take full advantage of POP-processed images and to provide
the user with an acceptable data base for subsequent inter-
pretation purposes. Under this aspect post processing means
  - supression of noise
  - further enhancement of tonal variations
  - enhancement of linear features
  - generation of color composits
  - geometric correction.
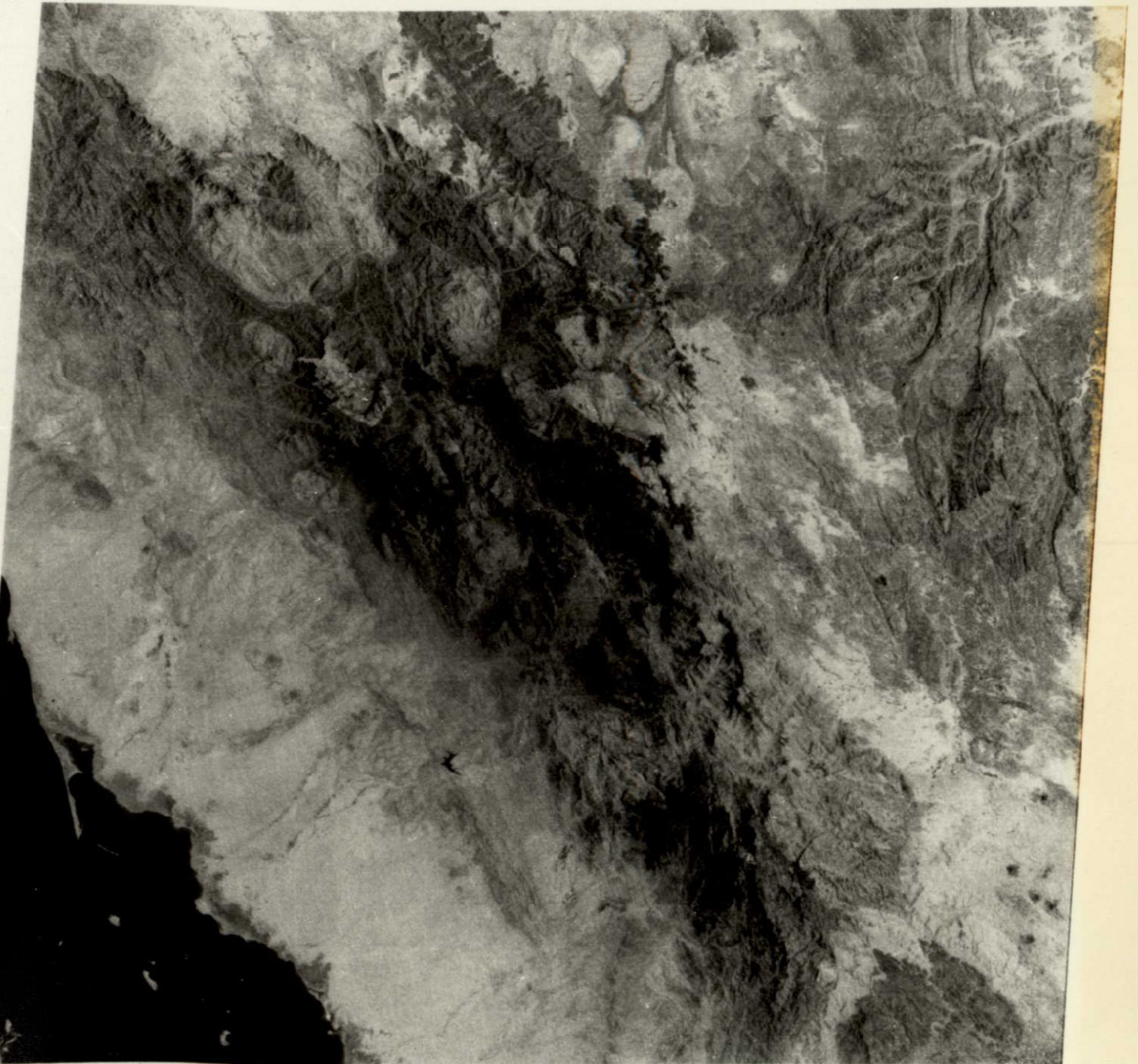
Fig. 38: Landsat MSS 5 Saudi Arabia EROS buld products

Fig. 39: Landsat MSS 5 Iran EROS bulk products

On the basis of above Landsat scenes our capabilities and
work in applying POP and PTP-techniques are demonstrated.

3. Ratio Processing (POP)

Ratio processing is understood to result from dividing
intensity values of corresponding picture elements in adja-
cent spectral bands. New ratio values are presented in the
form of a new image. There are two properties of band ratio-
ing which makes this simple technique extremely useful espe-
cially for geological applications:

a) Suppression of unwanted atmospheric and illumination
   effects:
   If we assume that the physical characteristics of electro-
   magnetic radiation are very similar in adjacent narrow
   spectral bands, the impact of atmosphere and illumination
   variations should also be very similar. Thus by band-
   ratioing it is possible to decrease the above effects e.g.
   to eliminate shadows as a disturbing feature which depend
   on the illumination angle and the surface relief.

b) Enhancement of spectral properties of lithological units:
   It has been reported, that ratio intensities of adjacent
   wavelength regions are very sensitive to variations in the
   mineralocial composition of rock types. By this it is
   an excellent tool to discriminate between various rock
   types or even to enhance lithological boundaries not visible
   on the basis of the original spectral bands.

The examples of fig. 4o which represent an entire Landsat
frame may illustrate above mentioned properties. Fig. 4o,
a,b,c exhibits MSS bands 4, 5 and 6. The ratios defined on
a subset of the Landsat frame are displayed by fig. 4o d,e.
Fig. 4o d which corresponds to the ratio 4/5 clearly demon-
strates the suppression of intense shadow effects exhibited
by the strong relief. Furthermore the appearance of various

geological phenomena become visible. Above ratio image in
combination with the original spectral bands provides for
some areas information not recorded on geological maps
available.

A further ratio image (fig. 4o e) between MSS bands 5/6
shows rather vegetated areas in dark and black than
an increased differenciation of geological features.

A typical case for post processing (PTP) is f.e. the geo-
metrical rectification of POP-results or their representation
in form of color composites. Fig. 41 demonstrates a geo-
metrical corrected sub-area and fig. 42 a,b the comparison
between a normal false color and a ratio color display.
The examples of fig. 42 a,b are photographed from a TV
screen and are characterized by a decreased quality.
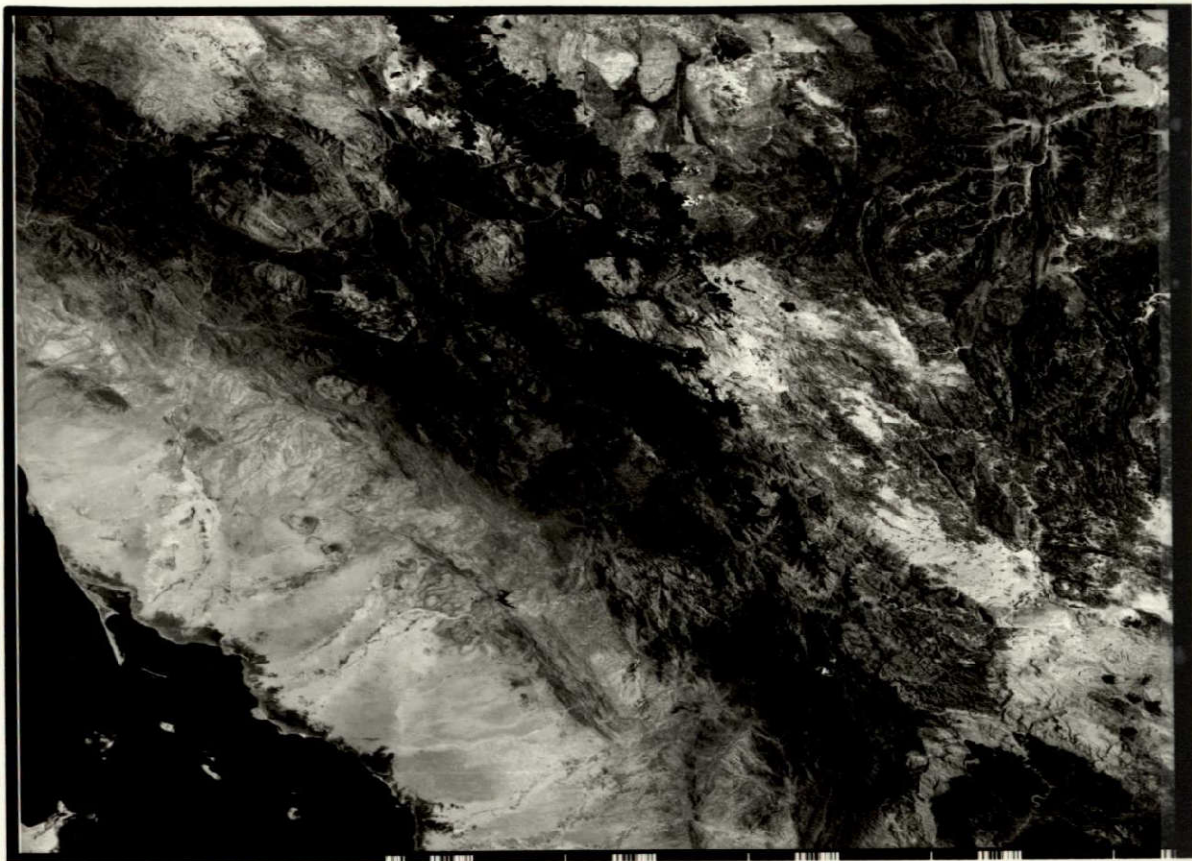
Fig. 4o a: Landsat MSS band 4

ORIGINAL PAGE IS
OF POOR QUALITY
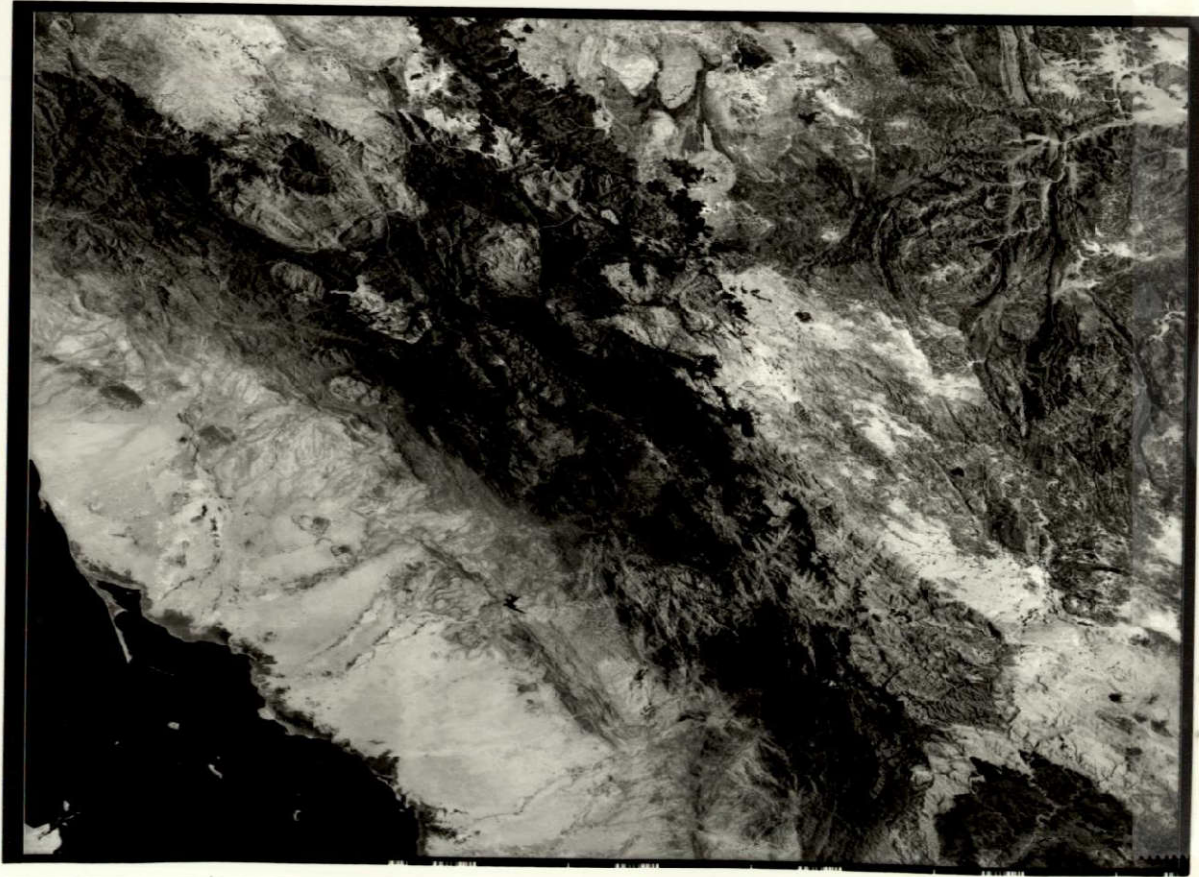
Fig. 4o b: Landsat MSS band 5
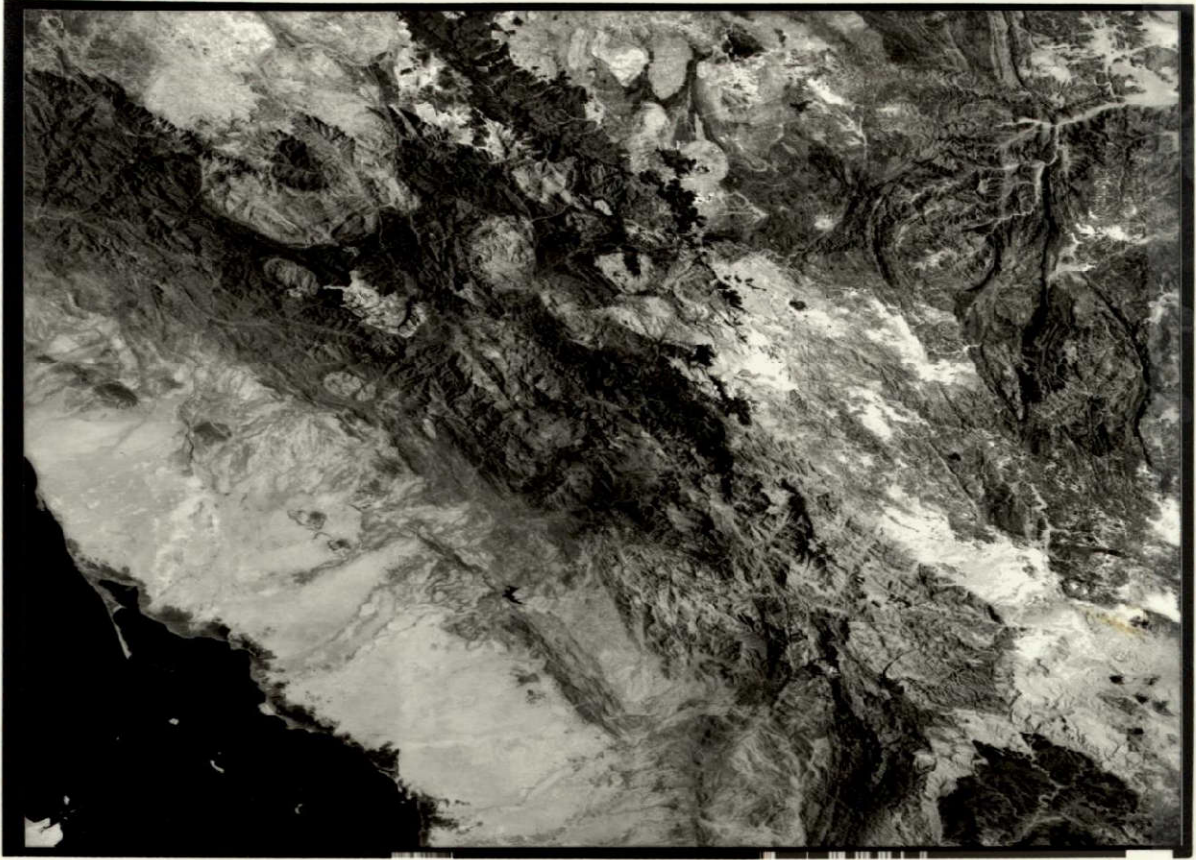
Fig. 4o c: Landsat MSS band 6

Fig. 4o d: Ratio MSS 4/ MSS 5
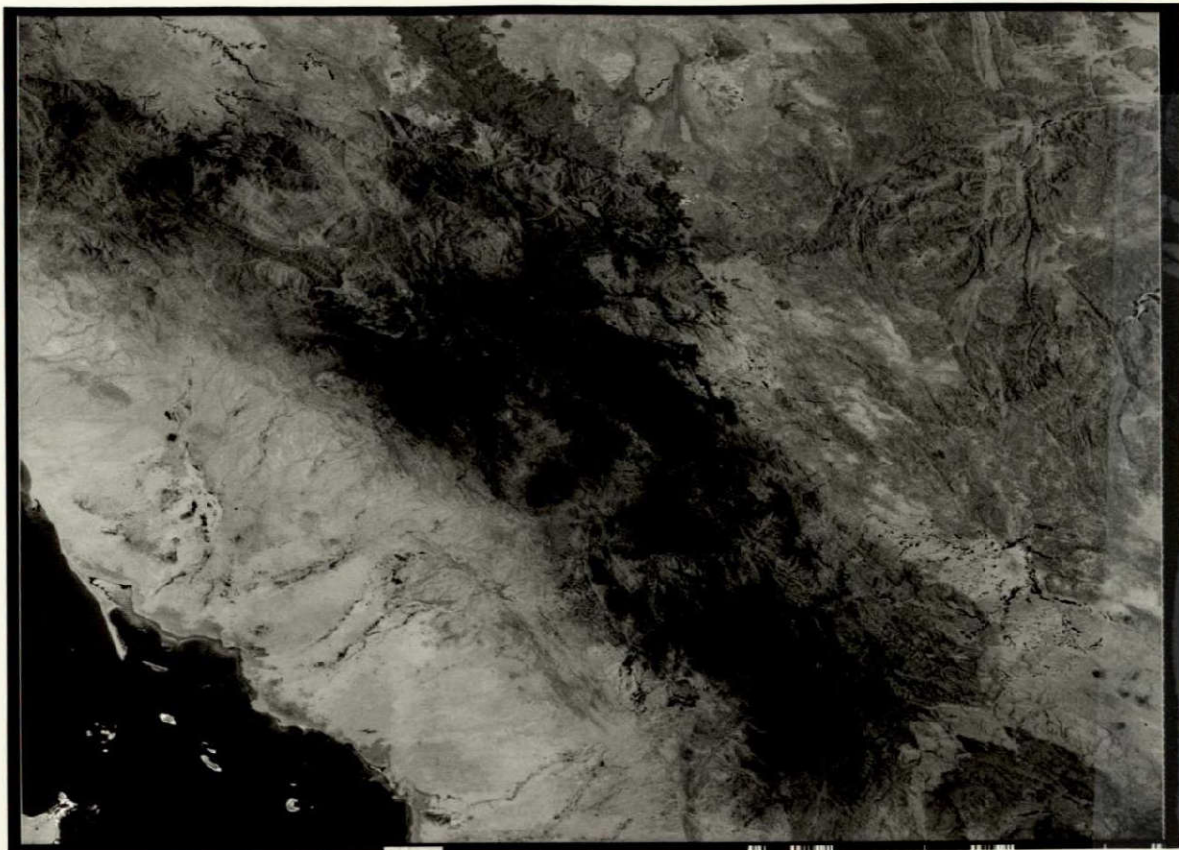
Fig. 4o e: Ratio MSS 5/MSS 6

Fig. 41: MSS 4 geometrically rectified.

Fig. 42 a: False color representation
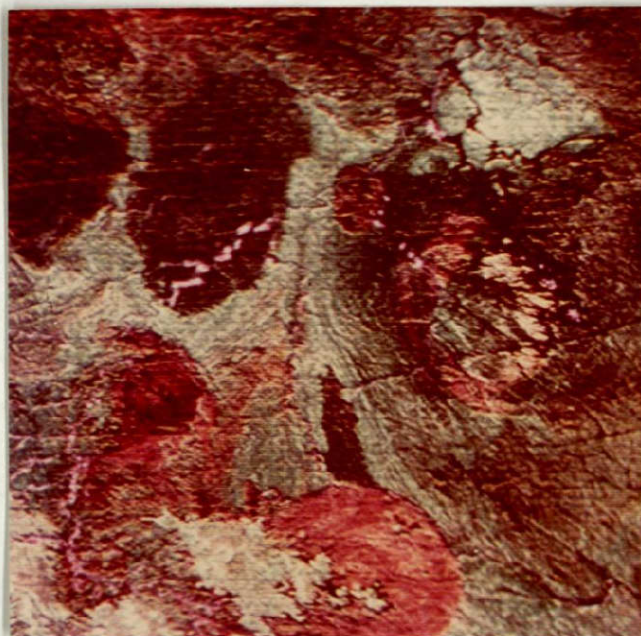
Fig. 42 b: Ratio color representation.

4. Principal-Component-Transformation (POP)

The principal-component (PC) -transformation is a well known
technique and of special significance for data reduction
purposes. The PC-transformation represents basically a linear
combination of the original bands by calculating the weighting
factors for the transformed images via the covariance matrix.
So f.e. out of 4 spectral bands 4 new, transformed and now
not correlated images of decreasing information content can
be calculated. Experience with multispectral data has shown,
that by the first component normally more than 5o percent of
the information present in the original bands can be expressed.
The remaining percentage is distributed over the lower order
transformations also in a decreasing way. By this the 3rd and
4th components only contribute with a few percent of information.

The transformed images of the test area clearly demonstrate
how most of the grey-tone variance (information) is contained
in the first component (fig. 43 a).

Of special interest for the photogeological interpretation
are the transformations of lower information content after
problem oriented processing.
The 2nd, 3rd and 4th axis of fig. 43 a,b,c,d have been post
processed by carrying out a 3 x 3 convolution in combination
of a histogram egalisation. Above low order transformations
are characterized by some tonal contrast not detectable on
the original data.
Of special interest is the enhancement of a rock border within
the granite. Fig. 44 a,b exhibits two color renditions based
on enhanced lower order transformation.

Fig. 43: Principal components of a 512 x 512 subarea
taken from Landsat scene (fig. 39).
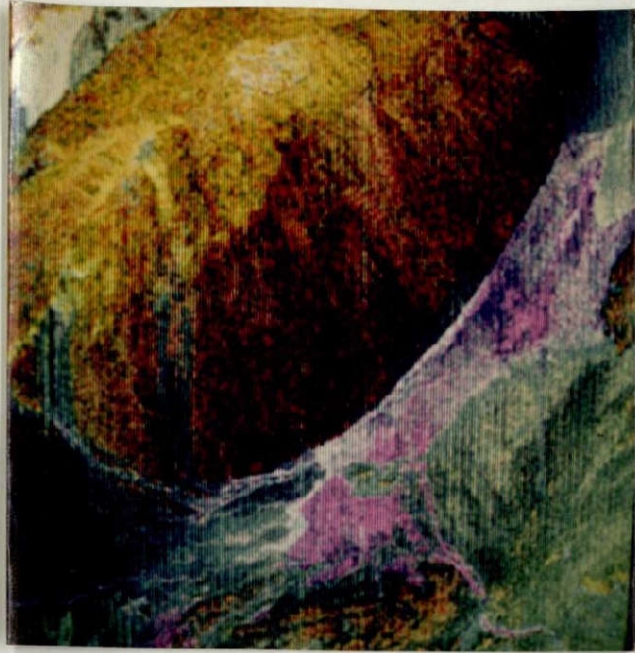
ORIGINAL PAGE IS
OF POOR QUALITY
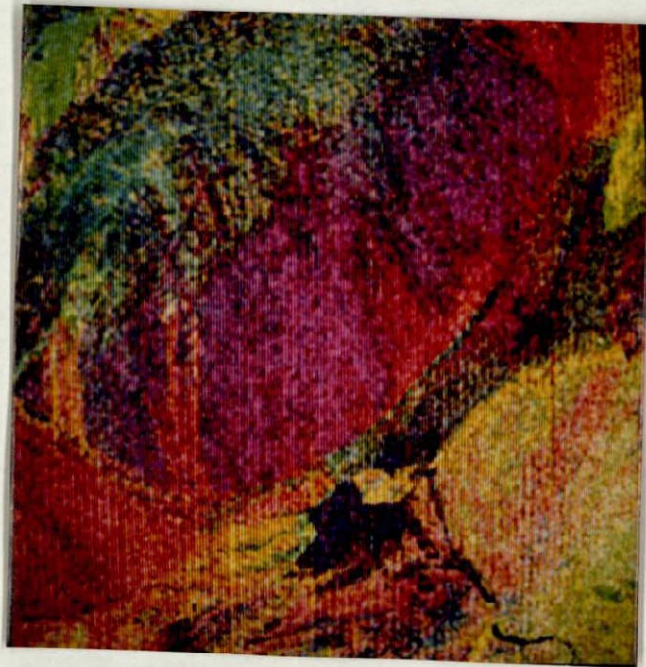
Fig. 44: Color renditions composed of enhanced low
order transformations.

5. Image Filtering (PTP)

Very often it can be observed that especially the problem
oriented processed data (ratios, PC-transforms are
characterized by also enhanced noise pattern.
With respect to Scanner data striping noise is very critical.

This noise manifests itself in the form of stripes in the
scanning direction, and can be under some circumstances very
disturbing for an interpretation or an automatic processing
of the image. Since this is a totally technology-dependent
problem, it can be foreseen that an improvement in the sensor
technology in the next Landsat-series satellites will tend
to elliminate this problem. However, the Landsat-1 satellite
has been sending image data to earth for three years and the
Landsat-2 will possibly do well a long time also.

That represents an extraordinarily amount of data which will
have to be processed for years to come, for its own sake
and also in conjunction with images from future systems.

Therefore, a method for the ellimination of this problem in
already existing imagery is of very great importance. Some
restrictions should be imposed on such a method: First, it
must be fast. Second, it must be a standard algorithm applicable
to all data without the need to be adjusted to each new picture
and third, and perhaps most important, it must not destroy
information contained in the picture.

In the following chapter very recently started work in above
field of post processing is discussed.

Problem Description and Already Existent Methods

The nature of the problem source can be easily understood
considering the structure of the MSS. In each spectral
channel six lines are scanned through six different detectors.
Obviously, if each one of the detectors had exactly the same
characteristics the problem wouldn't exist, but they have
different gain and offset.
This produces the undesired effect that even an homogeneous
object will not produce an homogeneous picture.
In most of the pictures, this noise cannot be appreciated at
first glance. As example, four spectral channels of a sub-
scene of a Landsat frame are shown in fig. 45. In fact, only
in picture regions where the signal to noise (S/N) ratio is
very low, can it be observed easily.

In some cases, however, the effect of processing is a reduction of
the S/N ratio, as in the case of channel ratios and
differences, and for the principal components transformation.
This last processing is shown in fig.46 . As can be seen, the
third and fourth principal components have a lower S/N ratio
and therefore the striping noise is easily visible.

Various methods have been proposed for correcting this effect.
The most obvious would be to measure the gain an offset of
each different detector (as is actually done in most scanners
through a calibration lamp) and afterwards to modify the data
according to the obtained coefficients.

This is perhaps the most reasonable method, and it has the
single disadvantage that the coefficients can vary from time
to time.

Another method uses local statistics in the picture to elli-
minate the variation produced in each line due to the
detectors. We will concentrate here on a method based on
the coherency of the noise, that is, on its frequency
characteristics.
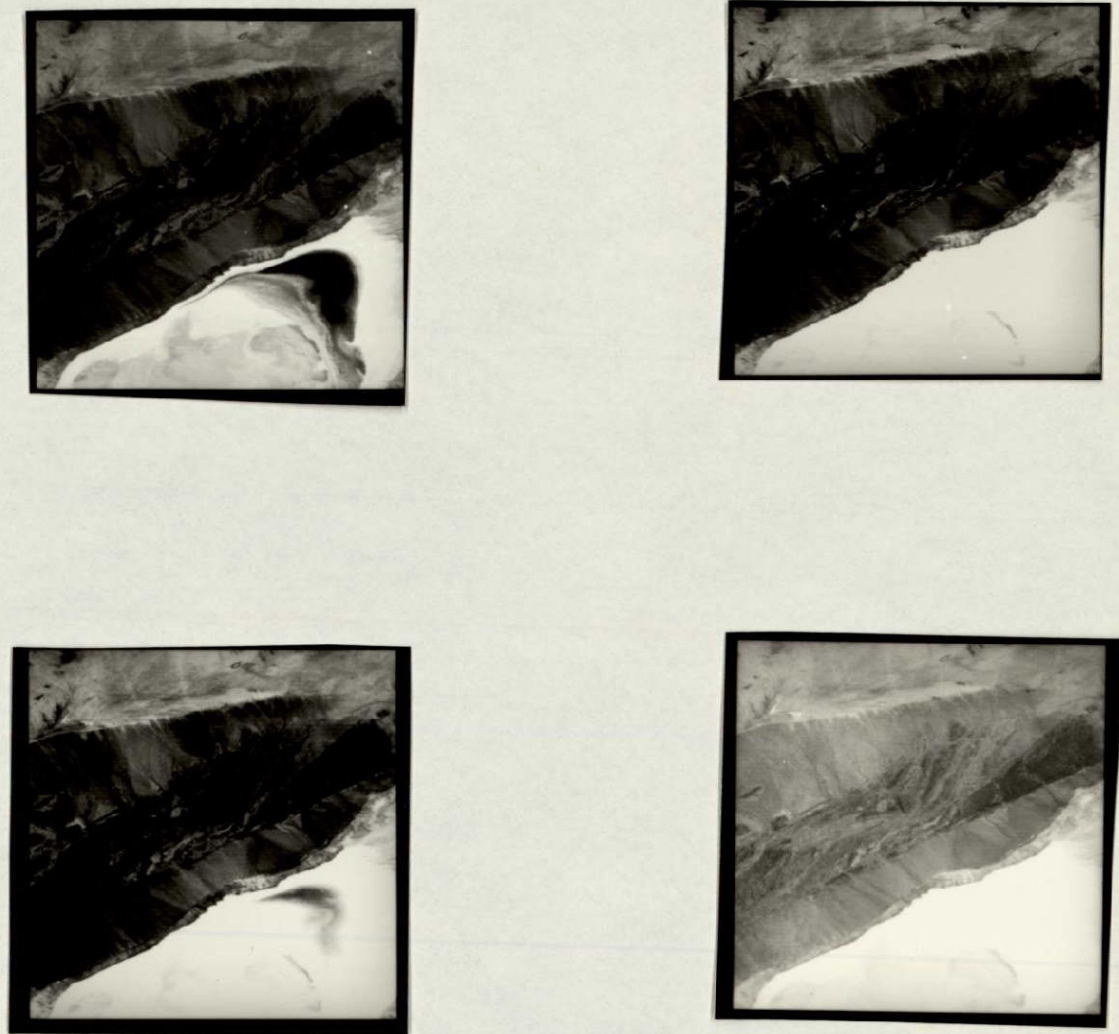
Fig. 45: Display of the 4 Landsat MSS bands striping
         effect detectable only in areas with low S/N ratio.

Fig. 46: Principal component transformation of Landsat
MSS bands, fig. 45 (256 x 256 pixels).

Spectrum Analysis

Since it is known that the noise is one-dimensional, an also one-dimensional Fourier transform will be enough in order to evaluat. its frequency characteristics. For this trans-formations we choose the image of fig.46 d, and applied the fast Fourier transform along the columns. The result is shown in fig. 47 .

The noise can be seen to consist of two components of two very well defined frequencies, namely

$$f_1 = \frac{21}{128} \frac{1}{\Delta x}$$

$$f_2 = \frac{42}{128} \frac{1}{\Delta x} = 2 f_1$$

(a)

$\frac{1}{\Delta x}$ = sample frequency, in this case could be assumed to be

$\frac{1}{79}$ m

Obviously, after the Nyquist theorem, we can only have frequencies such that $f \leq \frac{1}{2\Delta x}$ and with this rule the frequencies mentioned above can be easily deduced from fig. 47.
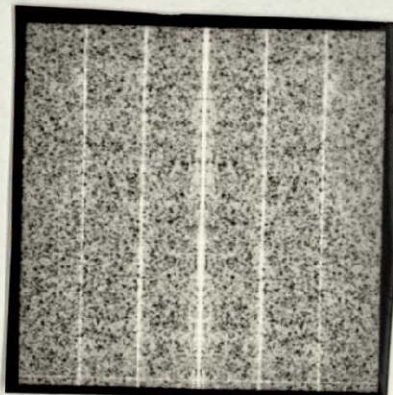
Fig. 47: One-dimensional fourier transformation of fig. 46 d.

Filtering in the Frequency Domain

From the known relation for two signals and their respective
Fourier transforms:

$$S * f = S \cdot F$$

(b)

Where $*$ devotes convolution and S and F are the Fourier
transforms of s and f, it can be easily seen that the multi-
plication of the signal transform S with an adequate filter
and doing afterwards the inverse Fourier transform would
eliminate the noise correponding to the filter transform F.
In our case it would mean to apply a filter which eliminates
the frequencies f_1 and f_2 (a filter transform with zeroes
at this frequencies) and which presses all other frequencies
(ones). That would be an idealized multiband bandpass filter.

This method was applied to the last two images in fig.46
and the results can be observed in fig.48 .

It should be pointed out that this is a relatively very time
consuming algorithm, because of the double application of
the Fourier transform (direct and inverse) and because
the picture must be transformed in column direction and
is normally linewise stored in mass storage, a transposing
operation being therefore necessary prior to the filtering
operation.
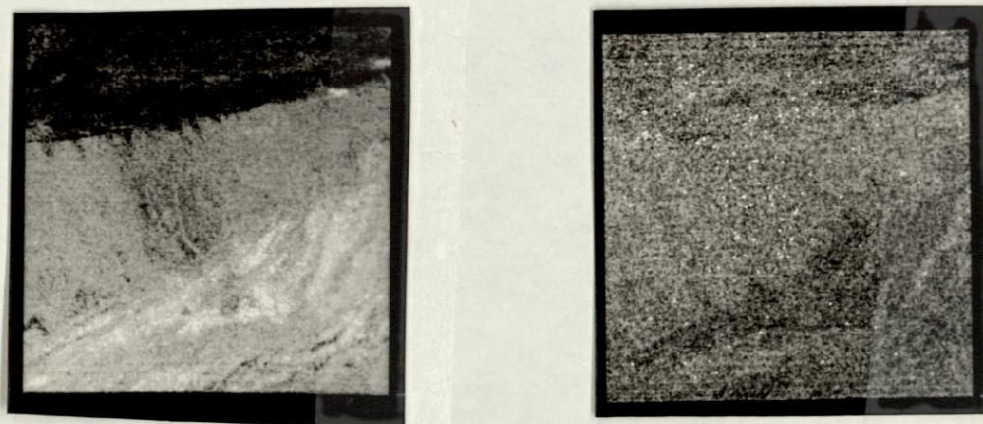
Fig. 48 a/b: 3rd and 4th principal component after filtering
in the frequency domain.

Design of a One-Dimensional Finite Impulse Response Filter

A very well known class of filters, the finite impulse
response (FIR) filters, is specially attractive for imple-
mentation, because very efficient algorithms already exist
for the design. A general expression for such a filter can
be written as follows

$$y\ (k)\ =\ \sum_{i=0}^{N-1}\ h\ (i)\ x\ (k-i) \qquad (c)$$

where N is the length of the filter, h (i), i = o ... N-1 its
coefficients (A) and x (k) is the input sequence or signal
(in our case a picture line or column) y (k) is the output
,or filtered sequence.

That is the expression for a discrete convolution, and ob-
viously, if we succeed in designing a filter which approximates
the ideal frequency response of the desired bandpass filter,
with only few coefficients, a considerable increase with respect
to the implementation with the Fourier transform could be attained.

A first problem must be in our case mentioned. We cannot
approximate a band pass filter with a finite number of
coefficients, so that
1) the relation (b) does not apply for the method applied
   in the foregoing section and therefore the results
   obtained in fig. 48 are not totally correct;

2) the FIR filter we will obtain only approximates the
   desired frequency response. Moreover, since we want to
   use as few coefficients as possible, this approximation
   cannot be very good;
3) if we increase the number of coefficients, a direct
   implementation through convolution will be impossible,
   so that we will be obliged to use the implementation in
   the frequency domain.

The expression for a bandstop filter is:

$$H(u) = \begin{cases} \emptyset, W_1 < u < W_2 \\ 1, u \leq W_1, \ u \geq W_2 \end{cases} \quad 0 \leq u \leq \pi$$

The inverse Fourier transform of this expression would be:

$$h(n) = \frac{1}{\pi} \left(\frac{\sin W_1 n}{n} - \frac{\sin W_2 n}{n} \right)$$

which has coefficients extending to $+\infty$, and therefore such filters cannot be exactly approximated by the filters of (c).

In our case we limited ourselves to the design of such a filter following an algorithm proposed by Mc CLELLAN and reducing the number of coefficients to 15.

The resulting filter has linear phase and is antisymmetric. Because of this antisymmetry we can save almost half the multiplications because the expression (c) can be written.

$$y(k) = \sum_{i=0}^{\frac{N-1}{2}-1} h(i) \quad X(k-i) - x(k-N+i+1) +$$

$$+ h\left(\frac{N-1}{2}\right) \cdot X\left(k-\frac{N-1}{2}\right) \tag{d}$$

The coefficients and design parameters of this filter is shown in fig. 5o

As already mentioned, the filter is only an approximation to the ideal case, first because it can only approximate the given frequency response, and second because we cannot specify frequency bands as narrow as desired. Obviously, the filter will cause a degradation because it will filter frequencies we don't actually wish to filter and moreover because of the ripple introduced by the approximation.

The result of filtering are shown in fig.51, for all four spectral channels, and even if we have filtered the striping noise, the degradation caused by the filter itself is evident.

```
*****************************************************************

              FINITE IMPULSE RESPONSE (FIR)
              LINEAR PHASE DIGITALFILTER DESIGN
              REMEZ EXCHANGE ALGORITHM

              BANDPASS FILTER

        FILTER LENGTH =  15

              IMPULSE RESPONSE
              H(  1) =  -.68341404E-02 = H(  15)
              H(  2) =  -.19531188E+00 = H(  14)
              H(  3) =   .16992465E-01 = H(  13)
              H(  4) =   .69750877E-01 = H(  12)
              H(  5) =   .38706068E-03 = H(  11)
              H(  6) =   .16015114E+00 = H(  10)
              H(  7) =  -.10545385E-01 = H(   9)
              H(  8) =   .58824886E+00 = H(   8)
```

	BAND 1	BAND 2	BAND 3	BAND 4
LOWER BAND EDGE	0.000000000	.150000000	.230000000	.315000000
UPPER BAND EDGE	.100000000	.180000000	.270000000	.345000000
DESIRED VALUE	1.000000000	0.000000000	1.000000000	0.000000000
WEIGHTING	1.000000000	10.000000000	1.000000000	10.000000000
DEVIATION	.342570848	.034257085	.342570848	.034257085
DEVIATION IN DB	-9.304991948	-29.304991948	-9.304991948	-29.304991948

	BAND 5	BAND
LOWER BAND EDGE	.390000000	
UPPER BAND EDGE	.500000000	
DESIRED VALUE	1.000000000	
WEIGHTING	1.000000000	
DEVIATION	.342570848	
DEVIATION IN DB	-9.304991948	

```
EXTREMAL FREQUENCIES
    0.0000000     .1500000     .1656250     .1800000     .2700000
      .3150000     .3306250     .3450000     .5000000

*****************************************************************
```

Fig.: 5o
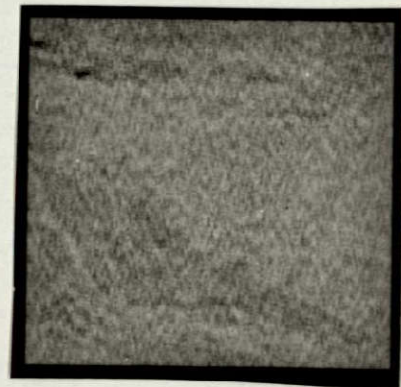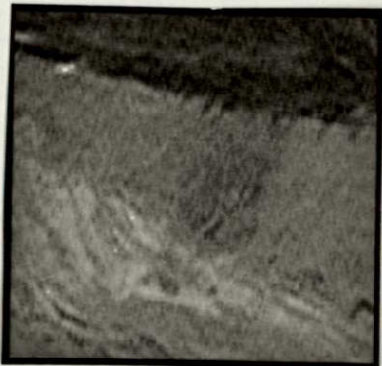
Fig. 51: FIR filter PC components.

BLANKET RELEASE FORM

In accordance with Memorandum of Understanding No. _____ between STID and

OSSA _____ ; OART _____ ; OTDA _____ ; OMSF _____ ; the attached document can be

Announced ✓ ; Not Announced _____ ; and has a distribution limitation as

follows:

☑ UNLIMITED

☐ U.S. GOVERNMENT AGENCIES AND CONTRACTORS ONLY

☐ U.S. GOVERNMENT AGENCIES ONLY

☐ NASA AND NASA CONTRACTORS ONLY

☐ NASA HEADQUARTERS OFFICES AND CENTERS ONLY

☐ NASA HEADQUARTERS ONLY

Remarks:

☑ NASA CR *158058* ☐ TMX _____ ACCESSION NO. _____

Analyst *F 3/5/79*

FF No. 864

Conclusions

Some aspects of the difficulties in the application of an
FIR filter for our particular problem are evident.
First, the effect of different band widths on the resulting
filter and therefore on the filtered image should be studied.
This must include also the number of coefficients, but it seems to
be impossible to approximate a filter with so few coefficients
as to allow the implementation as a convolution sum. Therefore,
the design with a large number of coefficients and the filtering
in the frequency domain should be carried out.
This would obviously not be an operative solution.

The second approach would be to design an infinite impulse
response filter (IIR), which can be implemented in a recursive
form and can provide sharper edges in the frequency response with
fewer coefficients than the FIR.

PART II

TECHNICAL DESCRIPTION OF THE IMAGE PROCESSING
SYSTEM ISI 47o AND ITS USE
FOR EDUCATIONAL PURPOSES

Technical description of the analog-digital image processing system ISI 47o

1. Software

Introduction

In this section the structure and capabilities of the image processing system software (originally called SWING) will be described. If the reader is interested in details of the programming system FORTH, which served as frame for the implementation of SWING, or if he needs some basic concepts for understanding the mechanics of SWING, he will find enough material in the literature referenced in this report (1), (2), (3), (4), (5).

The basic elements of SWING are:
- the Image Control Block (ICB)
- the Image Stack (IS)
- the Image Processing Loop (IPL).

In the following the structure of this elements and the interactions between each other will be described.

The Image Control Block

This is practically a list of variables resident in a core area. Each one of this variables or table entries, identified with a specific name contains an attribute of the image associated with the table.
Several of this areas are reserved at time of SWING loading, so that when the user wishes to get access to a definite physical image he only needs to associate it with any of the already existing tables.

A physical image can be a file on disc or one of the existing devices (TV monitor, optronics, magtape format, etc.).
The relation between physical images and ICBs can be represented graphically as in fig.52.
Fig.53 represents an ICB and how its entries are referenced.
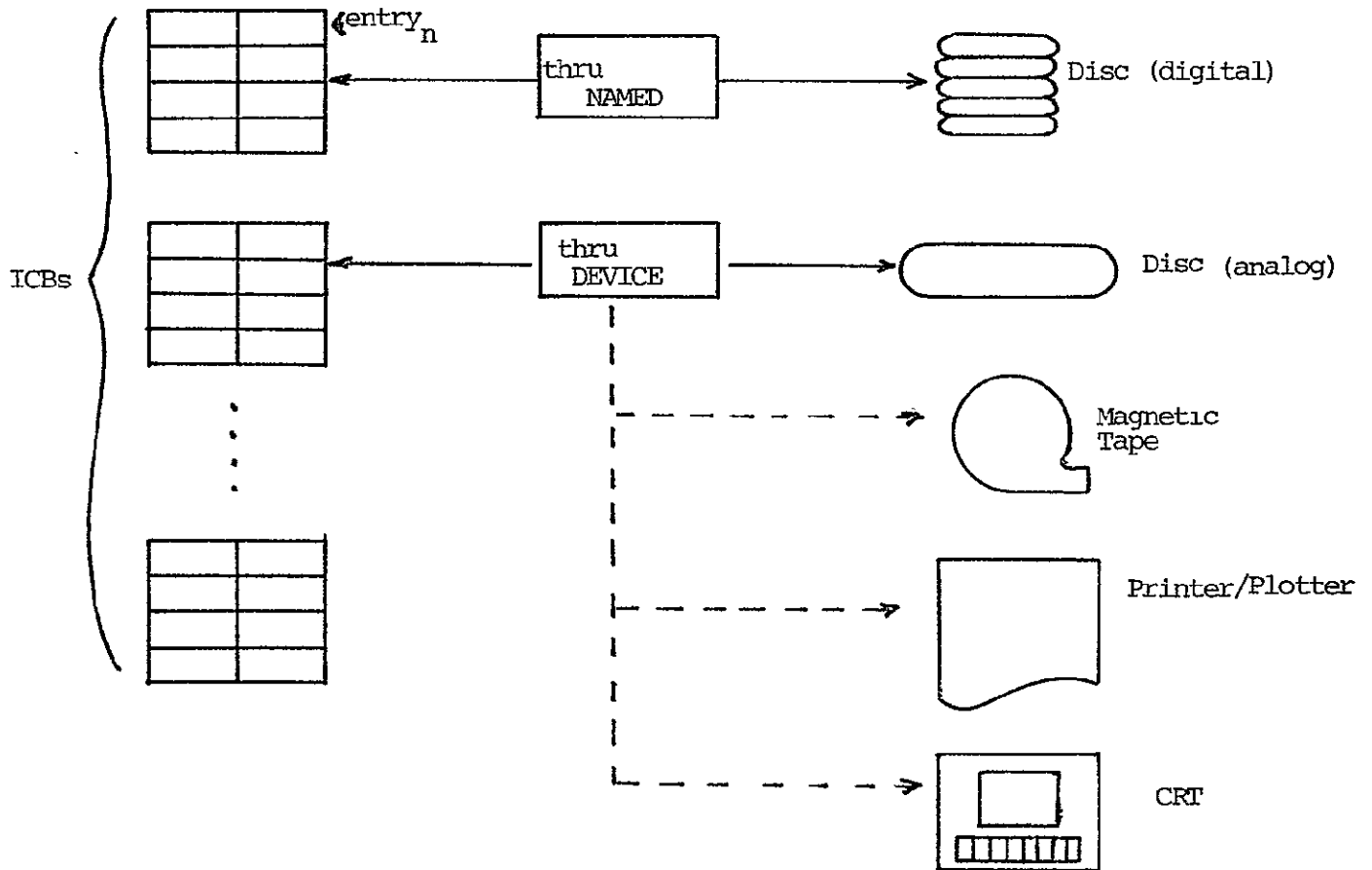
Fig.52:   Allocation Image/ICB

IMAGE ——→ [←—]   [ICB execution] Base   ICB
(user parameter)   Address   [   ] ID (name of entry)

                                                 [   ] NAME

                                                 [:]   :

                                                 [   ] →PREC

                                                 [   ] : NAME

Example: execution of ID

[CONTENTS of ID] ⎤
                 ⊕ ——→ = Address of this entry in primary ICB
[CONTENTS of IMAGE] ⎦
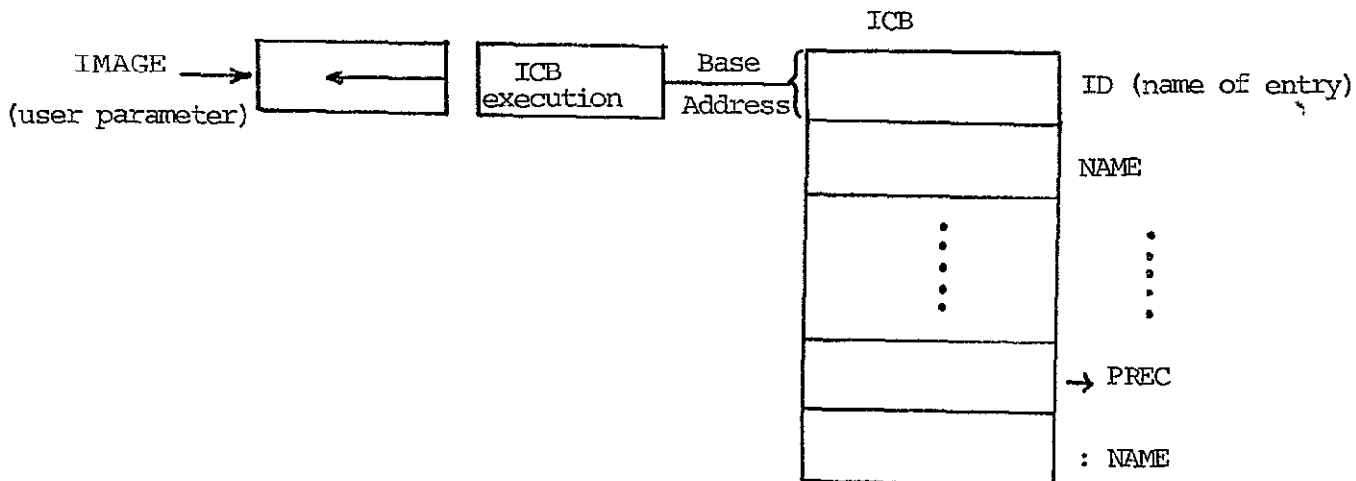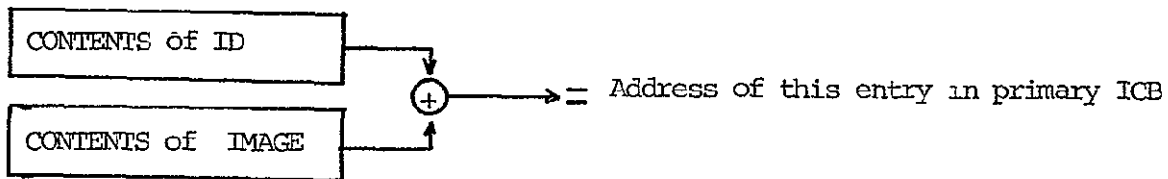
Fig. 53 : ICB's entries reference

Some of the entries in the ICB can be changed before starting
the processing so as to allow a choice of bands, subimage to
be processed, etc. Furthermore, an image file on disc will be
created by association of the file with an ICB and setting
interactively the parameters which define the image.
Each ICB has a name, and this is the name of a FORTH word which
at execution time will put the basis address of the ICB on
an entry of the user's control block. To obtain the contents of
a specified entry in the primary ICB only the bias of this
entry with respect to the basis address need to be known,
as shown in fig. 53. The ICB entry will be in the newest
referenced IBC.

The Image Stack

It works like a normal first in-last out list, where the basis
address of the ICB is stored each time that an ICB is
referenced by its name as mentioned above.
In this way several ICBs can be stored and afterwards retrieved
for processing. This characteristic allows the concatenation of
processing commands.

The Image Processing Loop

A large class of image processing algorithms works on the
arguament picture in a sequential mode, normally processing
the whole picture line by line.
At each picture element the same operation will be applied for
the whole picture, depending on the result desired.
Independently the whole input/output management and the
supervising of the sequential process don't need to be of
concern for the person interested in the processing.
The aim of the IPL is to assume this control of a previously
defined process, and the mechanics of the IPL are shown in fig. 53.

The key to the whole is the value of a status indicator, the variable ISTATE, which tells in which stage of the operation the system is.

The PROCESS area of fig.54 is given in more detail in fig. 55. This table is filled by the user with arguments (images and parameters) through the processing commands. It could be assumed to be a program at the highest possible level (the image processing language).

The user enters data and addresses pointing to executable code in the process in the following way

$$\text{image }_1 \ldots \text{ image }_n \text{ parameter}_1 \ldots \text{ parameter}_m \text{ command}$$

The command fills the PROCESS as shown, but the contents of it will not be executed.

The command TRANSFER includes the contents of the PROCESS within an IPL and starts it.

The process will be executed beginning with the first ICB, which puts its basis address on the stack, then the second and so forth. The parameter list will be jumped over and the sequence continues entering the operation driver.

The code executed by the operation driver depends also on the status variable ISTATE and its structure is shown in fig. 56. If this variable has the value 3, the code defined by the user will be executed.

The user can easily determine which operation driver he needs for a specified operation and which parameters his program will receive at execution time. Usually they are byte addresses of input and output data and number of pixels. He can retrieve the parameters entered before the TRANSFER from the PROCESS and operate with them and with the picture data.

Normally he only needs to observe some easy rules and can write in FORTH or symbolic assembler the code he wants to be executed.

Initialize IPL

PROCESS

(Process area)

ISTATE ? | O | No → | 1 | No → | 2 | No → | 3 | No → | 4 | No → | 5 |
Yes   Yes   Yes   Yes   Yes

lock buffer.
increment
ISTATE

initialize
band. increment
ISTATE

initialize row.
increment
ISTATE

increment row.
if ready with
all rows incre-
ment ISTATE

Set next band
to be processed
ISTATE ← 2
if all processed
inc. ISTATE.

Free locked
Buffers.   END
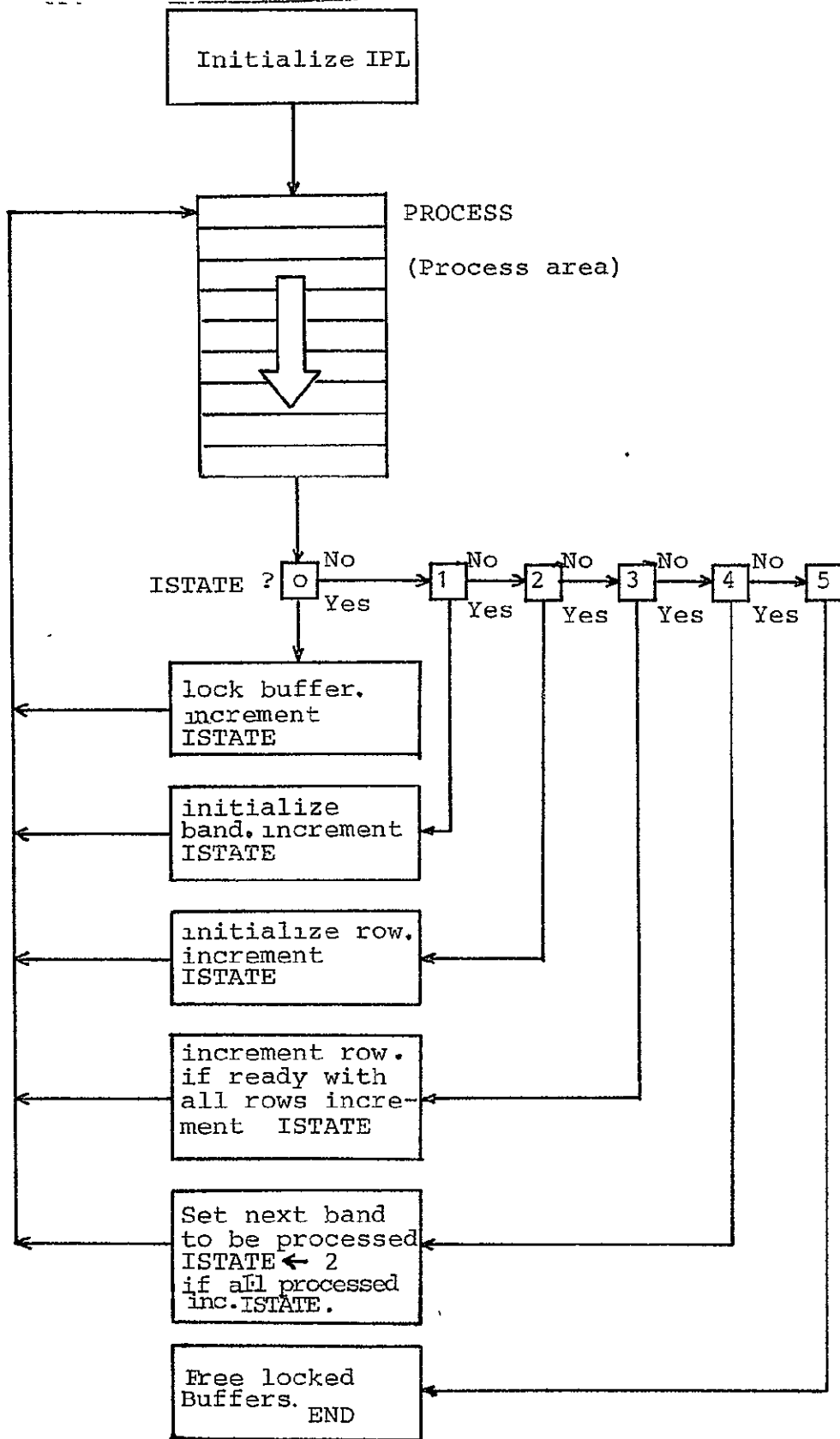
Fig.54: Control Flow of Image Processing Loop.

Lower
Memory

Code Address of Image$_1$
$\vdots$
C.A. of image$_n$
C.A. of word which jumps to end of parameter list
$\vdots$ parameter list $\vdots$
C.A. of Operation Driver
C.A. of code for this processing command
Next blocks similar to preceding one. One for each processing command.
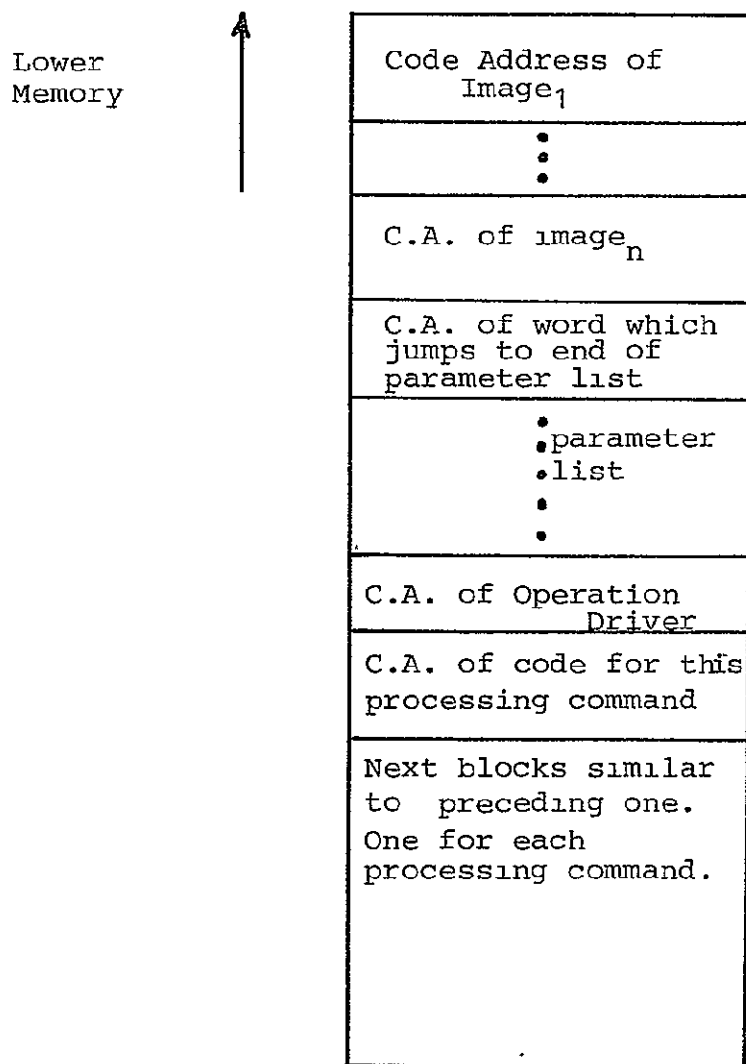
Fig. 55:   Contents of Process Area.

from last ICB
execution in
process

continue in
process

o   No ──────→ 1   No ──→ 2   No ──→ 3   No ──→ 4   No ──→ 5

Yes   Yes   Yes   Yes   Yes

Validate argument
image attributes

Allocate core
buffer

Set pointers to
1st band in
device

I/O Management
and do user
programmed process

Output contents of
in core remaining
buffers

Reset parameters
for next transfer
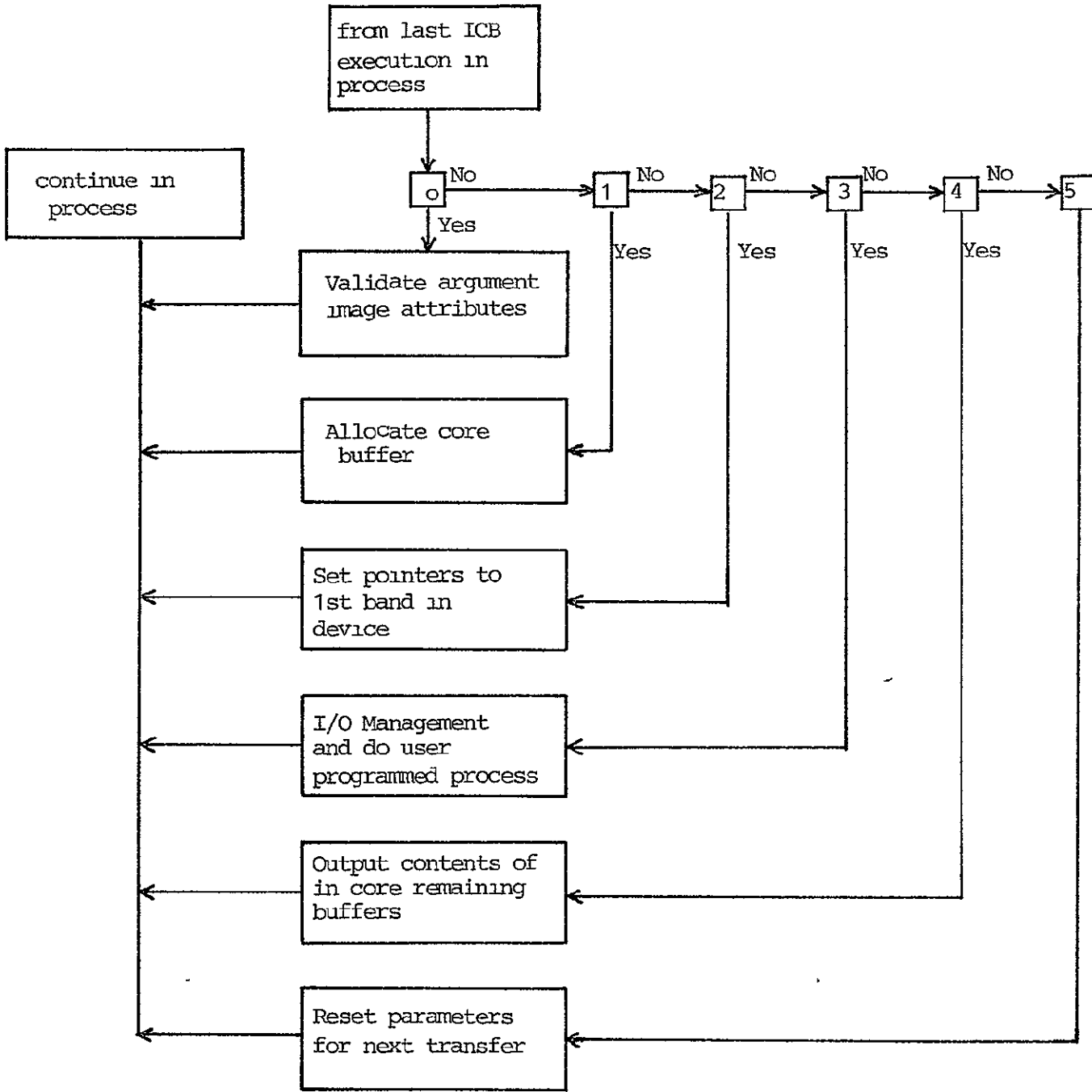
Fig.56:   Basic Structure of Operation Driver.

1)   FORTH - An application oriented language - Introductory
     Programmer's Guide
     Forth, Inc. - Manhattan Beach, California

2)   FORTH Technical Mannual
     Forth, Inc.

3)   FORTH-PDP-11 Supplement
     Forth Inc.

4)   Minicomputer Programming in FORTH. E.D. Rather, C.H. Moore,
     Forth Inc.

5)   FORTH: A New Way to Program a Mini-Computer.
     C.H. Moore, Astron. Astrophys. Suppl. 15, pp 497-511.

Image Processing Language Syntax and Available Commands

The syntax was already specified in the previous section.
The language consists of commands preceded   (or followed)
by arguments.
These arguments can be images (input, output) and parameters
(constants).
After the arguments and the code corresponding to a command
have been prepared for a posterior execution by TRANSFER,
the output ICB remains on the image stack. This ICB can
serve as input image for the following command, so that more
of them can be chained together. The chaining images don't
need to be existing ones, because since the process is executed
line by line, only the first and the last in the line need to be
physical images where the results will be stored. Of course,
some processes cannot be chained because they require global
information of the proceeding step, as is the case for the
principal components transformation, where the covariance
matrix of the whole image is needed before. Other cannot be in-
cluded in the process because they don't work in a sequential
way, as is the case for the image transpose.
Nevertheless, there are a large class of processes which can be
carried out sequentially and therefore can be programmed as a
chain of already existing processes, like the hyperbox
classification.
Finally, the next pages show a list of the available commands
with a short description of the operation associated with them.

Transient and buffer management utilities

BUFFERGET   Modify buffer area in order to allow processing of images larger than 1 K byte x 1 K byte

TEGSPACE   Restore original configuration of buffer area modified previously by BUFFERGET.

$WORDS

Loading word   Load   transients loaded by loading word (after that not deletable by C)

CWORDS   Delete commands loaded by $WORDS

Optronics Commands

inimage	raster size	!OPTRONICS	Enter a field corresponding to the size of <u>inimage</u> and <u>raster size</u> in the optronics film map file, with the position determined by the MAF.
		OPTRONICSHOW	Display on TV-monitor the optronics film map file.
		OPCLEAR	Clear the optronics film map file (for a new sheet of film)

Loading Words

GRIDS	Load support for the GRID processing command
PATTERNS	Load pattern generator
PRINTING	Load system diagnostic support
TAPING	Load magnetic tape support

Words associated with the PROCESS

C   clear the PROCESS and FORGET all transients

R   clear the PROCESS

MORE   allows adding more commands to the PROCESS after a TRANSFER

CDUMP   print a PROCESS dump

TRANSFER   execute the PROCESS

Image and system status utilities

	*HEADING	Print disk image heading content report
	*STATUS	Print ICB content report
	ICBS	Print report of all ICBS
n	ISTATUS	Print a STATUS report for top n images on the image stock
	STATUS	Print STATUS report.

Image File Management

            *ALLOCATE   Allocate a disk image file

            *CLOSE   Close a disk image file

            *CREATE   Create a disk image file (ALLOCATE is faster, use CREATE only if a zeroed file is needed)

            *OPEN   Open a disk file image

<u>Other commands</u>

TMP   Generate a TEMPORARY ICB

1 NULL   Generate a NULL ICB

image   ITRANSPOSE   transpose <u>image</u> (allowed size = 2^n x 2^n)

Image Statistics Utilities

	QHIST	Print 16 category histogram
at	NHIST	Print detail of histogram beginning with at
n	ZGFHIST	Print histogram with adjusted maximal percentage n
	STATISTICS	Print STATISTICS report
	?HISTOGRAM	Print STATISTICS report and histogram content report
	?COVMAT	Print actual covariance matrix
	?PRINCIPAL	Print actual eigenvalues and eigenvectors
	CORREL	Print actual matrix of correlation coefficients
	?MAPPED	Print mapped histogram

inimage	COVMAT	b	Calculates covariance matrix
inimage outimage	HCTRANS	bw	Principal components (inimage)→outimage
inimage outimage h.scale			
v.scale 1st col. 1st row	?TEXT	b	Writes a text on outimage beginning at 1st row 1st col. and extending horizontally. The character size is given by h.scale and v.scale
inimage (1) outimage (1)	1 > FFT	dw	one-dimensional Fourier Transform
inimage (1) outimage (1)	1 < FFT	dw	one-dimensional Fourier Transform (Backwards)
inimage (1) outimage	POWER	dw	power spectrum (inimage) → outimage
$inimage_1$ $inimage_2$ outimage	IFMUL	dw	$(inimage_1)$ ✶ $(inimage_2)$ → outimage
inimage (dwnd) outimage (word)	SF > W		(inimage)+n → outimage
outimage width position	STEPFILT	dw	create notch symmetric filter at (positon) with (width)
outimage width position	EXPFILT	dw	create exponential filter (smooth notch) at (position) with (width)
inimage (byte) outimage (word)	FIRFILTER		Filter inimage with filter coefficients stored on tape
inimage (DWORD) outimage (byte)	PSCALE		logarithm (inimage)→ outimage with output values between $\emptyset$ - 255
inimage	WEXTREM	w	Determine maximum and minimum of inimage and store on inimage file
inimage	FEXTREM	dw	Determine max. and min. of inimage and store in inimage file.

(1)   two band image (real and imaginary)

Piecewise Table Mapping Utilities

	PIECEWISE	Load piecewise mapping table words
	TBLGET	Gets are for piecewise table
	RELTBL	Releases table per piecewise table
start end value	FILLTBL	Fill piecewise table from start to end with value
startpos endpos startval endval	LINEAR	Sets piecewise table from startpos to endpos with values from startval to endval
start end	LSEG	Sets piecewise table from start to end with own values
start end	PASS	Sets piecewise table from start to end with own values, ∅ below, 255 above
	TBLSHOW	Print piecewise table
position value	VSET	Stores value at position of the piecewise table
	ZAPTBL	Zeroes piecewise table
	?MAPPING	Print mapping table

Processing Commands

inimage outimage gain bias	*+TBL	b	$(\underline{inimage} * \underline{gain}) + \underline{bias} \rightarrow \underline{outimage}$
inimage outimage mult div	*/TBL	b	$(\underline{inimage} * \underline{mult}) / \underline{div} \rightarrow \underline{outimage}$
inimage outimage mult	*TBL	b	$\underline{inimage} * \underline{mult} \rightarrow \underline{outimage}$
inimage outimage div	/TBL	b	$\underline{inimage} / \underline{div} \rightarrow \underline{outimage}$
outimage	+DIAG	b	Send an upward sloping diagonal ramp (up from left to right) to $\underline{outimage}$
inlimage in2image outimage	+SCATTERGRAM		Add the scattergram of $\underline{inlimage}$ (byte) and $\underline{in2image}$ (byte) to $\underline{outimage}$ (word)
outimage	-DIAG	b	Send a downward sloping diagonal ramp (down from left to right) to $\underline{outimage}$
inimage outimage low high	-NOTCH	b	Map values between $\underline{low}$ and $\underline{high}$ (inclusive) to 0, others to 255
inimage outimage	16STEPS	b	Map continuous $\underline{inimage}$ to 16 steps in $\underline{outimage}$
inimage outimage	8STEPS	b	Map continuous $\underline{inimage}$ to 8 steps in $\underline{outimage}$
image outimage adj gain atten bias	<BYTE		$(((\underline{inimage}\text{ (byte)} + \underline{adj}) * \underline{gain} / \underline{atten}) + \underline{bias} \rightarrow \underline{outimage}$ (wor
image outimage adj gain atten bias	<WORD		$(((\underline{inimage}\text{ (word)} + \underline{adj}) * \underline{gain} / \underline{atten}) + \underline{bias} \rightarrow \underline{outimage}$ (byt
inlimage in2image outimage	ADD	bw	$\underline{inlimage} + \underline{in2image} \rightarrow \underline{outimage}$
inimage outimage	B>W		$\underline{inimage}\text{ (byte)} \rightarrow \underline{outimage}$ (word)
inimage outimage	BITCOUNT	b	$bitcount\ (\underline{inimage}) \rightarrow \underline{outimage}$
inimage outimage low high	BTWN	b	Map values between $\underline{low}$ and $\underline{high}$ (inclusive) to 255, others to 0 (Does not generate a mapping table.)
image outimage CLASSIFY values		b	Classify $\underline{inimage} \rightarrow \underline{outimage}$, 0 is not in, 255 is in, $\underline{values}$ specify a hyperbox

Command	Name	Type	Description
inimage outimage thresh n	CLEAN	b	Zeroes non-zero cells with fewer than n neighbors which are greater than or equal to thresh and sets to 255 all cells with n or more neighbors which are greater than or equal to thresh
inimage outimage adj gain atten bias	CNVT		$(((\text{inimage} + \text{adj}) * \text{gain}) / \text{atten}) + \text{bias} \rightarrow \text{outimage}$ (byte $\rightarrow$ word or word $\rightarrow$ byte)
inimage outimage	CONTOUR	b	Contour inimage $\rightarrow$ outimage
inimage outimage	CONV	b	Convolve inimage $\rightarrow$ outimage (3 x 3 blocks)
inimage outimage	COPY	bw	inimage $\rightarrow$ outimage
inlimage in2image outimage	DIV	bw	inlimage / in2images $\rightarrow$ outimage
inlimage in2image outimage	EQ	b	inlimage = in2image $\rightarrow$ 255 $\rightarrow$ outimage else 0 $\rightarrow$ outimage
inimage outimage thresh n	EQINT	b	Map inimage $\rightarrow$ outimage in n equal-width levels based on the histogram of inimage ignoring values with less than thresh occurrences
inimage outimage n	EQPROB	b	Map inimage $\rightarrow$ outimage in n levels each having equal probability as determined by the histogram of inimage
inimage outimage	EXPMAP	b	Adjusted exponential function
inimage outimage	GRID	b	Superimpose a grid on inimage. Requires GRIDS.
inlimage in2image outimage	GT	b	inlimage > in2image $\rightarrow$ 255 $\rightarrow$ outimage else 0 $\rightarrow$ outimage
inimage outimage	HISTOGRAM	b	Gather histogram of inimage and place with outimage if possible
outimage	HRAMP	b	Send a horizontal (constant left to right) ramp to outimage
inlimage in2image outimage	LAND	bw	inlimage AND in2image $\rightarrow$ outimage
inlimage outimage	LNMAP	b	Adjusted logarithm function
inlimage in2image outimage	LOR	bw	inlimage OR in2image $\rightarrow$ outimage
inlimage in2image outimage	LT	b	inlimage < in2image $\rightarrow$ 255 $\rightarrow$ outimage else 0 $\rightarrow$ outimage

inl1image in2image outimage	LXOR	bw	inl1image Exclusiv OR in2image --▷ outimage
inimage outimage mod	MODTBL	b	inimage modulu mod --▷ outimage
inl1image in2image outimage	MUL	bw	inl1image * in2image --▷ outimage
inimage outimage thresh max	NMAX	b	Normalize to maximum max using thresh as the threshold based on histogram
inimage outimage thresh min	NMIN	b	Normalize to minimum min using thresh as the threshold based on histogram
inimage outimage thresh min max	NORM	b	Normalize to minimum min and maximum max using thresh as a threshold. Based on histogram
inimage outimage low high	NOTCH	b	low ≤ inimage ≤ high ⇒ 255 --▷ outimage else 0 --▷ outimage
	PRESERVE		Preserve mapping table with disk file of input image

inl1image in2image outimage numgain numbias dengain denbias RATIO b

Compute ratio:

$$\frac{(inl1image * numgain) + numbias}{(in2image * dengain) + denbias} \longrightarrow outimage$$

inimage outl1image out2image	REPLICATE	b	Replicate inimage to both outl1image and out2image
inimage outimage inlow inhigh outlow outhigh	RERANGE	b	Rerange inlow to inhigh to the range of outlow to outhigh
inimage outimage	REVERSE	b	Reverse the values, (255 minus inimage) --▷ outimage
n	SCALAR	b	Create an image with a value of n; used in place of an ICB reference
inimage outimage vnum vden hnum hden	SCALE	b	Scale up or down by vnum/vden in the vertical direction and by hnum/hden in the horizontal direction
inl1image in2image outimage	SCATTERGRAM		Create the scattergram of inl1image and in2image in outimage

inimage outimage   SD_TRETCH   b   Map using standard deviation stretch

inimage outimage   SHOWHISTO   b   Show the histogram of inimage on outimage

inimage outimage   SHOWMAP   b   Show the mapping table of inimage on outimage

inimage outimage thresh   STRETCH   b   Stretch the above thresh value range of inimage to 0 through 255 based on histogram

inlimage in2image outimage   SUB   b   inlimage - in2image --▷ outimage

inimage outimage   SQRTMAP   b   Adjusted square root function

inimage maskimage outimage thresh   TMASK   b   If maskimage > thresh, copy the corresponding cell of inimage --▷ outimage else do nothing

inimage outimage   USETABLE   b   Use the piecewise mapping table

outimage   VRAMP   b   Send a vertical ramp (constant columns) to outimage

inimage outimage   W▷B   inimage (word) --▷ outimage (byte)

Image Editor Commands

startrow endrow startcol endcol	!WINDOW	Set the window as specified
n	+D	Move the window down n rows
n	+L	Move the window left n columns
n	+R	Move the window right n columns
n	+U	Move the window up n rows
	.WINDOW	Print the window limits: startrow: endrow, startcol: endcol
	D	Move the window down 1 row
value startrow startcol endrow endcol	DRAW	Draw a line with value from (startrow, startcol) to (endrow, endcol)
value row column	I!	Store value at (row, column)
row column	I?	Print the contents of (row, column)
row column	I@	Fetch the contents of (row, column) onto the parameter stack
	GETWINDOW	Set the window from the MAF-1 frame
	L	Move the window left 1 column
	POSITIONING	Load +D, +L, +R, +U, D, L, R, and U for use
	R	Move the window right 1 column
value	RFILL	Fill the window with value
	SHOW	Show the contents of the window
	SWIN'	Use the subimage of the active image as .ie window
	U	Move the window up 1 row

DV-8 Commands

	ALIGN	Align on next track; allows up to 4 bands to be shown simultaneously
a b	ALTERNATE	Alternately display track a and b 10 times for 1 second each
	GETFRAME	Read the MAF-1 frame and place on the parameter stack
	LOCATE	Display last output which was written out using the active ICB
	NTK	Display next track
	PTK	Display previous track
start stop n	REPEAT	Repeat SWEEP n times
n	SEEK	Seek to channel n
start stop	SWEEP	Display tracks start through stop in turn for 2 seconds each
track	TRACK	Seek to channel 1 of track
n	TSK	Skip over n channels before beginning output
?CURSOR		Read cursor values and put them on the parameter stock.

Image Attributes

	NAMED name	Sets the filename to <u>name</u>
	NULL	Selects the null device
p	PRECISION	Sets the precision (p = BYTE or WORD/DWORD
	PRIMARY	Selects the active ICB as the primary ICB also
n	ROWS	Set image size to $\underline{n}$ rows
rows columns	SIZE	Set image size to the specified number of <u>rows</u> and <u>columns</u>
	SPAREBANDS	Set the number of spare bands to $\underline{n}$
startrow endrow startcol endcol	SUBIMAGE	Set the subimage
n	SYMBANDS	Set the number of symbolic bands to $\underline{n}$
	TAPE	Select SWING magnetic tape as the device (not implemented)
	TEMPORARY	Select the temporary device
	UNDER username	Set the current user id and the ICB user id according to username
	WHOLEIMAGE	Set the subimage to the size of the image
	RECORDER	Select Optronics film recorder as the device (output only)
	TELESPAZIO	Select TELESPAZIO tape as the device (input only)
	OLIVEN	Select Bendix M^2S tape as the device (input only)

Image Attributes

	12BAND	Select 12 channel tape as the device (input only)
	ALL	Select all bands (data and symbolic) for processing
	ALLDATA	Select all data bands for processing
	ALLSYM	Select all symbolic bands for processing
	BAND n	Select band n for processing
	BYTE	As in BYTE PRECISION
	CAMERA	Select camera as the device (input only)
n	COLUMNS	Set image size to n columns
	COPYOF from	Copy the ICB from to the active ICB
	CRT	Select the terminal as the device (output only)
	CSUB to	Copy subimage from active ICB to to ICB; make to active
n	DATABANDS	Set the number of data bands to n
	DISK	Select (digital) disk as the device
	DISPLAY	Select analog disk as the device (output only)
	GETSUB	Set subimage from the MAF-1 frame
	HARDCOPY	Select the printer/plotter as the device (output only)
	LANDSAT	Select LANDSAT tape as the device (input only)
	LIKE from	Copy selected items from the from ICB to the active ICB

Image Header Editor Commands

n	!ANCILLARY name	Setup current user id and name as the n-th ancillary file
value	!HASPECT	Set horizontal aspect to value
value	!HSCALE	Set horizontal scale to value
value	!LAT	Set latitude to value
value	!LONG	Set longitude to value
value	!VASPECT	Set vertical aspect to value
value	!VSCALE	Set vertical scale to value
number	?ANCILLARY	Print ancillary file name and user id of the n-th ancillary file
	?CAPTION	Print the caption
	?HASPECT	Print the horizontal aspect
	?HSCALE	Print the horizontal scale
	?LAT	Print the latitude
	?LONG	Print the longitude
	?VASPECT	Print the vertical aspect
	?VSCALE	Print the vertical scale
	CAPTIONED caption	Set the caption
	HDREDITOR	Load all of the above commands except ?CAPTION and CAPTIONED (which are normally loaded)

2. Hardware

A detailed description of the system hardware ist out of
the aim of this report. Only a brief description of some
unusual components appearing in fig.58 will be given,
specially concerning the analog system ISI 15o.

The analog system communicates with the computer through
the DV-8, which is capable of D/A-A/D conversion and video
formatting of the data. This permits the digitalization of
TV frames from the video disk and the storage of D/A converted
and video formatted pictures in the video disk. A total of
6oo TV frames can be stored and selected for display nor-
mally with the disk controller or by a program through the
DV-8. The VP-8 and AP-3 allow some very simple image mani-
pulations to be carried out in real time (arithmetric
operations, false color, equidensities, etc.) and trans-
parencies can be read on video disk through a TV camera.
A description of the very well known digital components is
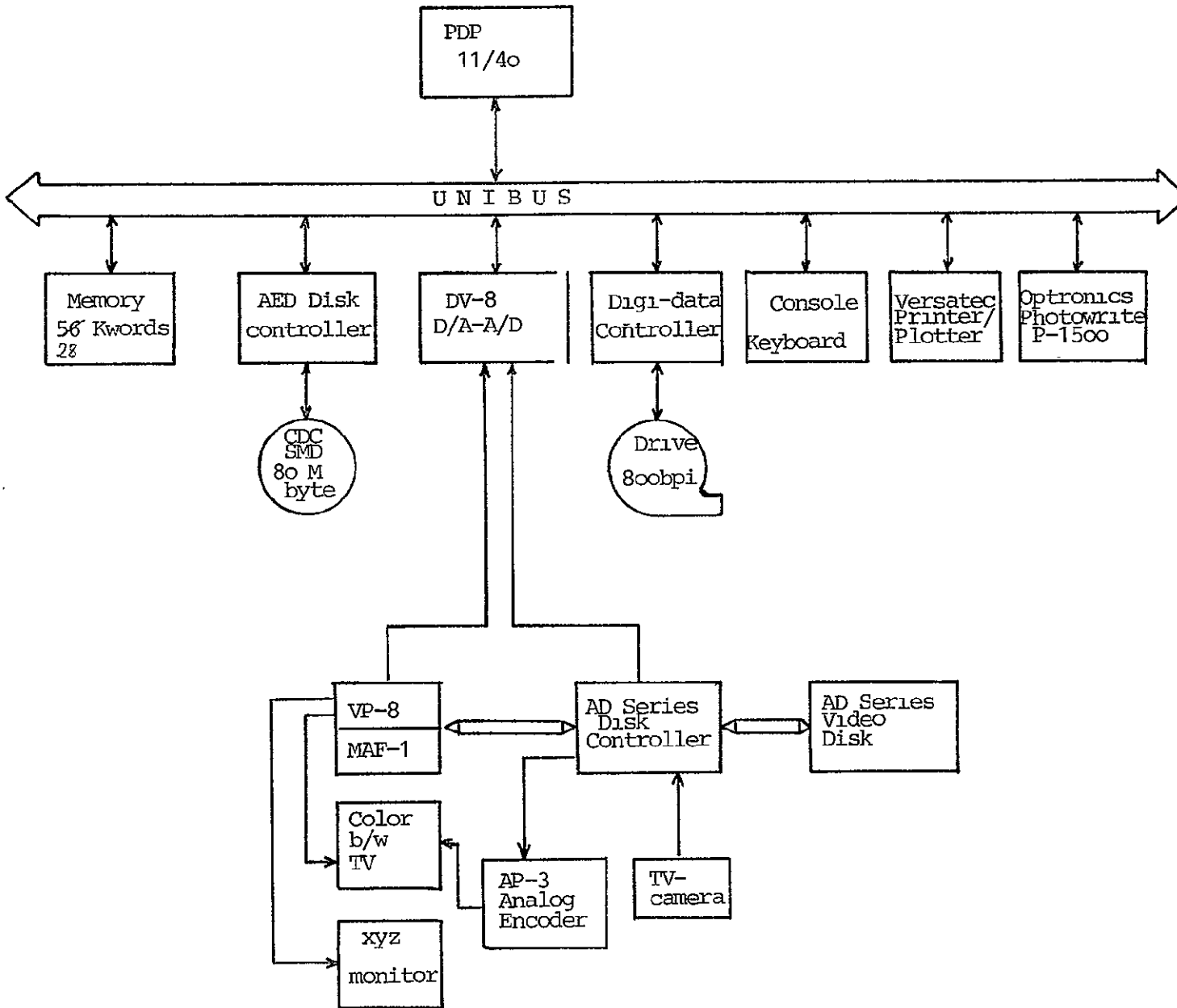not necessary.

View of the image processing system.

Fig. 58 :   Hardware Configuration

8. The Use of the System 47o for Educational Purposes

The combination of analog and digital data processing
techniques - the hybrid concept - probably has disadvantages
with respect to the user's interactivity through the
TV-display which is optimally given on the basis of a
digital refresh memory.
Nevertheless, we have decided to move towards a hybrid
data processing concept, because there exist certain
advantages which are indispensible with respect to the
introduction and training at earth scientists in the use
of remote sensing data.
During the last years we have experienced that there exists
a tremendous communication gap between technical oriented
and science oriented people. The lack of communication
becomes evident, if the earth scientist becomes involved
in digital processing of data.
From the technical side a variety of possibilities to process
multispectral data are offered. The operator normally is not
able to identify the earth scientific problem and the earth
scientist is not capable to identify the kind of processing
required or even to recognize the information exhibited by
multispectral data.
Because of above mentioned problems and the significance
of applying image data processing techniques we are using
our hybrid system under two aspects:

1) To introduce potential users of remote sensing
   methods to the data he has available.

2) To help establish experience in handling the
   data.

In the following a short description of above aspects is
given.

Under normal situations the unexperienced user community
is confronted to bulk data products such as black and white
copies of individual bands or color composites.

This kind of data probably exhibit a trememdous amount of
information identifiable immediately.
In order to fully utilize and recognize the information
content, the user must be in a position to carry out some
additional manipulations on the data. We have learned,
the best results in terms of motivation and output were
obtained if the scientist is experiencing the effects of
processing on the data personally.
Under this aspect the hybrid data processing concept is
optimally suited and we are using the following approach:

1) Make available of 1 or 2 CCT's exhibiting the
   area of interest.

2) Digital enhancement of the area of interest
   (histogram stretch) transfer and storage of
   enhanced data onto the video disc for display
   and analog processing purposes.

3) Introduction of analog processing system to the
   user. In order to fully use the analog system, a
   training of 1⁻2 hours is sufficient.

4) The user is left with the analog system where he
   can perform in realtime.
     - ratio processing
     - linear transformations
     - flicker operations
     - color composition of originally or analog
       preprocessed data
     - density slicing on original or analog
       preprocessed data
     - pointwise readings of densities
     - density profiles.

Normally the user spends several hours manipulating
the data.

5) Discussions with the user about the earth scientific
   problems he wants to investigate.
   The experience has shown, that after spending some
   hours with the analog system, the user is capable
   to discuss his requirements and he is able to
   demonstrate to the operator the phenomenon he is
   interested in.
   In many cases he even experienced and extracted additional
   information

6) Digital processing of the data.
   On the basis of previous discussions the operator
   tries to digitally enhance and display the identified
   phenomena in order to provide the user with a high
   quality film product (photo-write) for further inter-
   pretation.

Above described approach has been carried out with earth
scientists representing geology, vegetation sciences,
hydrology and oceanography. Of special interest is the
experience that the requirements towards the application
of automatic classification procedures is decreasing on
the basis of increased experience in handling the data.
This matter of fact is probably related to the increased ability
of the user to critically explore multispectral data
which has to be built up in an itterative learning process.

PART III

SUMMARY OF USER REQUIREMENTS WITH RESPECT TO

OPERATIONAL SATELLITE REMOTE SENSING AND

ITS IMPACT ON THE DEFINITION OF AN EUROPEAN

SATELLITE SYSTEM

With respect to Landsat 1 and 2 investigations
which are being carried out with users re-
presenting various desciplines, during the
last years the capabilities of Landsat and
additional user requirements were discussed
in detail. In addition to this we participated
in activities of ESA's Remote Sensing Working
Group, RSWG, (Chairman J. Bodechtel), which set
up multinational working parties to define user
related requirements from the European stand-
point.

In the following chapter a summary of our
experience concerning key applications and
resulting user requirements is given. The
manifold discussions led to a concept of an
earth resources satellite which was defined
together with Messerschmitt-Bölkow-Blohm (MBB).

The basis knowledge of the earth for solving environmental problems more and more assume global proportions. The application of spaceborne and airborne remote sensing techniques has proved their potential for various scientific and economic disciplines. The evaluation of Landsat and Skylab data has shown that global and continental (european) user requirements can be met with spaceborne techniques. Imagery from satellites in relatively low earth orbits and subsequent interpretation has to be part of the efforts aimed at accomplishing these permanent future tasks in an efficient manner. The final goal will be the application of those techniques in application oriented operational satellite systems.

For the definition of tasks concerning earth observation by spaceborne remote sensing techniques, outstanding advantages are:

- synoptic view and analysis of regional conditions and interrelationships of large and medium size areas
- continuous observation and monitoring of dynamic features as well as permanent targets on the earth surface.

Multispectral and multitemporal data acquisition from satellite platforms for large scale phenomena, interrelationships and changes are approaching within the next 1o years on operational phase. Satellites will be the first order platform for global and regional tasks.

Europe defined and further has to define its own needs and a global system has to meet and include if possible all those requirements. Certain scientific and problem areas of static phenomena and dynamic processes in natural resources monitoring and management, in environmental monitoring, in monitoring changes in phenology, land use and hydrology, only to mention some tasks, have to be solved by remote sensing and equipment and programs have to be adapted to these needs.

In fulfilling the need of continuous monitoring with high
repetition rate, beside Earth and Ocean monitoring-satellites,
the data of weather satellites like Meteosat, will be useful
for largescale correlation of fast changing phenomena.

Within a research program the more operational aspect of
remote sensing has to be considered. This involved not only
investigations concerning the feasibility of remote sensing
as a basis, but also the definition of relevant applications
and as a final goal the optimization of technical and
scientific requirements.
Intensive studies on the spectral behaviour of surface
features are carried out. The present investigation is main-
ly restricted to the visible and infrared part of the
spectrum. Future basic investigations will have to concentrate
more on the microwave region of the spectrum not least due
to its independence of the weather.

One further task is the development of automatic evaluation
models based on spectral characteristics varying in illumi-
nation and seasonal changes. Those models are the basis for
the indispensable automatic data evaluation for thematic
cartography of different and varying earth surface features.

The latter goal will be a main requirement to keep the data
output on a level which is compatible with the data evaluation
capacity and capability of the user community.

1. Key Applications for an Operational System

The overall objectives can be envisaged for both regional
and global tasks. Of first order are the regional tasks

- to monitor dynamic features in developed regions such
  as Europe, and possibly in selected areas within the
  developing regions;

- to provide basic resources information for developing

regions to be used within the framework of development aid programs.

Global aspects are
- to monitor the global oceans,
- to monitor the global atmosphere, in particular with respect to the climate and climate changes, and air quality measurements,
- to map global resources such as basic food supplies, soils and forests.

The involvement depends on internal Euroepan priorities. High priority must be given to the implementation of regional space systems providing data that can be applied both in Europe and within the framework of development aid programs.

It is important to consider that the interest of Europe extends beyond its political boundaries. It includes global monitoring of the oceans and atmosphere, the use of remote sensing data within the framework of development aid programs, and to monitoring global resources (e.g. food supplies and raw materials) of vital interest to a continent highly industrialized and poor on natural resources.

The main emphasis is placed on the management and conservation of known resources, rather than in the exploration and exploitation of new resources. The two main exceptions to this general rule are the continental shelf areas and Greenland. This emphasis in resource management leads to the requirements to monitor at high resolution the changing features of the European landscape.

The dynamic character of the main requirements plus near continuous cloud cover over many European regions, point to the need to develop high resolution all-weather remote sensing capabilities.

The following table lists key areas where an operational satellite system could support to solve important tasks.

Key Applications of Major European Interest

Land Use

Land use mapping and classification, ecological mapping, regional and urban planning, real time land use data-bank for dynamic parameters.

Agriculture and Forestry

Statistical information on agricultural products = crop inventory, yield prediction for key crops.
Agrometeorological monitoring
Forst inventory, monitoring of the green wave.
Soil moisture and irrigation monitoring.
Monitoring of vegetation desease and stress.

Extractive Resources

Basic studies in tectonics, lithology for mineral exploration and prospecting - thematic mapping.
Monitoring of changing secondary indicators (e.g. vegetation, soil moisture) for detecting anomalies due to subsurface geology, mineralization, thermal anomalies etc.

Inland Water Resources

Monitoring of snow coverage and snow melt,
Calculation of run off.
Areal monitoring of precipitation and soil moisture.
Monitoring of frost line and permafrost.

Oceanography and Coastal Zones

Sea currents, chlorophyll-concentration, upwelling areas, sea ice monitoring.
Continental shelf operations.
Pollution (oil) monitoring of coastal zones.
Contineous monitoring of interior (mediterranea and baltic) and marginal (northern sea and shelf) seas.

Polar Zones

Thematic mapping and monitoring of Greenland and
arctic islands.
Ice surveys, perma frost.
Vegetation monitoring, sea ice monitoring.

Development Aid

Topographic and thematic mapping   1:1oo.ooo.
Mineral resources exploration.
Planning and inventories in agriculture, forestry and
land use.
Disaster monitoring and damage assessement.

2. Requirements for Operational Applications

Europe's own needs and special requirements lead consequently
to an own segment in a global monitoring system. The sensors
configuration, orbit and repetition characteristics, spectral
and resolution specifications have to fullfill Europe's specific
needs and have to be comparable and where possible compatible
with other mainly US systems in operational world wide
satellite remote sensing.

The key problem areas for operational application, which cannot
be met by existing experimental systems are
- spatial resolution
- spectral band selection and combination
- repetition rate.

For land application the main analytical sensor with high ground
resolution will be for the near future in the optical field of
the spectrum. To fill the gaps for the required repetition
rate in an operational system and to fullfill specific tasks
active microwave sensing is indispensable, also if the complete

use of this technique needs further basic investigations
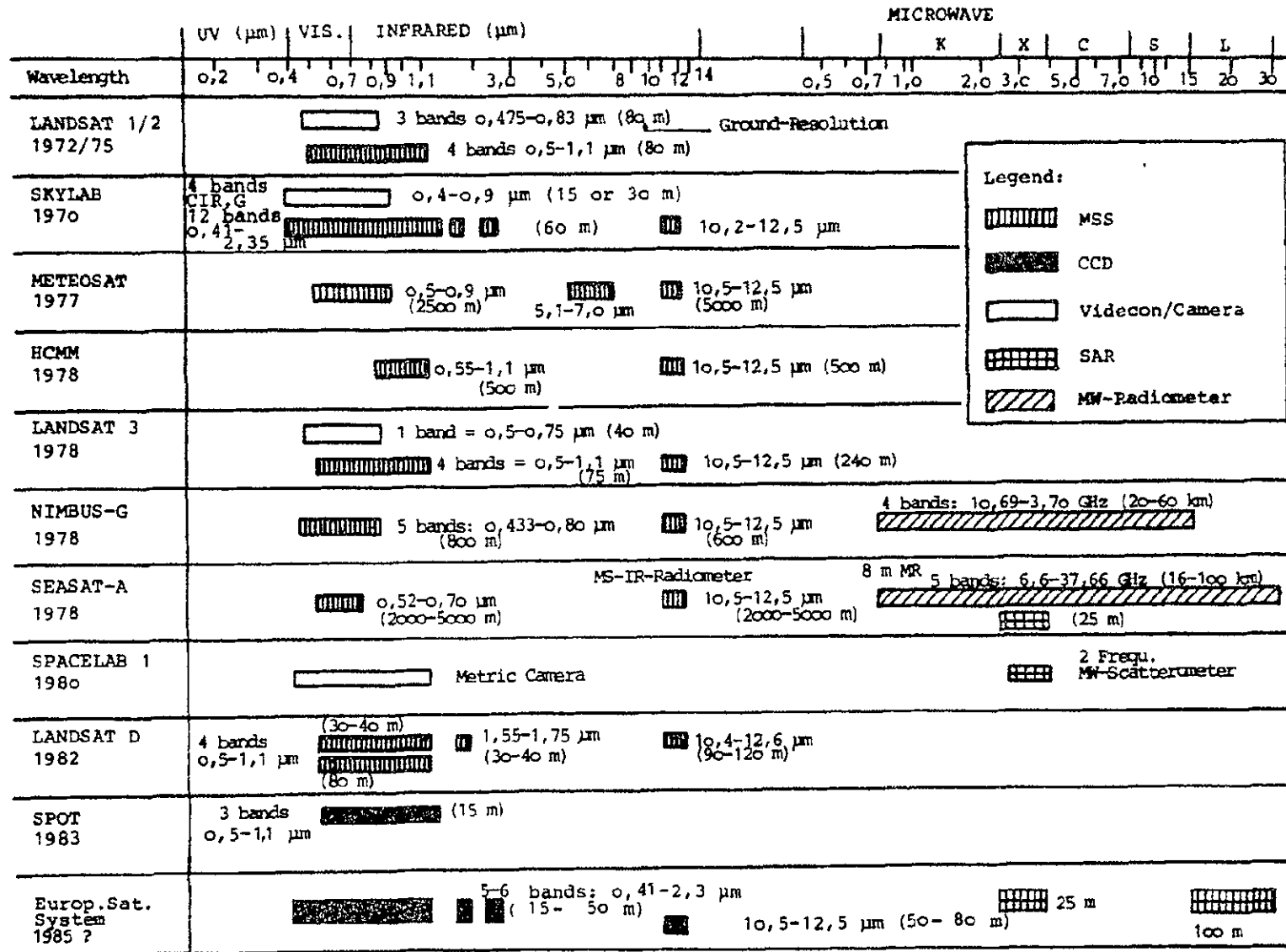via SPACELAB experiments.

For sea application the combination of microwave and optical
sensing with coarse and medium ground resolution and high
spectral resolution in the optical field seems the ideal
combination.

Fig.59 shows the existing and planned earth observation
satellites, their spectral bands, sensors and ground reso-
lution (in brackets) and where a proposed european satellite
would fit in. Fig . 60 demonstrates the time frame and expect-
able life time of these earth observation satellites.
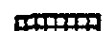
The requirements on spectral band location for the optical
part of the spectrum (fig .61) demonstrates that in general
4 - 6 bands with varying bandwidths are required. Especially
in the medium IR but also in the visible certain technology
has to be developed.

Systems with flexible spatial and spectral resolution can
be achieved by using modular opto-electronic multispectral
scanners. This sensor should provide images in the visible
and infrared spectral ranges, using the CCD technique based
on the "pushbroom" process.

Generalized requirements meeting the major applications shows
fig. 62.

Fig.59: Imaging Systems in earth observation satellites

	1972	73	74	75	76	77	78	79	80	81	82	83	84	85	86

LANDSAT-1

LANDSAT-2

LANDSAT-3   ?

LANDSAT-D

SEASAT   ?

NIMBUS-G   ?

HCMM   ?

SPOT   ?

EUROPEAN SAT-
SYSTEM   ?
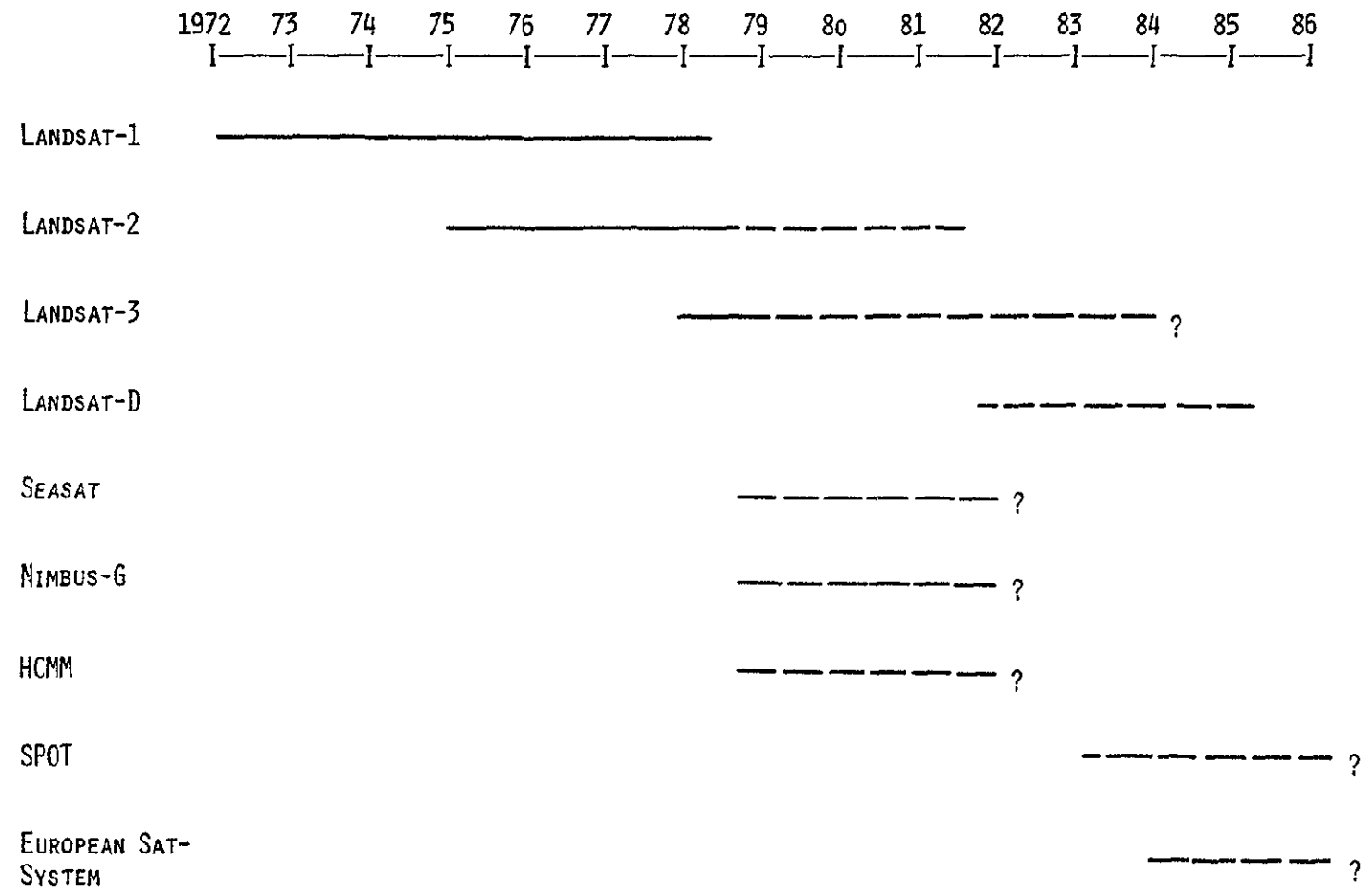
Fig. 60: Existing and projected satellite systems.
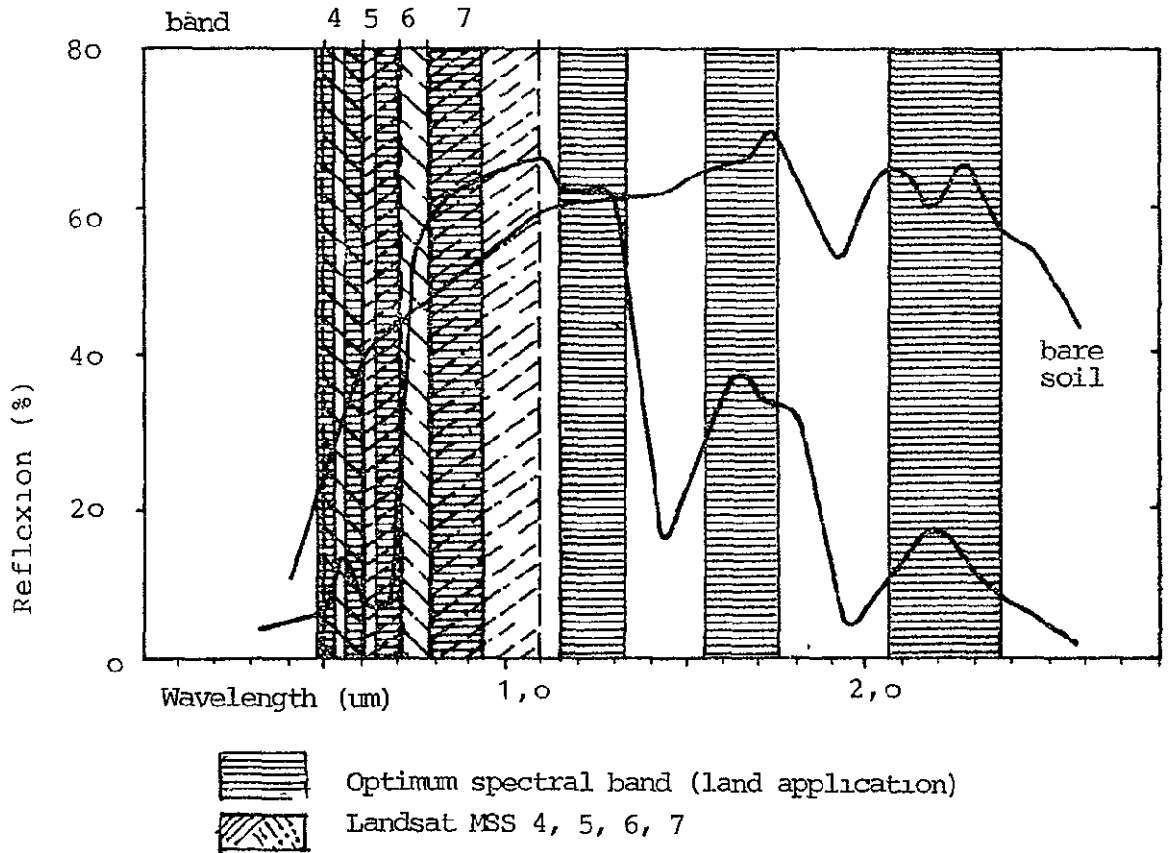
Fig. 61:   Major spectral bands for land application.

LAND USE — 4-6 BANDS VARIABLE (3o-1oo NM BANDWIDTH)

AGRICULTURE/FORESTRY — 4-6 BANDS / BANDWIDTH 3o-1oo NM

EXTRACTIVE RESOURCES — 4-5 BANDS (1oo NM BANDWIDTH)
PANCHROMATIC FOR STEREO

INLAND WATER RESOURCES — 4 BANDS (2o NM) 1x1oo NM BAND
2 BANDS (1oo - 3oo NM)

OCEANOGRAPHY & COASTAL ZONES — 5 - 6 BANDS = CZCS

POLAR ZONES — 5 - 6 BANDS: VARIABLE BANDS

DEVELOPMENT AID — 4-6 BANDS VARIABLE (BANDWIDTH 1oo NM)
2 BANDS 1o NM

λ 0,4 0,5 0,6 0,7 0,8 0,9 1,o 1,1 | 1,3 2,5 | 1o 12 UM

TO BE DEVELOPED

Fig. 62: Requirements of spectral band locations

The repetition rate for most monitoring tasks can be full-
filled with 7 - 9 days period. To guarantee for continuous
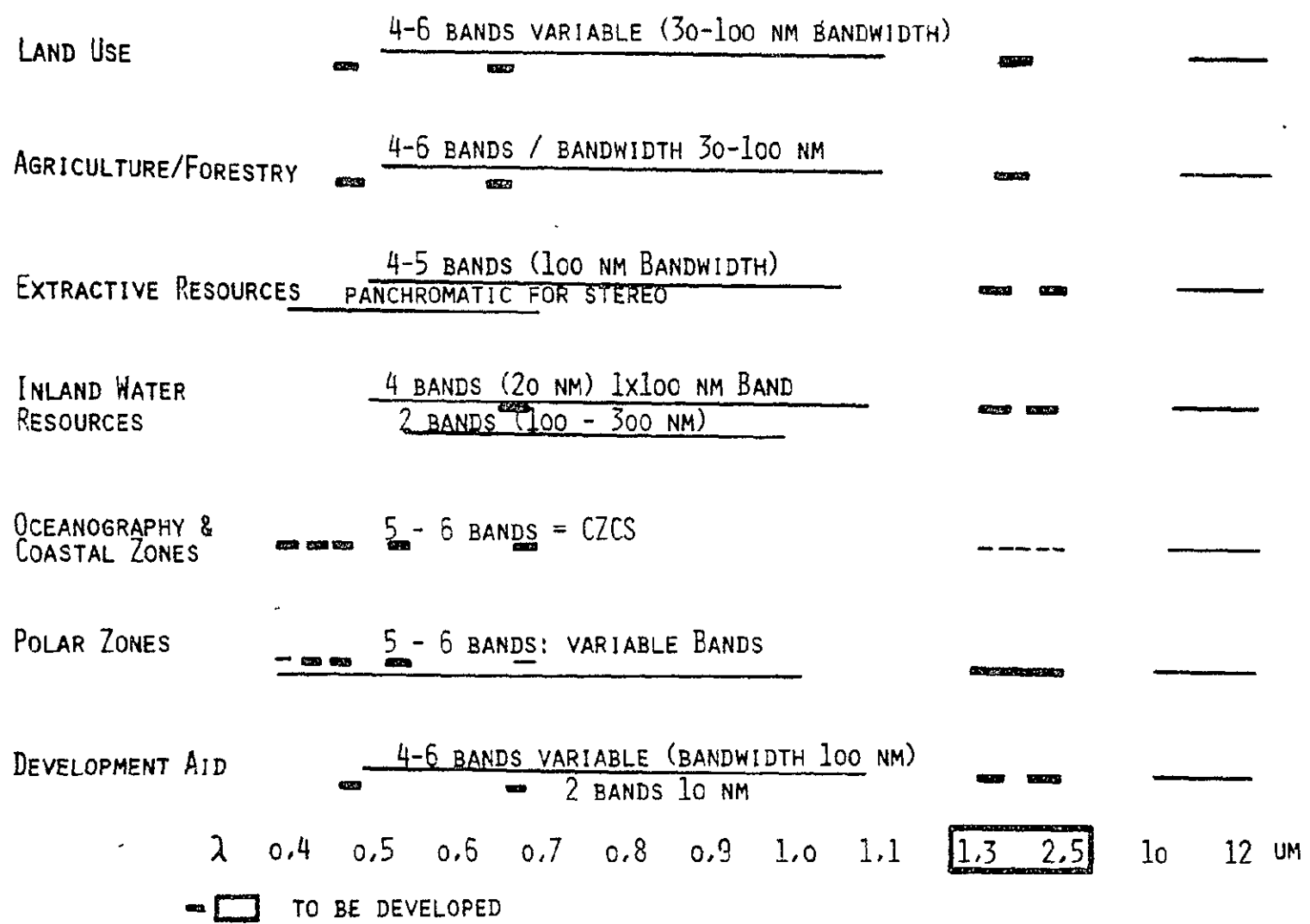monitoring and in the case of agriculture expecially for the
growing season weather independant sensing is indispensable.
As exeption are tasks in oceanography where daily repetition
rate is required (fig. 63).
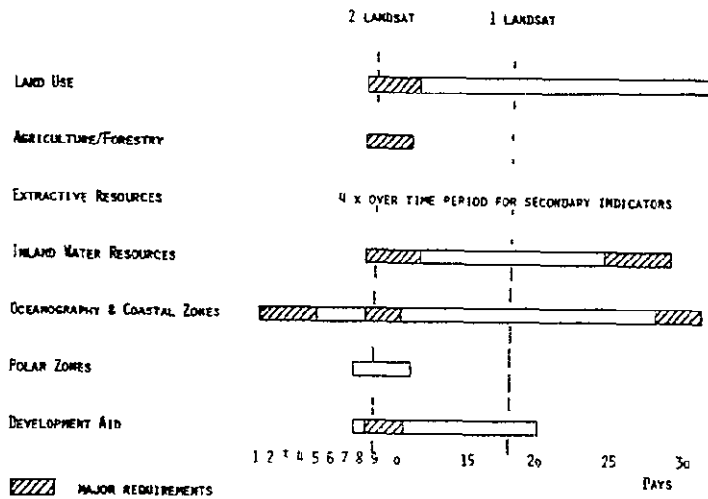
Fig. 63: Repetition rate in days.

The other driving factor for European tasks are the require-
ments on the ground resolution. Fig. 64 shows in the visible
to medium IR and the active microwave region requirement for
multispec-ral sensing around 2o m resolution. The require-
ments in the thermal IR and passive microwave radiometry are
around 8o m, large scale oceanography requires less than 5oo m
with high repetition rate.
Summarizing all requirements fig. 65 shows the European needs
in the different fields of earth observation in comparison

GROUND RESOLUTION

LANDSAT-3
(VIDECON)

LANDSAT -D

SPOT,

LANDSAT 1,2,3

LAND USE

AGRICULTURE/FORESTRY

EXTRACTIVE RESOURCES

INLAND WATER RESOURCES

OCEANOGRAPHY & COASTAL ZONES

POLAR ZONES

DEVELOPMENT AID

1o 2o 3o 4o 5o 6o 7o 8o 9o. 1oo/M

Fig. 64: Ground resolution

| | 0,38 - 2.5 µM | | 1o - 12 µM | | >1 CM |
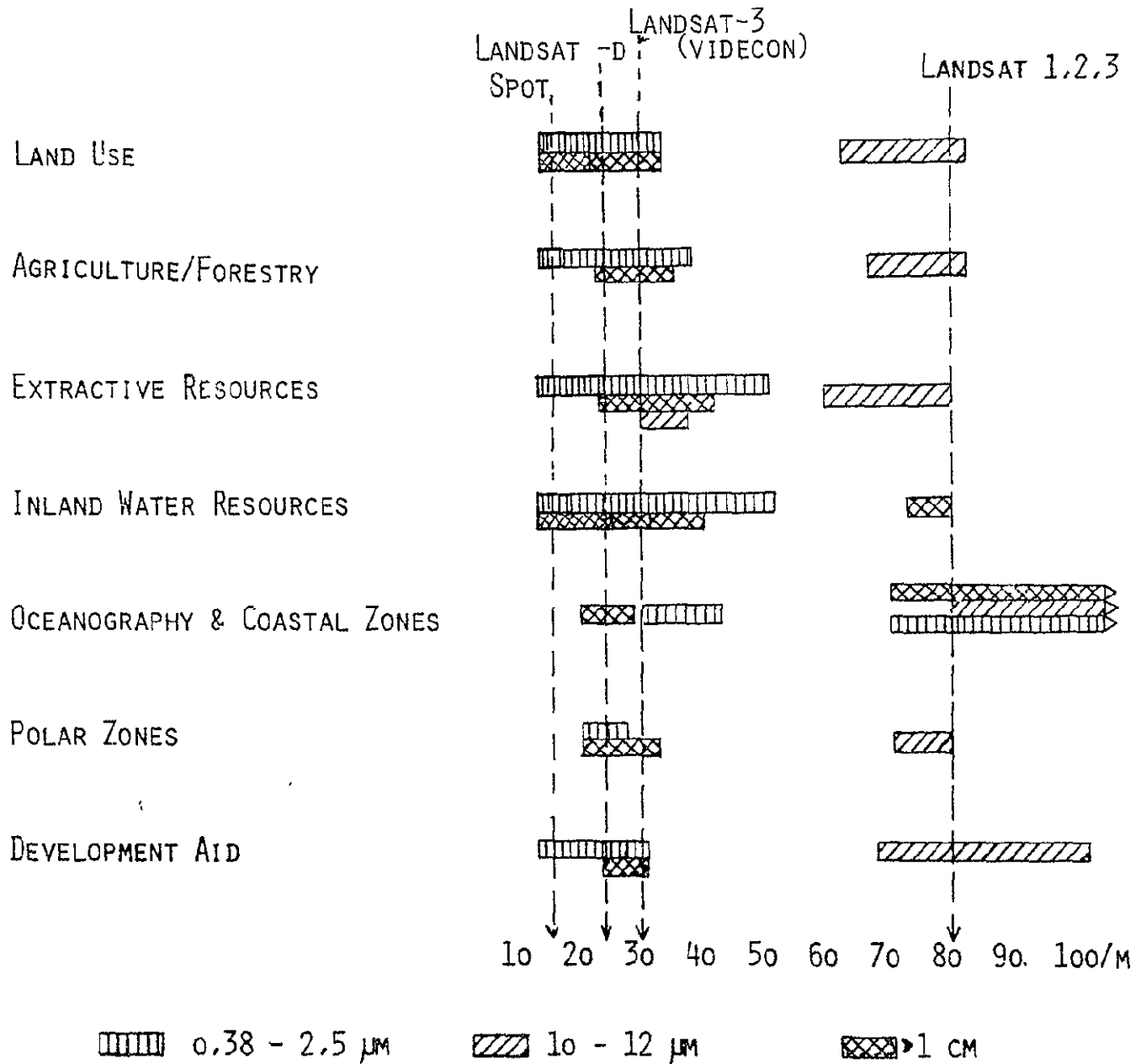
Fig. 65
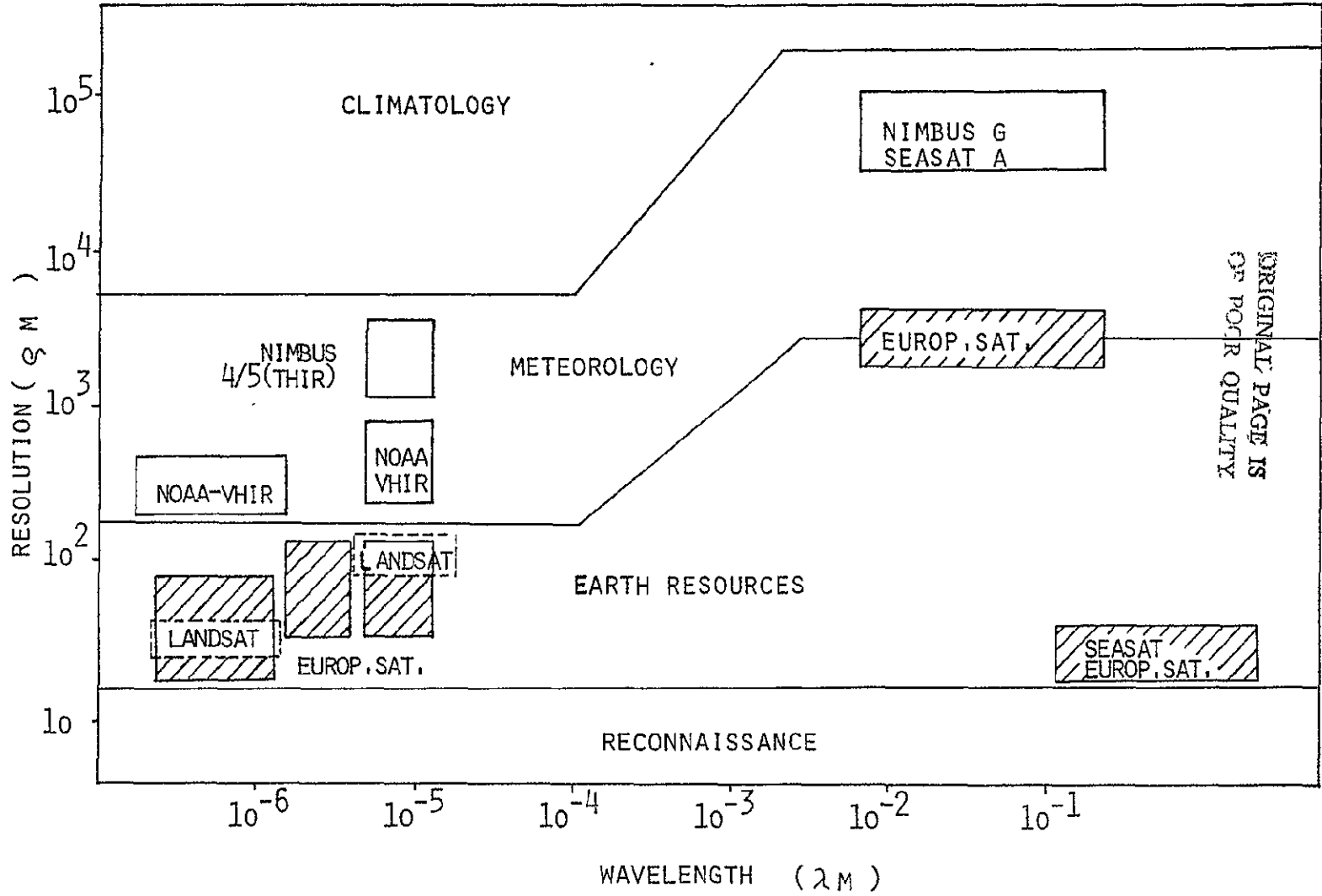
with American systems in a diagram ground resolution versus wavelengths. It demonstrates the overlapping and differing areas.

In conclusion the tasks in the different applications cannot be met with one payload configuration. Three different systems are required for land application, coastal zones and water resources and oceanography and polar zones.
Driving factor for using different payload configurations are the differing requirements on optimum spectral band and ground resolution. Possibly coastal zone requirement could be met by land application payload configuration. Though at least two systems according to fig. 66 are required for major monitoring and inventory tasks.

APPLICATION	SYSTEM REQUIREMENTS
AGRICULTURE/FORESTRY LAND USE EXTRACTIVE RESOURCES DEVELOPMENT AID	OPTICAL PAYLOAD (MED. AND HIGH GROUND-RESOLUTION) TWO FREQUEN. SAR
COASTAL ZONES WATER RESOURCES	OPTICAL PAYLOAD (MED. GROUND-RESOLUTION HIGH SPECTRAL RESOLUTION) SAR + IMAG.MICR.RADIOMETER
OCEANOGRAPHY POLAR ZONES	OPTICAL PAYLOAD (COARSE GROUND-RESOL.) IMAG.MICR.RADIOMETER

Fig.66: Typical European satellite
        systems

Operational earth observation satellites under European and
global aspects will be either dedicated to special tasks for
a limited number of applications with special orbital and
sensor requirements or to a multidisciplinary approach in
two possible payload configurations. In general the following
parameters including European needs have to be considered:
Sun-synchroneous orbit of 57o or 98o km altitude.
A spatial resolution of the sensors in the visible and near
infrared between 2o and 3o m regarding the small-scale pattern
of intensive land use areas.
In a global system including non european satellites a net
of two or three satellites within an orbital distance of
12o$^{\mathrm{o}}$ latitudes to observe fast changing targets and their
regional interrelationship.
Great emphasis to be given to microwave systems due to the
global varying climatological conditions and for the monitor-
ing of special phenomena.

3. Proposal for a Pre-Operational European Satellite

Within the limits of the above described applications, and
requirements, an Earth-observation payload can be met in
the medium term by European technology. In particular, with
a view to earlier pre-operational use, preference should be
given to sensor systems whose basic operational character-
istics are known. On the basis of users' experience, the
peculiarly European requirements for optical and passive
microwave systems may already be laid down. In order to meet
the operational requirements, Argus proposes the following

- A modular, opto-electronic, multispectral scanner
  (MOMS) with 2o-m resolution in the visible and near
  infrared and 6o-m resolution in the thermal infrared.

  Taking advantage of earlier German pre-development
  work, this sensor could be developed by 198o using
  American components, or by 1983 with excluxively
  European ones.

- A passive multifrequency microwave scanner radiometer
  (PAMS) with a resolution of 3 to 5 km at 33 GHz, 6 to
  8 km between 19 and 1o.6 GHz, and about 12 km at 5,5 GHz.

These sensor systems cater for the pre-operational and expe-
rimental requirements as follows:

Pre-operational_aspects

MOMS:

- The provision of high-resolution, synoptic satellite
  images for the various branches of environmental
  planning within the EEC.

- Improved classification cpability, and the provision
  of topographical data (stereo images) with a geo-
  metrical resolution of some 3o-m for developing
  countries' purposes.

- Thematic mapping of geological, hydrological and vegetation phenomena in developing countries.

- Provision of thematic maps.

PAMS:

- All-weather observation of oceanographic phenomena in the Central and North European areas (coastline, coastal zones, Mediterranean and Arctic Sea areas).

- Acquisition of data on snow phenomena over extensive areas.

Experimental aspects

MOMS:

- Investigation with a view to the acquisition of relevant spectral signatures.

- Optimization of the spectral regions to be used for specific applications.

PAMS:

- Investigations of the applications potential of passive microwaves for acquiring data of hydrological phenomena over extensive areas (soil moisture).

- Use of passive microwave processes in connection with the employment of the opto-electronic payload for atmospheric correction.

Last but not least, active microwave systems (SARs) appear to be essential for continuous operational, meteorological independent monitoring tasks. Admittedly, extensive fundamental research and costly technical development will be necessary in this area, in order to be able to set up a

multifrequency system for the quantilative automatic utili-
zation of the data.

ARGUS, a Modular Satellite System

Argus is a modular satellite system, designed to be launched
by Ariane. The design allows the progressive addition and
use of purely optical payloads up to and including passive
microwave scanners and active radar systems.

- The basic support module,measuring 1.8 x 1.8 x 1 m,
  consists of the basic structure, thermal-control system,
  power-conditioning arrangements and the system for trans-
  mitting, receiving and handling data. These sub-systems
  themselves are in turn modular, so that the respective
  requirements of the various configurations can easily
  ba met. Attached to the basic module is the solar array,
  which is also modular and adaptable to the various power
  and performance requirements.

- The optical module consists of the interchangeable
  camera element, whose measurements correspond to those
  of the basic support module. The camera element can be
  mounted either on the cut-away side of the module or on
  one of the narrow faces. In every case, the optical
  module has a heat-radiation system pointing away from
  the sun and, if required, a tape recorder for inter-
  mediate storage while contact with the ground is lost.

- The microwave module consists of a basic rectangular
  block measuring 1.8 x 1.8 x 4 m. An integral part of it
  is a 2.8 x 4 m paraboloid antenna. The latter is mounted
  along the diagonal of the side surface and extends some
  2o cm beyond the block in either direction in the flight
  path. In passive operation, a linear receiver system

is mounted on the Earth-pointing side of the block,
making possible phase-controlled scanning by the
antenna radiation pattern at right angles to the
satellite's flight path (scanning radiometer). The
receiver system is designed for two frequency bands:
5.3 and 1o.6 GHz. The ancillary elements required for
operating the antenna are located in the block above
the basic structure.

In place of the passive microwave module, an active side-
looking synthetic aperture radar (SAR) can be mounted.
Fig. 66 shows a 1o-m long SAR antenna consisting of five
planar arrays each 2.2 x 2 m. After deployment, it is
swung out of the orbital plane to the required angle of
sight.

In the passive operating mode, a further antenna for the
3o-GHz band can also be mounted on the microwave module.
It operates directly, without a reflector, on the phase-
selection principle, and also allows the receiver-antenna
pattern to scan at right angles to the flight path. This
antenna may be inclined to the Earth at angles between O
and 9o$^{\mathrm{o}}$ and can be folded against the block during launch.

3.1 Payload

Modular Opto-Electronic Multispectral Scanner (MOMS)

Based on Landsat 1 and 2 experiences optical sensor systems
have to lead from experimental systems to flexible operational
systems adapted to the broad variety of requirements.
A system with flexible spatial and spectral resolution can
be achieved by using the modular opto-electronic multi-
spectral scanner (MOMS). This sensor provides images in the

Modular Remote Sensing Satellite System

BASIC SUPPORT MODULE	1 KW SOLAR ARRAY	VISIBLE NEAR AND THERMAL INFRARED CAMERAS

BASIC SUPPORT MODULE	1 7 KW SOLAR ARRAY	VISIBLE NEAR AND THERMAL INFRARED	10 & 20 GHz PASSIVE MICROWAVE

BASIC SUPPORT MODULE	2 KW SOLAR ARRAY	VISIBLE NEAR AND THERMAL INFRARED	10 & 20 GHz MICROWAVE PASSIVE	30 GHz PASSIVE MICROWAVE

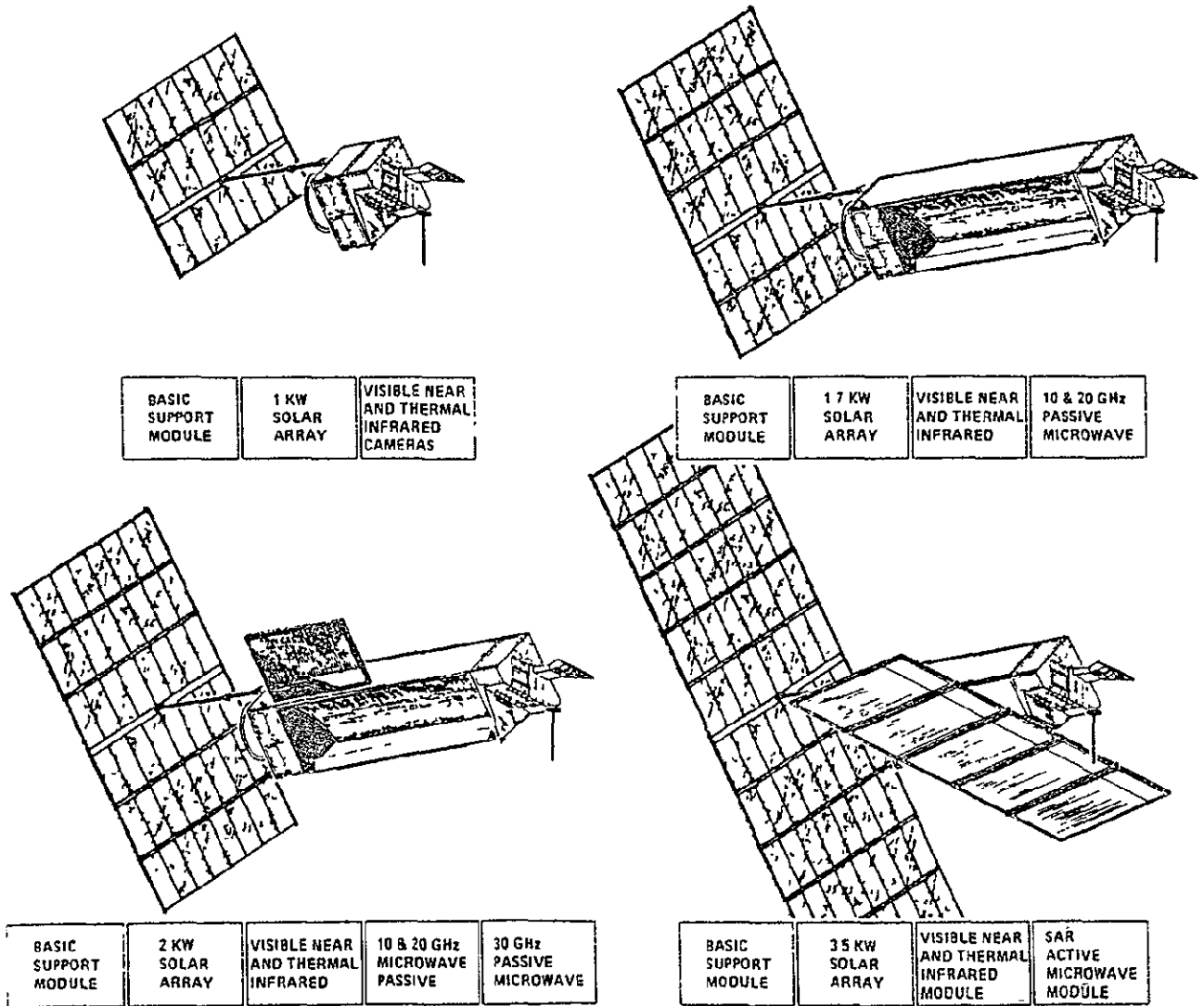| BASIC SUPPORT MODULE	3 5 KW SOLAR ARRAY	VISIBLE NEAR AND THERMAL INFRARED MODULE	SAR ACTIVE MICROWAVE MODULE

Fig.66:   Argus modular multidisciplinary Earth-resources satellite system

visible and infrared spectral ranges by electronic scanning
with semi-conductor detector arrays, using the CCD technique
based on the "pushbroom" process.

This technique, which is specially suited to producing
geometrically exact orthogonal images, represents a marked
technical advance over the presently used scanners with
mechanically driven scanning mirrors. In addition to its
small weight and satisfactory dimensions, this system's
imaging geometry is very flexible. Thus, for orbits between
6oo and 9oo km, the spatial resolution (maximum 2o m) and the
image swath width (6o - 24o km) can be adjusted to suit the
measurement tasks and the texture of the area covered. These
characteristics also apply to stereo images.

A separate module with its own optical system is provided
for each spectral channel and for stereo images. The basic
version of the MOMS shown in fig.67 comprises six modules
and a tape recorder; the latter can, when appropriate,
be exchanged for a stereo module. The principles of the
individual modules are shown in fig. 68 . A given image area
is viewed twice through two lenses by three of the suitably
adjusted elements and sensed by a detector array of six
linearly arranged CCD elements each with 17oo pixels. This
process enables an exact reconstruction of the image lines
without distortion due to the mechanical lateral limitation
of the CCD elements.

The effective length of the detector line can thus be
lengthened virtually at will. By means of appropriate
specifications, it can be suited to the image width and the
resolving power. The process makes it possible to use CCD
elements with fewer pixels (e.g. 5oo instead of 17oo) with-
out loss of image. This means that the system can be
developed regardless of the availability of American CCD
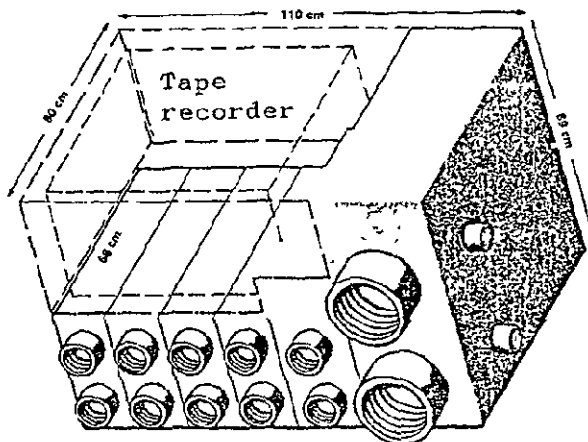elements.

FIG. 67   Modular opto-electronic
          multi-spectral scanner (MOMS)

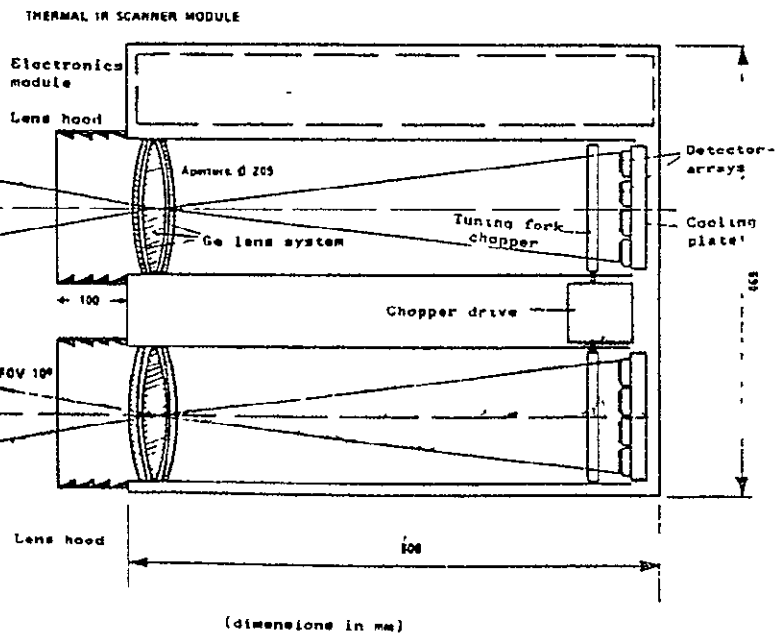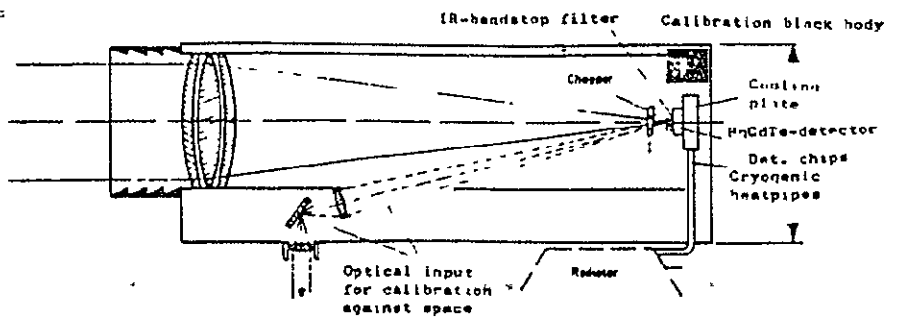|	Channels 1 - 3	channel 4	channel 5	channel 6
Spectral region (μ)	o,45 – 1,o	0.45 – 1	1.5-1.7/2.1-2.3	10.5 – 12,5
Spectral bandwidth (μ)	0.05 – 0 1	0.02	Variable	2 0
Max spatial resolution (m)	20 / 40 / 60	60 / 100	60 / 100	60 / 100
	o. 25 / 50	50 / 100	50 / 100	50 / 100
Image swath width (km)	55 / 110 / 240	110 / 240	110 / 240	110 / 240
Temperature resolution (K)				0 5 – 1.0
Number of detector chips	2 x 3 x 1728	2 x 3 x 1728	2 x 4 x 500	2 x 4 x 500
Type of detector	Si photodiodes	Si photodiodes	InSb or PbS	HgCdTe
Pixels per scanning line	- 10368	10368	4000	4000
MOMS - Overall characteristics				
Total mass (kg)	77 (including cooling radiator and tape recorder)			
Dimensions (cm)	110 x 69 (front face) x 80			
Maximum digital data rate (Mbps)	approx 45 (forgoing maximum performance			
Development time:	approx 5 years (including Spacelab tests)			

Fig. 69: Characteristics of the scanner system
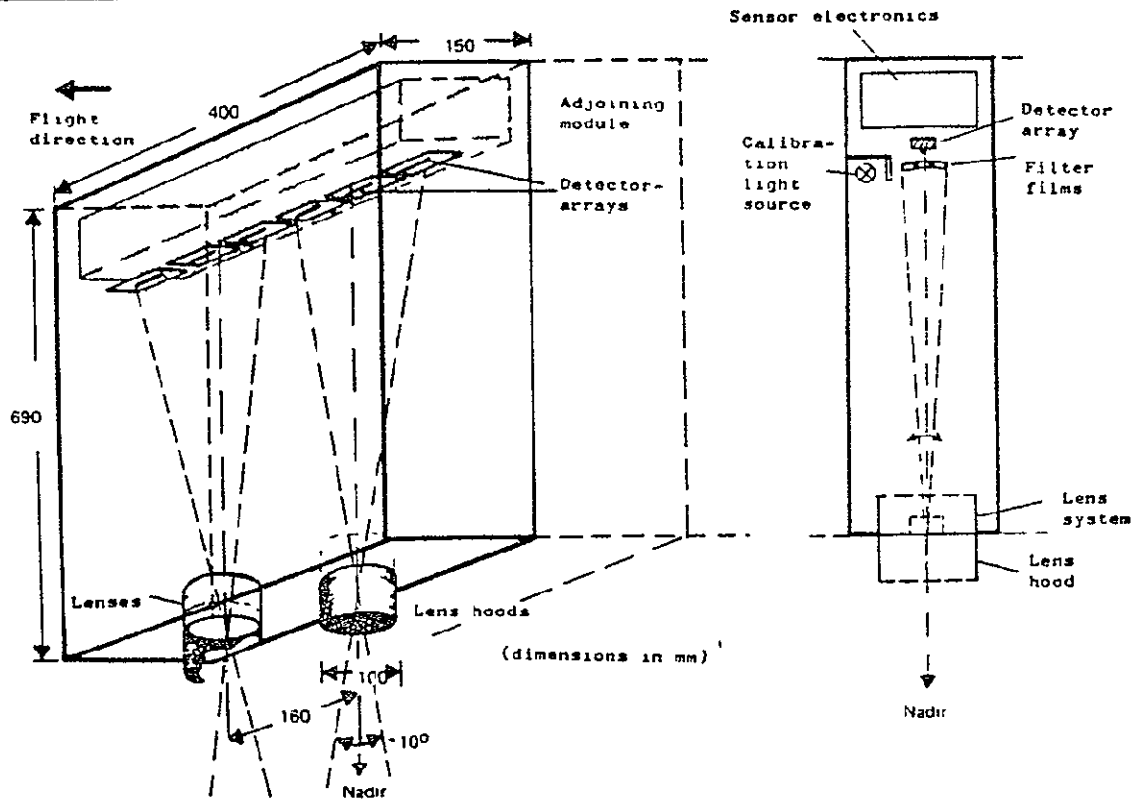
Fig. 68: Principle of the multispectral scanner module
for visible to near IR.

The stereo module operates on the same principle, but has
two detector arrays parallel to one another, arranged symme-
trically about the image central axis at a distance
appropriate to the base-to-height ratio. This enables the
simultaneous viewing in the flight path of a swath both in
front of and behind the satellite. The resultant radio-
metric and geometric image quality is better than has
hitherto been achieved in space: an essential feature
for mapping, particularly in the developing countries.

In the visible region, standard optical systems with
apertures of some 1o-cm are satisfactory, and germanium
lenses of some 2o-cm in the infrared. The latter are avail-
able at short notice in Germany.

Such small apertures are possible because each spectral
band has its own lens. In contrast, the systems that have
hitherto been customary used a wide aperture together with
beam dividers, which have been eliminated in the MOMS.

The spectral band covered by a module is determined by the
type of detector used and by a filter located between the
lens and the detector array. For the basic version, combi-
nation filters are provided with triply variable centre
frequencies and bandwidths. Fig. 69 shows the various
types of detector and the corresponding sensor character-
istics. One of the channels also provides a high spectral
resolution of o,o2 bandwidth in the o,45 – 1,1 u band,
albeit with reduced spatial resolution (6o instead of 2o m).
This channel is used to cover specific absorption bands and
radiation maxima. Particular phenomena can thus be selective-
ly recognised, for example cereal diseases in the o,62 –
o,68 u band and chlorophyll from o,64 to o,67 u.

The system's high measurement accuracy is ensured by care-
ful calibration during operation. This compensates electronically
for the sensitivity variation of the individual diodes of the
CCD elements.

Applications	Frequencies (GHz)				
	5,3	10,6	19,35	22,25	30 – 35
Surface temperature measurement ($\Delta T_{abs} \approx 1$ K/280 K)					
– Land areas	O	◉	O		O
– Water areas	◉	◉	◉		
Ice/water assessment	◉	◉			◉
Snow/ice/land assessment	◉	◉	◉	O	
Determination of snow moisture	O	O	O	O	
Determination of age of ice	O	O	O	O	
Determination of soil moisture:					
– total	◉	◉	O	O	O
– through vegetation cover	O	O			
– with penetration	◉	O			
Determination of type of soil	O	O	O		O
Measurement of cloud layer thickness and precipitation rates	O	◉	◉	◉	
Measurement of atmospheric moisture			◉	◉	
Spectral measurement of sea states (with variable polarisation)	O	O	O		
Salinity determination					

O fully applicable   ◉ supporting measurements recommended

Fig. 71: Typical application of a multichannel microwave scanning radiometer

	Channel 1	Channel 2	Channel 3	Channel 4
Frequency (GHz)	5.3	10.6 [*]	19.35 [*)]	33
Wavelength (cm)	5.7	2.8	1.55	0.9
Type of antenna	Cyl.-parab.	Cyl.-parab.	phased array	phased array
Antenna aperture (m)	4 x 2.6	4 x 2.6	1.8 x 1.5	1.8 x 1.5
Image swath width (km)	200 – 220	200 – 240	200 – 220	220 – 280
Spatial resolution (half beamwidth, degrees)	1.15 x 0.9	0.6 x 0.45	0.75 x 0.5	0.42 x 0.3
Spatial resolution (km)	12 x 9.5	6 x 4.7	8 x 5.7	4.4 x 3
Antenna gain (db) (after deduction of losses)	43 approx.	45 approx.	47 approx.	70 approx.
Temperature resolution (K, at instrument) – 200-MHz bandwidth	0.08	0.1	0.25	0.4
ditto – 100-MHz bandwidth	0.15	0.3	0.7	ca. 1

PAMS — Overall characteristics

Masses: Cylinder parab. antenna + radiometer phased-array antenna + radiometer	75 kg / 115 kg
Mean electric power requirement	120 W + 230 W
Development time	about 5 years (including SPACELAB testing)

*) Radioastronomy port

Fig. 72: Characteristics of the passive microwave scanning radiometer

Fig. 7o shows the first test image obtained by a flight version of an opto-electronic module.

Passive microwave scanning radiometer (PAMS)

The modular, extensible microwave scanning radiometer represents a first step towards the employment of microwave sensors, which are required for an operational satellite remote sensing system. The current operational use of passive microwave systems, e.g. in the Nimbus satellites, for meteorological and oceanographic purposes may be extended to Earth sensing even before active radar systems are available in Europe. An improvement in resolving power from some 14o-km (Nimbus) to 5-1o km enables the investigation and all-weather monitoring of important small-dimension phenomena in coastal and continental-shelf regions, as well as on land.

PAMS is designed for this task. As shown in fig.71 , it is a multi-channel system enabling the acquisition of the ground signatures of various types of phenomena at 5,3, 1o,6, 19,35, and 33 GHz. The frequency of 22,5 GHz, which is of value for determining the water-vapour content of the air, is provided as an option. At a temperature resolution of under o,5 K, the resolving power at all frequencies is better than about 1o km.

Figure 66,p.   , shows the PAMS' two antenna systems. They employ electronic beam scanning based on the phased array technique. A linear phased array with a cylindrical reflector having a 4-m axial aperture is provided for the frequencies of 5,3 and 1o.6 GHz. For 19,35 and 33 GHz, a planar phased array of 1,8 m aperture is fitted. A further similar antenna for 22,25 GHz is provided as an option and can be mounted beside the planar antenna.

The development of the antenna system involves only small technical risks. The characteristics in fig.72 are based on

Fig. 7o: First test image obtained by an opto-electronic
module (o,4 - 1,o u).

previous experience. The cylinder system can be developed from the Helios antenna, which has already been proven in space in order to achieve the required surface accuracy of about 1/2o of a wavelength, the reflector design is based on carbon-fibre technology; it is likewise available. The only significant new item to be developed is the phase-shift electronics for electronic beam scanning. This involves no fundamental problems, however, and the same is true of the planar system.

In order to achieve high ground and temperature resolution, it is necessary to limit the scanned image swath width, which in the case of PAMS lies between 22o and 28o km, as shown in fig. 73 . These figures take account of satellite velocity and the integration time required per image pixel. The image data from PAMS are transmitted to Earth in digital form, as for the optical system, and stored there on tape for further processing. In addition, the passive system has a data rate that is smaller by two orders of magnitude than an active system giving the same resolution, since, as in the case of optical scanning, only one signal value is assigned to each image pixel. Image recovery and evaluation on the ground can therefore be accomplished for both MOMS and PAMS using the same equipment and related software as for Landsat data, whereas extensive new development is required in connection with the processing of radar data.

3.2. Orbit Selection

The selected orbit is a compromise between the requirements for good resolution by the sensors, maximum repetition rate and lifetime. This led to the 593 km sun-synchronous orbit, of which details are given in fig. 74 . The altitude results from selecting a repetition rate of exactly 12 days, i.e. the orbital tracks of the twelfth day coincide exactly with those of the first day.

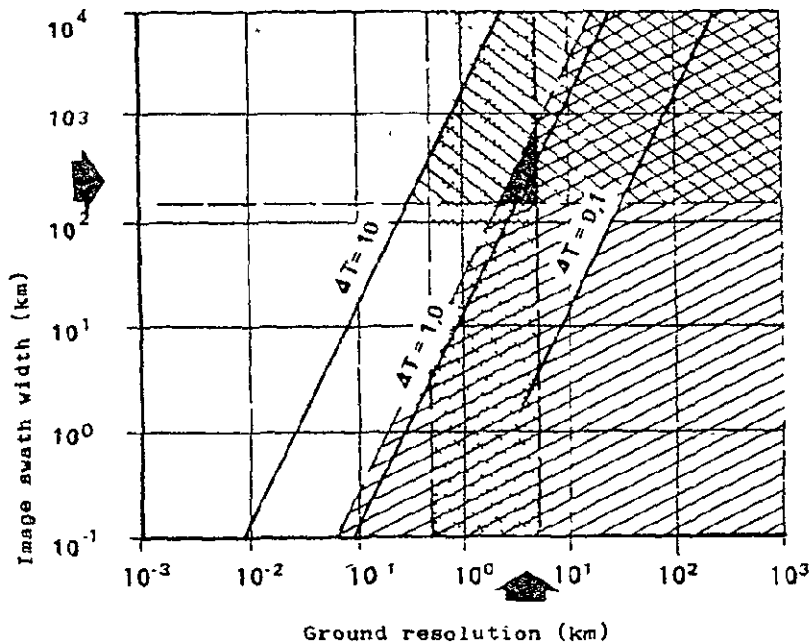Radiometer figure of merit (K) = 0.1 K, satellite velocity = 7 km/s

Fig.73: Spatial resolution plotted against image swath width
for a passive microwave scanning radiometer

Table IV: Orbit and coverage parameters

Inclination	97.747°
Orbit altitude	593, km
Orbital period	96.536 min
Number of orbits per day	14.917
Distance at the Equator between two successive orbital tracks on the same day	24.13° (= 2687 km)
Daily drift of orbital tracks referred to the Earth	2.01° (224 km)
Repetition rate for worldwide coverage by ground tracks	12.0 days
Intersection of 1st-day image swath with corresponding swath of 2nd day (swath width 200 km)	$\pm25.4^{\circ}$ latitude

Fig. 74: Orbit and coverage parameters.

Earth coverage

The requirement for measurements along the ground tracks at
approximately the same illumination conditions (constant
local time) leads to the necessity for the inertial drift
of the orbit's nodal line to be sun-synchronous. The incli-
nation resulting from this requirement is 97.747° with respect
to the equator.

Fig. 75 shows schematically the geometry of the orbit, the
satellite and the direction of the sun.

The ground tracks of this orbit were determined over a period
of two days and the essential coverage parameters deduced
therefrom. The worldwide plot is shown in fig. 76 , while fig.
7 7 shows the European coverage.

The daily drift of some 224 km (measured at the equator) -
resulting from the fact that there is not an exact number
of orbits in 24 hours - is necessary in order to achieve a
progressive, continuous coverage of the whole Earth in 12 days.

As can be seen in fig. 77 , the European region is crossed
each day by three north-south ground tracks and three south-
north tracks. The time difference at an intersection point
between the northbound and southbound ground tracks is some
ten hours. This means that if, for example, it is decided
that the northbound track shall cross the equator at 1o.oo,
any given area will be overflown twice a day: once in the
morning and once in the evening.

Communication with Ground Stations

Fig.77 shows the areas over which the satellite is in contact
with Redu and Fucino respectively. A minimum elevation of 5°
above the horizon is assumed, which is sufficient for TM/TC.
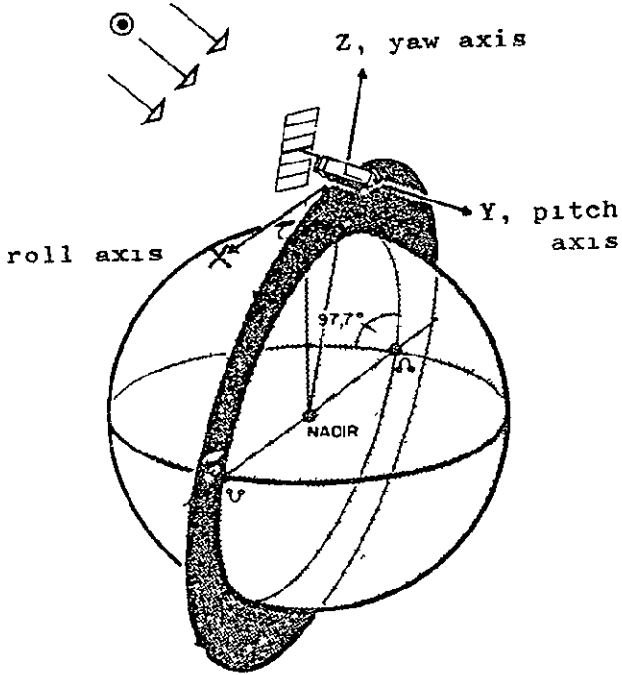Contact is maintained for a maximum of some 1o minutes longer.

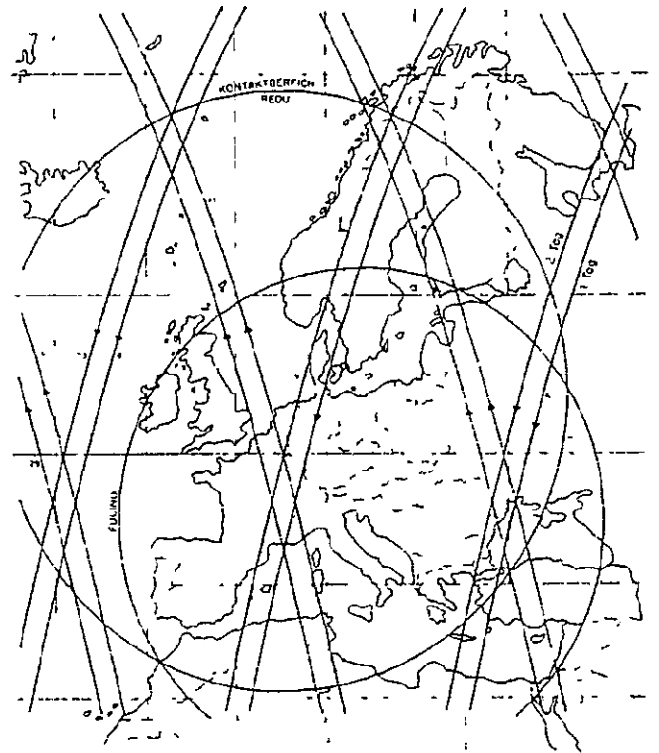Fig.75: Sketch of satellite's orbital geometry and attitude

Fig.77: Ground tracks over Europe, and coverage areas of Redu and Fucino during the two days after injection
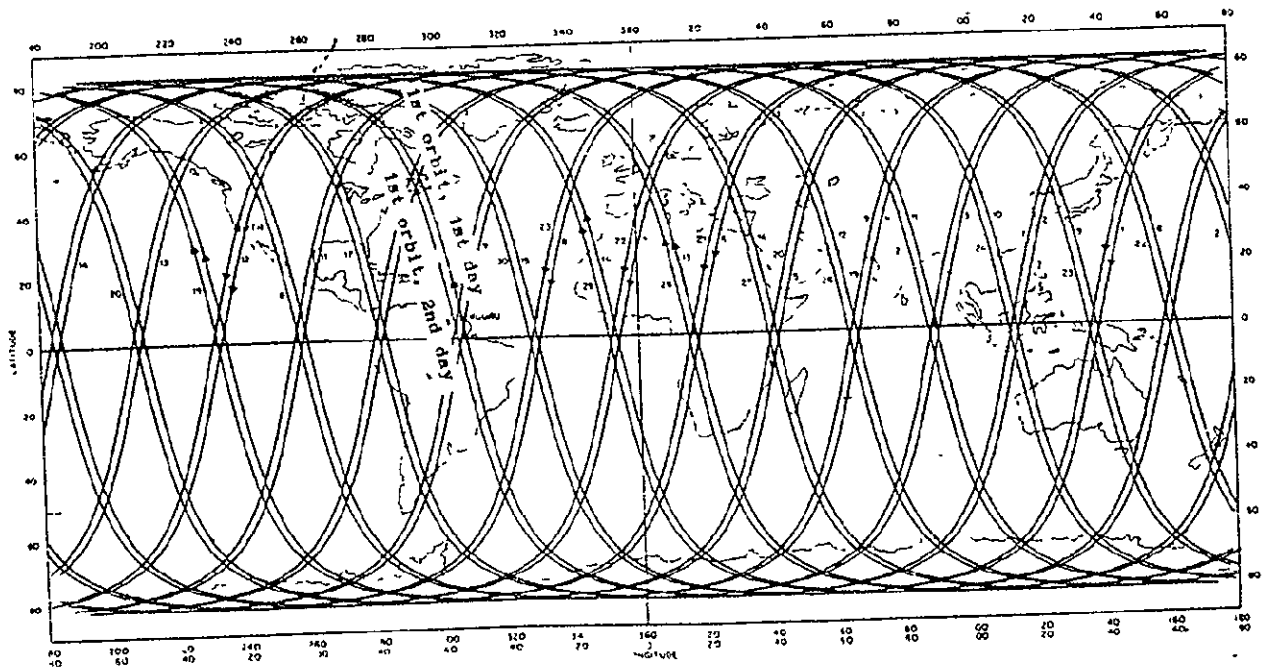
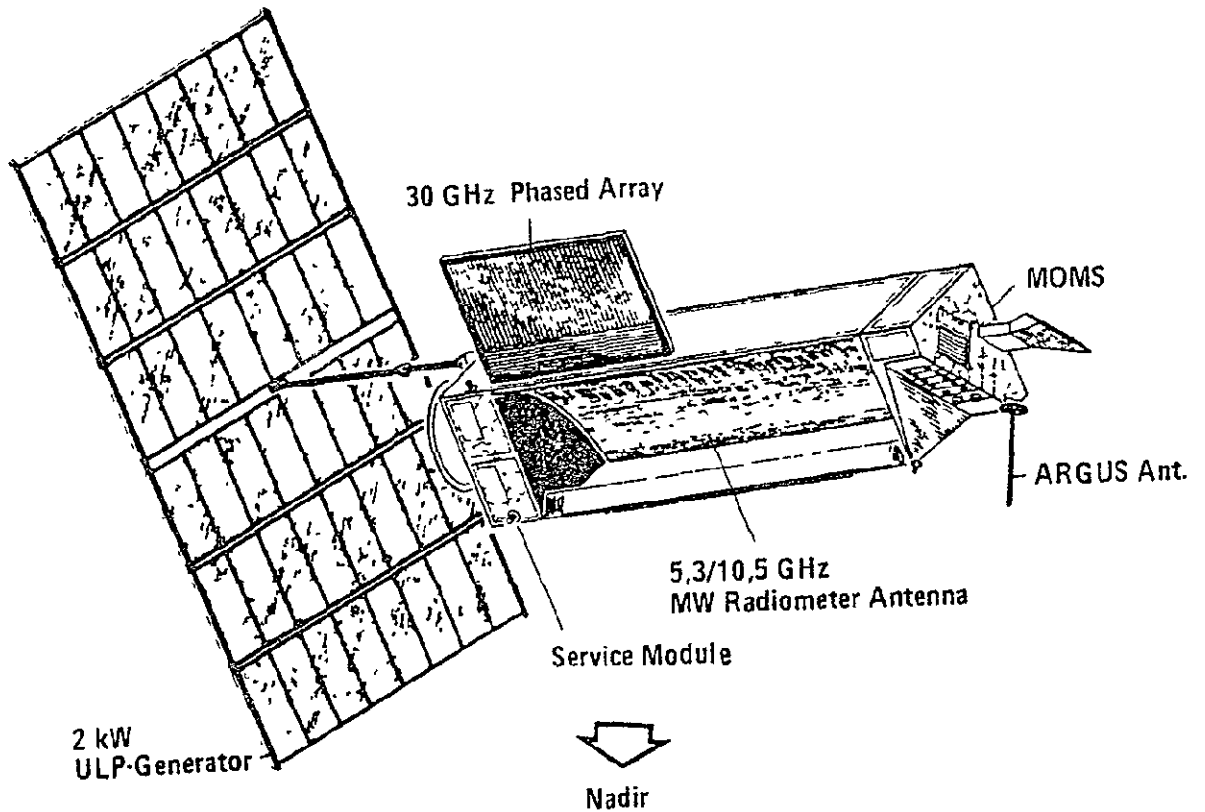Fig.76: Worldwide distribution of ground tracks during the two days after injection

Fig.78: Flight configuration of Argus satellite with optical multispectral scanner, two passive microwave radiometers (three frequencies) and 2-kw ULP solar generators

3.3 Description of the Satellite Concept

Satellite Design

Argus is designed for launching by Ariane or Space Shuttle into sun-synchronous low Earth orbit. Its main features are as follows (see fig. 78):

- Modular construction: power supply module, microwave module, optical payload module

- Three-axis stabilisation aligned on the nadir and the sun by means of momentum wheels and magnetic torquers

- System for correcting orbital inclination and altitude for a lifetime of three years.

- Steerable solar array, capable of extension up to 3.5 kW of electrical power using the MBB ULP technology (Ultra Lightweight Panels made on carbonfibre reinforced plastic).

- Full use made of the Ariane payload volume, with a rigid cylindrical paraboloid antenna for the microwave radiometer operating on 5.3 and 1o.6 GHz.

- Deployable planar antenna for a third microwave frequency of 33 GHz.

Its modular construction makes it possible to mount the SPOT payload proposed by CNES on the basic module, in addition to the payload described above, or else to mount an active radar system in place of the passive microwave radiometer.

The dimensions of the basic configuration shown in fig. 78 are based on the constraints imposed by the payload fairing in the launch configuration

The 1.8 m square cross section is suitable for the dynamic-
ally useable diameter of 2.8 m, and also gives maximum width
to the cylindrical-paraboloid antenna, which stretches
along a diagonal of the block.

The power-supply module consists of the cylindrical adapter
of 1.2 m diameter, the adjacent sandwich box structure and
the deployable solar array. The overall height of the basic
module has been kept to 1 meter, so that the whole 4 meter
height of the cylindrical Ariane fairing is available for the
microwave antenna. Access to the interior is by removeable
side panels.

The orbit-correction system is fitted in the adapter, while
the other bus components such as attitude control, batteries,
S-band TM/TC and solar-array drive are mounted in the square
main structure.

The solar array, which in the basic design gives 1.6 kW
after three years, consists of 6 ultra-lightweight (ULP)
panels, secured to a side wall. The drive shaft has three
joints, which are required for deploying the array and point-
ing the unfolded panels towards the sun. During one orbit,
the satellite turns once around the array-drive axis, so
that its longitudinal axis is at right angles to the orbital
plane and thus forms the pitch axis.

In order to allow the IR sensor to radiate heat, the optical
module is mounted on the microwave module. The cooling
radiator thus faces neither the sun nor any part of the
satellite. By slanting the horn and making its Earth-facing
side longer, the Earth's albedo is prevented from reaching
the inside of the radiator.

The paraboloid outline of the microwave antenna lies along
a diagonal of the rectangular basic module, so that the
radiator can be mounted on the corner in front of it. The
same arrangement is used at the upper end, by means of the

advancing corner of the optical payload module. The normal
of the cylindrical paraboloid points towards the nadir, and
the optical module is therefore similarly cut away in the
diagonal direction.

The cylindrical paraboloid and the backward-facing surfaces
have to be made of very rigid carbon-fibre reinforced plastic
in order to be able to carry the payload module which weighs
over 13o kg, and to remain correctly pointed.

Options and Possibilities of Extension

The Argus system can cater for:

- Because of its modular construction, various payload
  sensors, e.g. high-resolution optical sensors in the
  visible and infrared, passive microwave sensors (re-
  flector antennas and/or phased arrays), active micro-
  wave sensors (SAR or scatterometer), or combinations
  of optical sensors and microwave payloads.

- Various sun-synchronous orbits, e.g. orbit altitudes
  between 5oo and 12oo km and various orbit node-line
  arrangements (e.g. o6.oo to 18.oo, in which case
  between o6.oo and 13.oo Argus can remain pointed in
  the same direction towards the Earth).

The characteristics of the Argus system as designed for
Ariane and a 6oo km sun-synchronous orbit lie within the
following limits:

- Payload mass	1o/3oo/1ooo kg
- Payload power requirement	1ooo/45o/1oo W
- Payload bit rate	3oo/1oo/2o Mbps
- Memory capacity	up to about 10^{11} bits
- Mission duration	4, 3, or 2 years

- Overall mass   3ooo kg
- Overall power requirement   3,5 kW
        (3 years)

Telecommunications System

The sensors proposed for Argus would produce the following
provisional bitrates if an error-detecting code was used:

- MOMS	approx.	4o.o Mbps
- PAMS	"	4.3 Mbps
- IR-Radiometer	"	3.4 Mbps
- Housekeeping	"	o.3 Mbps
	Total:	48.o Mbps

These values are comparable to those for the optical payload
proposed for the first generation of SPOT (45 Mbps).

In view of the high data rate, real-time transmission to
a central ground station is envisaged, e.g. to the ESA Earth-
net (Fucino and Kiruna), assuming 3 day and 3 night orbits
per 24 hours, with a contact time of some 1o minutes for the
European region. For extra-European regions or the northern
fringes of Europe, it will be necessary to store data on
board for a short time (1o, 3o or 6o minutes), with the
result that the quoted telemetry rate will be increased by
a factor of between 2 and 3.

If no greater quantity of data can be stored, mobile receiver
stations will have to be sent to the developing countries.

Whereas the satellite platform TT & C system operates at
around 2 GHz in the unified S-band (USB), which is compa-
tible with ESA and NASA practices, the payload telemetry must

be transferred to higher frequencies, e.g. 8, 21.51 or 65 GHz,
which permit greater bandwidths and hence higher bitrates.
Using the 8 - 8.4 GHz band, the nominal Argus bitrate can be
transmitted to the ground using 2 bands, or the higher britrate
using 6 bands. The ground stations will be suitable for this
kind of working; typically, 6 HDDT per day will be recorded;
only the receiving antenna will have to be modified for this
frequency range.

The transmitted power in the 8-GHz band should amount to about
24 W per channel for a station 6oo km distant. However, in
order to use the whole contact time for data transmission
with approximately uniform quality, the transmitter power
must be higher, e.g. 4o W per channel, and the transmitting
antenna must have a shaped beam pattern with a gain at least
5 dB higher for angles greater than 60°. If a 0-dB antenna is
used, four travelling wave tubes with powers of some 2oo W
would be needed for transmitting some 14o Mbps.

Data management

A modular on-board data-management (OBDM) system is provided,
based on a programmed on-board computer (OBC). The OBC-
controlled data-and-command bus together with the remote
terminal units (RTU) enable flexible adaptation of the OBDM
to a wide range of payload requirements. In this connection,
a non-rigid (floating) telemetry format is recommended.

The OBC performs the following tasks:

- Data handling, i.e. data-bus and format control;

- Arrangement of the payload-specific data-recording
  times, spectral regions, ground resoltuion, track
  selection for MOMS, and quantification, i.e. data
  reduction is also possible;

- Data pre-processing, e.g. data redoction by means of
  delta modulation;

- Attitude determination tasks (Calmanfiltering) and attitude control, automatic position determination and orbit control;

- Management of the bus sub-systems, e.g. thermal control and power supply (batteries), in which connection fault monitoring and automatic switching of redundant components are important.

3.4 Availability of Major Components in Europe

- Multispectral scanner

The development of the MOMS here described is based on the following assumptions:

1) The modules for the visible to near infrared spectral region (channels 1-4 and stereo module) are directly derived from the aircraft experimental module developed by MBB under contract to the BMFT. There is no discernible risk associated with the development costs and time-schedule. Admittedly, the concept here described is based on the use of American CCD diodes, but comparable suitable detectors could equally be prdouced in Europe in less than 2 years.

2) For the module for the near-to-middle infrared region (Channel 5), suitable individual detectors exist in Europe, but as yet no linear arrays. Suitable CCD detectors indeed exist in the USA, but are currently not commercially available outside that country. The development work must therefore be undertaken in Europe. If need be, HgCdTe elements of channel 6 could be used for this region, with enlarged aperture.

3) The thermal IR module (Channel 6) is being developed from the existing French detector array using HgCdTe

elements, by increasing the number of detectors per element. Development costs and times are considerably greater than for the modules for channels 1 - 4, but there is not discernible risk.

The basic feasibility of the complete electronic multispectral scanning system using European and extensively German sensor technology has been established on the basis of an extensive market analysis and the study underlying this paper.

- Passive Microwave Radiometer

This cylindrical-paraboloid reflector is immediately available, with the present carbon-fibre/aluminium-core composite construction, as qualified for the solar arrays and paraboloid antennas of contemporary communications satellites. Carbon-fibre reinforced plastic wound skins up to 1o m long can be wound onto cores 2 m in diameter at MBB.

Microwave radiometer electronics are being developed in several institutes and firms in Europe, e.g. in the UK, Denmark, Switzerland and Germany (DFVLR) so that their use in 1983/84 seems assured.